



**Universidade do Minho**  
Escola de Engenharia

Márcia Cristina Teixeira Marques

Evaluation of the behaviour of bio-based  
nanostructures in food systems





**Universidade do Minho**  
Escola de Engenharia

Márcia Cristina Teixeira Marques

**Evaluation of the behaviour of bio-based  
nanostructures in food systems**

Dissertação de Mestrado

Mestrado em Biotecnologia

Trabalho efetuado sob a orientação da

**Doutora Ana Cristina Braga Pinheiro**

e do

**Professor Doutor António Augusto Martins de Oliveira Soares**

**Vicente**

## DIREITOS DE AUTOR E CONDIÇÕES DE UTILIZAÇÃO DO TRABALHO POR TERCEIROS

Este é um trabalho académico que pode ser utilizado por terceiros desde que respeitadas as regras e boas práticas internacionalmente aceites, no que concerne aos direitos de autor e direitos conexos.

Assim, o presente trabalho pode ser utilizado nos termos previstos na licença abaixo indicada.

Caso o utilizador necessite de permissão para poder fazer um uso do trabalho em condições não previstas no licenciamento indicado, deverá contactar o autor, através do RepositóriUM da Universidade do Minho.

**Licença concedida aos utilizadores deste trabalho**



**Atribuição-NãoComercial-Compartilhalgal**

**CC BY-NC-SA**

<https://creativecommons.org/licenses/by-nc-sa/4.0>

## AGRADECIMENTOS

A concretização desta dissertação de mestrado representa o culminar de uma etapa. Durante este percurso muitos foram os que ajudaram e contribuíram e aos quais não poderia deixar de agradecer.

Em primeiro lugar, quero deixar um agradecimento muito especial aos meus orientadores, Doutora Ana Cristina Pinheiro e Professor António Vicente, pela orientação, confiança, por todo o apoio e disponibilidade demonstrada.

À instituição de acolhimento, Centro de Engenharia Biológica (CEB) da Universidade do Minho pela disponibilização do espaço, equipamentos e recursos necessários à realização deste trabalho. Agradeço a todos os técnicos que de alguma forma colaboraram na elaboração deste trabalho, especialmente à Maura Guimarães.

Aos meus colegas do LIP agradeço por me terem recebido tão bem, pelo espírito de entreajuda e pelo excelente ambiente de trabalho que sem dúvida facilitaram imenso a realização deste trabalho. Agradeço em especial à Raquel pela ajuda ao longo da realização deste trabalho, por toda a paciência, amizade e disponibilidade demonstrada sempre que necessário.

Às amigas que a UM me deu, Bruna Dias, Bruna Freitas, Bruna Parente, Catarina Ferreira e Lúcia Roque, agradeço todo o apoio, motivação e amizade ao longo deste mestrado.

A todos os meus amigos, em especial à Ni agradeço a amizade, paciência interminável, motivação, apoio, disponibilidade e por me ter acompanhado sempre que precisava ao longo destes anos.

Um agradecimento muito especial ao Miguel por todo o amor, companheirismo, carinho, apoio, incentivo, paciência, motivação, otimismo e por transmitir-me sempre muita tranquilidade durante estes anos.

Finalmente, agradeço à minha família, em especial aos meus pais e irmão, tudo o que sempre fizeram por mim, todo o carinho, dedicação, paciência e amor.

## DECLARAÇÃO DE INTEGRIDADE

Declaro ter conduzido a elaboração da presente dissertação com integridade. Confirmando que em todo o trabalho conducente à sua elaboração não recorri à prática de plágio ou a qualquer forma de falsificação de resultados.

Mais declaro que tomei conhecimento integral do Código de Conduta de Ética da Universidade do Minho.

## RESUMO

O interesse crescente dos consumidores por alimentos mais saudáveis tem levado a indústria a desenvolver alimentos funcionais projetados especificamente para melhorar a saúde, o bem-estar e o desempenho de quem os consome. A curcumina é um polifenol natural que apresenta inúmeras atividades biológicas. No entanto, a curcumina tem baixa solubilidade em água, estabilidade química e biodisponibilidade. Podem utilizar-se sistemas de entrega nanoestruturados à base de lipídios para encapsular a curcumina. Neste estudo, desenvolveram-se nanopartículas lipídicas sólidas (SLNs) encapsulando a curcumina, incorporando-as posteriormente numa matriz alimentar à base de gelatina. As SLNs (antes e após a incorporação na gelatina) foram caracterizadas através do diâmetro médio, índice de polidispersão (PDI) e potencial zeta, por espalhamento dinâmico de luz (DLS). A gelatina e a gelatina-SLNs foram avaliadas quanto à cor, textura e reologia durante 21 dias de armazenamento. Realizou-se a digestão *in vitro* das SLNs e da gelatina-SLNs e mediu-se a bioacessibilidade, estabilidade e biodisponibilidade da curcumina. O grau de hidrólise (*DH*) da proteína e a produção de ácidos gordos livres da gelatina e da gelatina-SLNs foram avaliados nas fases gástrica e intestinal, respetivamente. Durante 21 dias, o diâmetro médio das SLNs manteve-se e o potencial zeta diminuiu ligeiramente. A incorporação das SLNs na gelatina não alterou significativamente o tamanho nem o PDI da partícula inicial. O potencial zeta das SLNs e da gelatina-SLNs é diferente devido ao facto de a gelatina ter carga superficial ligeiramente positiva. A diferença de cor total (TCD) da gelatina e da gelatina-SLNs permaneceu constante durante 21 e 14 dias de armazenamento, respetivamente. A adição das SLNs não levou a alterações nos parâmetros texturais da gelatina, contudo promoveram um comportamento mais sólido a esta matriz. O valor de *DH* da proteína na gelatina e na gelatina-SLNs foi de 47,8 % e 52,2 %, respetivamente. A produção total de ácidos gordos livres da gelatina-SLNs foi quase o dobro de SLNs. A bioacessibilidade e a biodisponibilidade da curcumina não foram estatisticamente diferentes entre as SLNs e gelatina-SLNs. No entanto, a estabilidade foi maior na amostra de gelatina-SLNs, sugerindo que esta matriz alimentar fornece um efeito protetor à curcumina. Finalmente, os resultados sugerem que as SLNs encapsulando a curcumina e incorporadas na matriz alimentar de gelatina constituem uma aplicação promissora para a indústria alimentar.

## PALAVRAS-CHAVE

Curcumina, digestão *in vitro*, gelatina, nanopartículas lipídicas sólidas, nanotecnologia

## ABSTRACT

The growing consumers' interest in healthier foods has led the food industry to develop functional foods specifically designed to improve human health, well-being, and performance. Curcumin is a natural polyphenol that presents numerous biological activities. However, curcumin has low water solubility, poor chemical stability, and low bioavailability. Lipid-based nanostructured delivery systems can be used to encapsulate curcumin. In this study, solid lipid nanoparticles (SLNs) encapsulating curcumin were developed and incorporated into a gelatine food matrix. SLNs (before and after incorporation in the gelatine) were characterized through mean diameter (Z-average diameter), polydispersity index (PDI) and zeta potential ( $\zeta$ -potential) by Dynamic light scattering (DLS). Gelatine and gelatine-SLNs were evaluated through colour, texture, and rheology during 21 days of storage. *In vitro* digestion of the SLNs and gelatine-SLNs was performed and curcumin bioaccessibility, stability, and bioavailability were measured. The degree of hydrolysis (*DH*) of proteins and the production of free fatty acids (FFA) of gelatine and gelatine-SLNs were evaluated at gastric and intestinal phases, respectively. During 21 days, the Z-average diameter of the SLNs was maintained and the  $\zeta$ -potential slightly decreased. The incorporation of the SLNs into gelatine did not significantly change neither the initial particle size nor PDI.  $\zeta$ -potential of SLNs and gelatine-SLNs is different and this is due to the fact that gelatine has a slightly positive surface charge. The total colour difference (TCD) of the gelatine and gelatine-SLNs remained constant during 21 and 14 days of storage, respectively. The addition of SLNs did not lead to changes in the textural parameters of the gelatine, however, they promoted more solid behaviour to this food matrix. The value of *DH* of proteins in the gelatine and gelatine-SLNs were 47.8 % and 52.2 %, respectively. The total production of FFA of gelatine-SLNs was almost double of that of SLNs. Curcumin bioaccessibility and bioavailability were not statistically different between SLNs and gelatine-SLNs. However, the stability was higher in the gelatine-SLNs sample, suggesting that this food matrix provides a protective effect to curcumin. Finally, these results suggest that SLNs encapsulating curcumin and their incorporation in the gelatine food matrix is a promising application for the food industry.

## KEYWORDS

Curcumin, gelatine, *in vitro* digestion, nanotechnology, solid-lipid nanoparticles



## LIST OF CONTENTS

DIREITOS DE AUTOR E CONDIÇÕES DE UTILIZAÇÃO DO TRABALHO POR TERCEIROS.....	II
AGRADECIMENTOS.....	III
DECLARAÇÃO DE INTEGRIDADE.....	IV
RESUMO.....	V
PALAVRAS-CHAVE.....	V
ABSTRACT.....	VI
KEYWORDS.....	VI
LIST OF CONTENTS.....	VII
LIST OF FIGURES.....	X
LIST OF TABLES.....	XIII
LIST OF GENERAL NOMENCLATURE.....	XIV
<b>1. MOTIVATION AND OBJECTIVES.....</b>	<b>15</b>
1.1. Thesis motivation.....	16
1.2. Research aims.....	17
1.3. Thesis outline.....	17
<b>2. LITERATURE REVIEW.....</b>	<b>18</b>
2.1. Food nanotechnology.....	19
2.2. Bioactive compounds and the need for encapsulation.....	20
2.2.1. Antimicrobials.....	21
2.2.2. Vitamins.....	21
2.2.3. Antioxidants.....	22
2.3. Formulation and design of nanostructured delivery systems.....	23
2.3.1. Encapsulation techniques.....	23
2.3.2. Bio-based materials.....	24
2.3.3. Nanostructured delivery systems.....	27
2.4. Characterization of nanostructured delivery systems.....	33
2.4.1. Physicochemical characterization techniques.....	33
2.4.2. Imaging techniques.....	34
2.5. Human gastrointestinal digestion.....	35

2.5.1. <i>In vitro</i> digestion models .....	37
2.6. Nanostructured delivery systems in food matrices .....	40
2.6.1. Food matrices .....	40
2.6.2. Nanostructured delivery systems incorporated into food matrices .....	41
2.6.3. Evaluation of food matrices .....	41
2.7. Application of nanostructured delivery systems in food industry .....	44
2.8. Toxicological aspects .....	44
<b>3. EXPERIMENTAL APPROACH .....</b>	<b>46</b>
3.1. Materials .....	47
3.2. Preparation of SLNs .....	47
3.3. Nanostructures characterization.....	47
3.3.1. Particle size .....	47
3.3.2. $\zeta$ -potential.....	48
3.3.3. Temperature stability .....	48
3.4. Incorporation of bio-based nanostructures in food matrices .....	48
3.5. Understanding the effects of bio-based nanostructures in food matrices' shelf-life .....	48
3.5.1. Colour evolution.....	49
3.5.2. Texture analysis.....	49
3.5.3. Rheology analysis .....	49
3.6. <i>In vitro</i> digestion.....	50
3.6.1. Digestion stock solutions.....	50
3.6.2. <i>In vitro</i> static digestion .....	50
3.6.3. Physicochemical characterization.....	51
3.6.4. Morphology .....	52
3.6.5. Evaluation of degree of hydrolysis of proteins by Lowry method .....	52
3.6.6. Evaluation of the release of free fatty acids.....	52
3.6.7. Curcumin bioaccessibility, stability and effective bioavailability .....	53
3.7. Statistical analyses .....	54
<b>4. RESULTS AND DISCUSSION .....</b>	<b>55</b>

4.1. Development of SLNs .....	56
4.2. Physicochemical characterization of SLNs.....	56
4.2.1. Particle size .....	56
4.2.2. Particle charge .....	58
4.2.3. Temperature stability .....	59
4.3. Incorporation of SLNs into gelatine .....	60
4.3.1. Physicochemical characterization.....	61
4.4. Evaluation the effects of SLNs incorporation in gelatine shelf life.....	62
4.4.1. Colour evolution.....	62
4.4.2. Texture evolution .....	64
4.4.3. Rheology evolution.....	65
4.5. <i>In vitro</i> digestion behaviour of gelatine with SLNs incorporated .....	66
4.5.1. Influence of digestion on particle size .....	67
4.5.2. Influence of digestion on particle charge.....	69
4.5.3. Influence of digestion on morphology .....	70
4.5.4. Evaluation of protein hydrolysis .....	71
4.5.5. Evaluation of release of free fatty acids.....	72
4.5.6. Curcumin bioaccessibility, stability and bioavailability .....	74
<b>5. CONCLUSIONS AND FUTURE REMARKS.....</b>	<b>77</b>
5.1. Conclusions .....	78
5.2. Future recommendations.....	78
<b>6. REFERENCES.....</b>	<b>80</b>
<b>7. ANNEXES.....</b>	<b>92</b>
Annex I – Evolution of the colour parameters of the gelatine and gelatine-SLNs.....	93
Annex II – Frequency sweep test.....	94
Annex III – Storage and loss modulus of the rheological analysis .....	95
Annex IV – Folin-BSA calibration curve .....	95
Annex V – Curcumin-chloroform calibration curve.....	96

## LIST OF FIGURES

<b>Figure 1.</b> Food applications of the nanostructures in the food industry. Adapted from (Paredes <i>et al.</i> , 2016; Singh <i>et al.</i> , 2017). .....	19
<b>Figure 2.</b> Chemical structure of curcumin.....	23
<b>Figure 3.</b> Bio-based nanostructured delivery systems that may be used for encapsulation of bioactive compounds for food applications. Adapted from (Souza Simões <i>et al.</i> , 2017).....	28
<b>Figure 4.</b> Physiological and physicochemical conditions present in the human digestive system (adapted from (Martins <i>et al.</i> , 2015; Gonçalves <i>et al.</i> , 2018)). .....	36
<b>Figure 5.</b> Schematic representation of pH-stat in vitro digestion model used to determine the digestion and release of nutrients. Adapted from (Li and McClements, 2010).....	38
<b>Figure 6.</b> Schematic representation of modified TNO gastric-small Intestinal Model (TIM-1) (Villemejane <i>et al.</i> , 2016). .....	39
<b>Figure 7.</b> Example of TPA curve with typical parameters. Adapted from (Kohyama, 2020). .....	43
<b>Figure 8.</b> Visual appearance of the developed SLNs.....	56
<b>Figure 9.</b> Evolution of Z-average diameter of the SLNs during 21 days of storage at 4 °C in the dark. The results are presented as the mean ± SD. ....	57
<b>Figure 10.</b> Evolution of PDI of the SLNs during 21 days of storage at 4 °C in the dark. The results are presented as the mean ± SD. ....	57
<b>Figure 11.</b> Changes of ζ-potential of SLNs during 21 days of storage at 4 °C in the dark. The results are presented as the mean ± SD. Different letters (a-c) indicate statistically significant between values ( $p < 0.05$ ). .....	58
<b>Figure 12.</b> Effect of temperature on the Z-average diameter of the SLNs. The results are presented as the mean ± SD.....	59
<b>Figure 13.</b> Effect of temperature on the PDI of the SLNs. The results are presented as the mean ± SD. ....	60
<b>Figure 14.</b> Visual appearance of gelatine (A) and gelatine-SLNs (B). .....	61
<b>Figure 15.</b> Z-average diameter of the SLNs and gelatine-SLNs. The results are presented as the mean ± SD.....	61
<b>Figure 16.</b> PDI of the SLNs and gelatine-SLNs. The results are presented as the mean ± SD. ....	62
<b>Figure 17.</b> ζ-potential of gelatine, SLNs, and gelatine-SLNs. The results are presented as the mean ± SD. Different letters (a-b) indicate statistically significant between values ( $p < 0.05$ ). .....	62

**Figure 18.** Evolution of TCD/ $\Delta E$  of gelatine and gelatine-SLNs during 21 days of storage at 4 °C in the dark. \* significantly different from correspondent values in gelatine from same day ( $p < 0.05$ ). ..... 63

**Figure 19.** Force-time curve obtained from TPA test of gelatine (A) and gelatine-SLNs (B) over 21 days of storage at 4 °C in the dark. The results are presented as the mean. .... 64

**Figure 20.** Complex viscosity ( $\eta^*$ ) versus time curve obtained from gelatine (A) and gelatine-SLNs (B) over 21 days of storage at 4 °C in the dark. The results are presented as the mean..... 66

**Figure 21.** Z-average diameter of SLNs and gelatine-SLNs as they undergo the different stages of *in vitro* digestion. The results are presented as the mean  $\pm$  SD. \*significantly different from correspondent values in SLNs in the same phase ( $p < 0.05$ ). Different letters (a-c) indicate statistically significant between values from same sample during different phases ( $p < 0.05$ ). ..... 67

**Figure 22.** PDI of SLNs and gelatine-SLNs as they undergo the different stages of *in vitro* digestion. The results are presented as the mean  $\pm$  SD. \*significantly different from correspondent values in SLNs in the same phase ( $p < 0.05$ ). Different letters (a-d) indicate statistically significant between values from same sample during different phases ( $p < 0.05$ )..... 68

**Figure 23.**  $\zeta$ -potential of SLNs and gelatine-SLNs as they undergo the different stages of *in vitro* digestion. The results are presented as the mean  $\pm$  SD. \*significantly different from correspondent values in SLNs in the same phase ( $p < 0.05$ ). Different letters (a-c) indicate statistically significant between values from same sample during different phases ( $p < 0.05$ ). ..... 70

**Figure 24.** Microscopy images of the SLNs and gelatine-SLNs as they undergo the different stages of the simulated *in vitro* digestion. .... 71

**Figure 25.** DH (%) during the protein hydrolysis in the simulated gastric digestion of the gelatine and gelatine-SLNs. .... 72

**Figure 26.** Total production of FFA after the simulated intestinal digestion of the gelatine, gelatine-SLNs, and SLNs. Different letters (a-b) indicate statistically significant between values ( $p < 0.05$ )..... 73

**Figure 27.** Bioaccessibility (%), stability (%), and bioavailability (%) of curcumin after *in vitro* digestion of SLNs and gelatine-SLNs. The results are presented as the mean  $\pm$  SD. \*significantly different from correspondent values in SLNs ( $p < 0.05$ ). ..... 75

**Figure A. 1.** Evolution of colour parameter  $L^*$  of the gelatine and gelatine-SLNs, during 21 days of storage at 4 °C in the dark. .... 93

**Figure A. 2.** Evolution of colour parameter  $a^*$  of the gelatine and gelatine-SLNs, during 21 days of storage at 4 °C in the dark. .... 93

<b>Figure A. 3.</b> Evolution of colour parameter $b^*$ of the gelatine and gelatine-SLNs, during 21 days of storage at 4 °C in the dark. ....	94
<b>Figure A. 4.</b> Frequency sweep test of the gelatine control.....	94
<b>Figure A. 5.</b> Storage modulus ( $G'$ ) and loss modulus ( $G''$ ) obtained from gelatine (A) and gelatine-SLNs (B) over 21 days of storage at 4°C in the dark. The results are presented as the mean.....	95
<b>Figure A. 6.</b> Folin-BSA calibration curve.....	95
<b>Figure A. 7.</b> Curcumin-chloroform calibration curve. ....	96

## LIST OF TABLES

<b>Table 1.</b> Main nanoencapsulation techniques and their advantages and limitations. ....	24
<b>Table 2.</b> Definition of some texture parameters that can be obtained from the force-time curve of the TPA test. ....	44
<b>Table 3.</b> Textural parameters obtained from the force-time curve from TPA test of gelatine and gelatine-SLNs over 21 days of storage at 4 °C in the dark. The results are presented as the mean $\pm$ SD.....	65

## LIST OF GENERAL NOMENCLATURE

CLSM	Confocal laser scanning microscopy
DH	Degree of hydrolysis
DLS	Dynamic light scattering
DSC	Differential Scanning Calorimetry
FFA	Free fatty acids
FTIR	Fourier transformed infrared spectroscopy
GI	Gastrointestinal
GRAS	Generally recognized as safe
MAG	Monoacylglycerol
NLCs	Nanostructured lipid carriers
PDI	Polydispersity index
SEM	Scanning electron microscopy
SGF	Simulated gastric fluid
SIF	Simulated intestinal fluid
SLNs	Solid lipid nanoparticles
SSF	Simulated salivary fluid
TAG	Triacylglycerol
TCD	Total colour difference
TEM	Transmission electron microscopy
TPA	Texture profile analysis
$\zeta$ -potential	Zeta potential



# CHAPTER 1

---

## MOTIVATION AND OBJECTIVES

### 1.1. Thesis motivation

The growing consumers' interest in healthier foods has led the food industry to develop new products with certain characteristics and new functionalities. Bioactive compounds are molecules that provide several benefits to human health, however their incorporation in food products is a major technological challenge. Many bioactive compounds are lipophilic (e.g. curcumin,  $\omega$ -3 fatty acids, lycopene, phytosterols, quercetin) and their utilization by food industry is limited due to their low bioavailability and difficulties associated with their incorporation into food matrices (McClements and Xiao, 2012). Curcumin is a natural polyphenol phytochemical extracted from the powdered rhizomes of turmeric (*Curcuma longa*) (Wang *et al.*, 2008). Curcumin has been the subject of much attention in recent years due to its great beneficial biological and pharmacological activities, such as anticancer, antioxidant, antimicrobial, and anti-inflammatory properties. However, curcumin is a strongly hydrophobic molecule with low water solubility, which hinders its incorporation into food products and has low bioavailability, which means that its beneficial properties may not be perceived when ingested (Ahmed *et al.*, 2012a). Many approaches have been taken into consideration to increase the chemical stability of curcumin in food matrices and in the gastrointestinal (GI) tract and to improve its oral bioavailability.

The creation of new encapsulation methodologies using nanotechnology allows the protection and release of bioactive compounds with several advantages when compared to microencapsulation, and the development of functional food products without affecting their quality is one of the researchers' focuses (Silva *et al.*, 2012; Cerqueira *et al.*, 2014). Several delivery nanostructured delivery systems have been developed for controlled release of bioactive compounds intended for food applications, namely, nanocapsules, nanohydrogels, and lipid-based systems. This technology has enormous potential for the development of delivery systems that allows the protection of bioactive compounds during food processing and/or digestion. Lipid-based nanosystems can be used in food and beverage industry to encapsulate lipophilic compounds, allowing the preservation of their unique properties, releasing them in the desired target and, simultaneously, preserving the organoleptic and nutritional properties of food products (Plaza-Oliver *et al.*, 2015). The first generation of lipid-based nanosystems was obtained using a lipid matrix composed of only solid lipids (saturated fatty acids), called solid lipid nanoparticles (SLNs). The SLN structure allows the incorporation of different types of bioactive lipophilic compounds, which are protected against degradative processes by the lipid matrix (Silva Santos *et al.*, 2019). SLNs present many advantages for lipophilic bioactive components such as curcumin, including improved stability and bioavailability, gradual release, and higher dispersibility in aqueous-based foods (Rafiee *et al.*, 2019).

Despite of the major advantages of nanostructured delivery systems for food applications, there are significant challenges that must be faced for the implementation of nanotechnology in the food sector. These main challenges are the need to produce edible delivery systems and the need to formulate them to be effective and safe for human consumption (McClements and Xiao, 2012). The first issue can be solved by producing nanostructured delivery systems entirely from food-grade ingredients using simple and economic methods and the second issue relates to the study of the behaviour of nanostructured delivery systems when subjected to physical-chemical and physiological processes that occur in the human GI tract using *in vivo*, or at least *in vitro* models (Pineiro *et al.*, 2016) . Also, the evaluation of the behaviour of bio-based nanostructured delivery systems, once incorporated into food matrices, is still a challenge due to the lack of standardized methodologies/techniques for the identification and characterization of nanostructured delivery systems in complex matrices.

The great potential of nanotechnology for the creation of new and healthier foods and the need to understand its behaviour under GI conditions, when encapsulating bioactive compounds and also incorporated in a food matrix were the main motivations for the development of this thesis.

## 1.2. Research aims

The main purpose of this thesis was the development of SLNs encapsulating curcumin and their incorporation into a food matrix. The specific aims of this work were:

- Production of SLNs encapsulating curcumin;
- Physicochemical characterization of developed SLNs;
- Evaluation of the stability of SLNs;
- Evaluation of the effects of SLNs in food matrix shelf life;
- Evaluation of the behaviour of food matrix with SLNs incorporated during *in vitro* digestion.

## 1.3. Thesis outline

This thesis was organized in a total of six chapters. Chapter 1 provides the thesis' motivation, research aims and outline of this thesis. Chapter 2 provides an overview on the state-of-art of nanotechnology applied to the food sector. Chapter 3 reports the list of all chemicals used in this work as well the experimental approach. The results obtained and further discussion are presented in Chapter 4. Chapter 5 outlines the main conclusions of this work and recommendations for future work. Chapter 6 provides the literature references.

# CHAPTER 2

---

## LITERATURE REVIEW

## 2.1. Food nanotechnology

The increase in population and in the consumers' demand for healthier products has led the food industry to pay more attention to processes such as production, preservation, safety, and sustainability of its products in order to provide consumers with high-quality, abundant products (Singh *et al.*, 2017). The application of nanotechnology in the food sector may represent a solution that allows developing products with desired characteristics and new functionalities (Neethirajan and Jayas, 2011). Nanotechnology refers to the manipulation of matter at atomic, molecular, or macromolecular scales with at least one dimension that ranges from 1 to 100 nm in length (Duncan, 2011). In the food industry, nanotechnology is mostly applied to packaging, antimicrobials, and encapsulation of food components (**Figure 1**). The importance of nanotechnology in food processing can be assessed considering its role in improving food products in terms of (i) food texture, (ii) food appearance, (iii) food taste, (iv) nutritional value of the food, and (v) the shelf life of the food (Singh *et al.*, 2017). In addition, when applied to food products, nanomaterials can prevent undesirable physical and chemical reactions, improve the solubility and bioavailability of functional compounds, and protect food against degradation (Singh *et al.*, 2017; Souza Simões *et al.*, 2017).

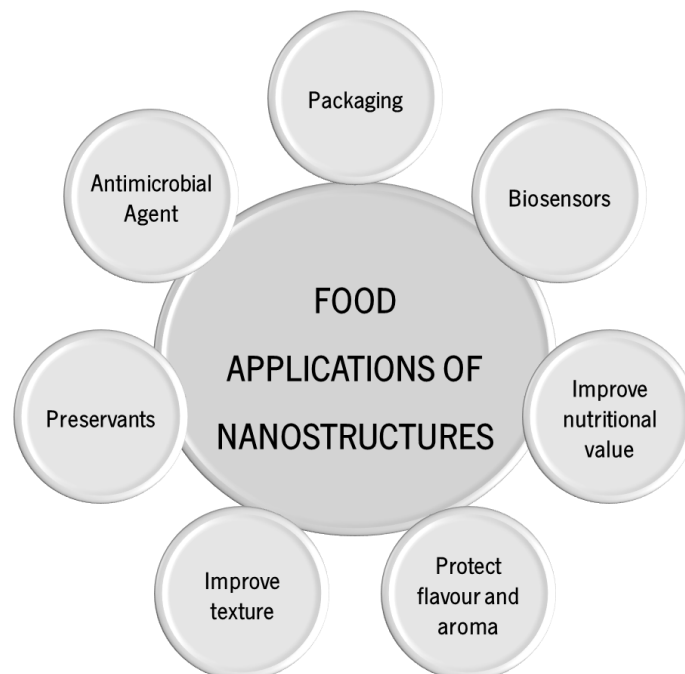


**Figure 1.** Food applications of the nanostructures in the food industry. Adapted from (Paredes *et al.*, 2016; Singh *et al.*, 2017).

The use of nanomaterials can be classified as direct or indirect. Direct use refers to the incorporation of nanostructured substances in foods, such as fragrances, coloring agents, antioxidants, and biological active components. Indirect use includes the application of the nanostructures in packaging technology and nanosensors (Pathakoti *et al.*, 2017).

In recent years, nanotechnology has shown immense potential, particularly in the development of new delivery systems that allow the protection of bioactive compounds during processing and/or digestion, and new features such as increased bioavailability and controlled delivery at specific locations (Cerqueira *et al.*, 2014). However, there are many challenges to be overcome, especially the formulation of safe products for human consumption (Pathakoti *et al.*, 2017).

## 2.2. Bioactive compounds and the need for encapsulation

Bioactive compounds are molecules that provide several benefits to human health by preventing or retarding the appearance of diseases through e.g., antioxidant, anti-inflammatory, or anticancer activities. Thus, bioactive compounds' properties should be preserved until the exact moment and specific site where they will be used (Souza Simões *et al.*, 2017). Since they are not synthesized by the human body, bioactive compounds need to be incorporated into our daily diet, as they are involved in several biological processes. In this way, the food industry has been using and incorporating these bioactive compounds in foodstuff. However, most of bioactive compounds are lipophilic and have limitations such as low water solubility, stability, and bioavailability, which can compromise the success of their incorporation in foods and their functionality (Gasa-Falcon *et al.*, 2020). Nanoencapsulation is a favorable alternative to facilitate the delivery of these poorly bioavailable compounds by increasing their absorption into cellular structures through favorable particle properties such as shape, size, and surface. This approach allows to increase bioactive compounds' potential solubilization, alter absorption pathways by modifying the rate and site of release, influence GI dispersion, and prevent bioactive compounds' premature metabolic degradation (Bazana *et al.*, 2019). The protection of bioactive compounds, such as vitamins, antioxidants, proteins, lipids, and carbohydrates may be achieved using this technique to produce functional foods with enhanced functionality and stability (Sekhon, 2010). Nanoencapsulation can bring several advantages, such as increase bioactives' efficiency, biodegradability, low toxicity, improvement of oral absorption, and controlled/sustainable release, but can also improve their stability under certain environments, such as heat, extreme pH, and GI fluids. Thus, delivery of bioactive compound through the GI tract is guaranteed and, consequently, their bioavailability and functionality are enhanced (Pinheiro *et al.*, 2017; Gasa-Falcon *et al.*, 2020).

### 2.2.1. Antimicrobials

Antimicrobial compounds play an important role in preventing or inhibiting the growth of microorganisms, such as bacteria and yeasts (Shah *et al.*, 2017). Among all antimicrobial compounds, enzymes, polysaccharides, and more recently, herbs, spices, essential oils, alcohols, ketones, phenols, acids, aldehydes, and esters have been commonly used for controlling the microbial growth (Tajkarimi *et al.*, 2010; Quirós-Sauceda *et al.*, 2014). The incorporation of these compounds as food additives increases the safety and shelf life of food (Quirós-Sauceda *et al.*, 2014). Food industry has shown an increasing interest in the use of essential oils since these are natural compounds obtained from plant extracts and demonstrate antimicrobial activity as well as a wide range of health benefits without known toxicity or side effects. However, its low solubility in water, high volatility and reactivity, and unpleasant aroma offer limitations for their use in food products (Souza Simões *et al.*, 2017). In this way, antimicrobials may be encapsulated to improve their compatibility with the food matrix, to enhance their efficacy, to improve release profile, to mask off-flavors, and/or improve their storage stability, transportation, and utilization (Shah *et al.*, 2017).

### 2.2.2. Vitamins

Vitamins are important organic compounds for the proper functioning of biological processes (Shah *et al.*, 2017). These are classified as water-soluble or fat-soluble. Water-soluble compounds include vitamins from the B complex (B1, B2, B3, B5, B6, and B12) and vitamin C (ascorbic acid) and fat-soluble compounds include vitamins A, D, E and K (Panigrahi *et al.*, 2019). Water-soluble vitamins are normally lost due to leaching in operations such as washing, bleaching, and cooking (Assadpour and Mahdi Jafari, 2019). Since the human body cannot produce vitamins (except vitamins D and B3), they must be obtained naturally from food or added to it (Shah *et al.*, 2017; Souza Simões *et al.*, 2017). When adding vitamins to foods it is important to pay attention to their stability, as these compounds are susceptible to degradation during processing, storage, and absorption in the GI tract due to several factors, such as exposure to light, oxygen, temperature, pH (Shah *et al.*, 2017; Souza Simões *et al.*, 2017; Ruiz Canizales *et al.*, 2019). Nutritional deficiencies in the uptake of vitamins can be caused by inadequate intake or use, malabsorption, increased excretion or destruction in the body or even due to increased needs, which can lead to the development of certain diseases, for example, cancer and diseases cardiovascular diseases (Souza Simões *et al.*, 2017). Vitamins are sensitive to many factors, such as high temperature, pH, and light, they may need to be encapsulated to ensure their stability. The encapsulation of vitamins

allows its incorporation in an aqueous medium, improves its ease of use, and prevents chemical degradation (Shah *et al.*, 2017).

### 2.2.3. Antioxidants

Free radicals and other reactive oxygen species (ROS) are products from normal cellular metabolic processes in the human body or from external sources such as exposure to X-rays, cigarette smoking, air pollutants, and industrial chemicals. It has been suggested that the oxidation of biomolecules is involved in several disorders, including cancer, cardiovascular disease, atherosclerosis, inflammatory condition and the process of aging (Mozafari *et al.*, 2006). Oxidation reactions are the main deterioration processes of fats, oils and lipid-based foods which result in decreased nutritional value and sensory quality.

Antioxidants can be enzymatic and non-enzymatic and can be obtained from natural sources such as vegetables, fruits, leaves, oilseeds, cereals and herbs, and play an important role in providing protection from free radicals and nitrogen species (Souza Simões *et al.*, 2017; Assadpour and Mahdi Jafari, 2019). Phytochemicals are plant-derived compounds, including polyphenols, flavonoids, isoflavones, resveratrol, and carotenoids that have high antioxidant and anti-inflammatory activity. Antioxidants such as vitamin E (tocopherols), vitamin C (ascorbic acid), carotenoids and phenolic compounds are often added to food products to protect the nutritional and sensory quality of food, eventually being introduced into the human body (Mozafari *et al.*, 2006). Antioxidants are often encapsulated to improve handling and use, to improve compatibility with the food matrix, and to prevent chemical degradation (Shah *et al.*, 2017). In many cases, phytochemicals are encapsulated to avoid unwanted sensory properties (for example, undesirable flavors and smells) in food products, allowing their use in higher concentrations without causing adverse effects to consumers (Mozafari *et al.*, 2006). Another example is the case of  $\beta$ -carotene which is sensitive to light and oxygen and can be encapsulated to inhibit its oxidation by limiting its exposure to light and oxygen (Shah *et al.*, 2017).

#### 2.2.3.1. Curcumin

Curcumin is a natural polyphenol phytochemical extracted from the powdered rhizomes of turmeric (*Curcuma longa*) (Wang *et al.*, 2008). Curcumin has three chemical entities in its structure: two aromatic ring systems containing o-methoxy phenolic groups, connected by a seven carbon linker consisting of an  $\alpha,\beta$  unsaturated  $\beta$ -diketone moiety (**Figure 2**) (Priyadarsini, 2014).



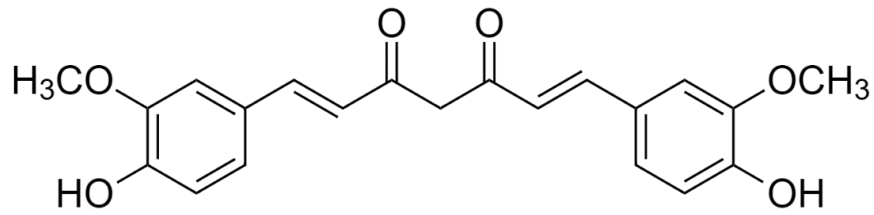


**Figure 2.** Chemical structure of curcumin.

Curcumin (E100) is used as natural colorant serving as an alternative to some artificial colorants. In the last years, curcumin has received an increased interest by the scientific community because it possesses significant beneficial biological and pharmacological activities, such as anticancer, antioxidant, antimicrobial, and anti-inflammatory properties. However, curcumin is a strongly hydrophobic molecule with low water solubility ( $11 \text{ ng}\cdot\text{mL}^{-1}$ ), which hinders its incorporation into food products and has low bioavailability, which means that its beneficial properties may not be perceived when ingested (Ahmed *et al.*, 2012a). Many approaches have been taken into consideration to increase the chemical stability of curcumin in food matrices and in the gastrointestinal (GI) tract and to improve its oral bioavailability. One of these approaches is the curcumin encapsulation in nanostructured delivery systems.

### 2.3. Formulation and design of nanostructured delivery systems

Encapsulation is a technique with potential applications in the pharmaceutical and food industries (Risch, 1995). This method allows protecting bioactive compounds (e.g. polyphenols, antioxidants, vitamins, and nutraceuticals) against deterioration (e.g. oxidation) during production and storage (Peters *et al.*, 2011). Furthermore, nanoencapsulation has the ability to increase bioavailability, control the bioactive compounds release, and allow targeted site-specific delivery (Ezhilarasi *et al.*, 2013; Souza Simões *et al.*, 2017).

#### 2.3.1. Encapsulation techniques

Nanoencapsulation techniques use either top-down or bottom-up approaches to produce nanostructured delivery systems. The top-down approach involves physical processing of the materials, which requires the application of precise tools that allow size reduction and modeling of the structure for the desired application of the nanomaterials that are being developed. The bottom-up approach presents more control over the properties of the structure since the materials are constructed by self-assembly and self-organization of molecules, which are influenced by factors such as pH, temperature, concentration, and

ionic strength. Both techniques have been optimized to achieve the desired properties for distinct food applications (Ezhilarasi *et al.*, 2013). The most important nanoencapsulation techniques and their main advantages and limitations are summarized in **Table 1**.

**Table 1.** Main nanoencapsulation techniques and their advantages and limitations.

Nanoencapsulation technique	Advantages	Limitations	References
<b>Freeze drying</b>	Remove water from nanocapsules without changing its structure and shape	Expensive, requires a long time of dehydration and cryoprotectants to conserve the particle size and to avoid aggregation	(Ezhilarasi <i>et al.</i> , 2013; Souza Simões <i>et al.</i> , 2017)
<b>Spray drying</b>	Simple, low cost, high-quality particle size with good yield, fast solubility, and good stability	Encapsulation of volatile or thermosensitive bioactive compounds	
<b>Coacervation</b>	Does not require high temperature, high core loading level, the structures formed are water immiscible	Commercializing the coacervated food ingredient due to the use of glutaraldehyde for cross-linking	(Ezhilarasi <i>et al.</i> , 2013; Khare and Vasisht, 2014; Souza Simões <i>et al.</i> , 2017)
<b>Fluid bed coating</b>	Low energy consumption, good reproducibility, reduced operating time and cost	High temperatures and direct exposure to hot air may limit application to highly sensitive compounds	(Souza Simões <i>et al.</i> , 2017)
<b>High-pressure homogenization</b>	Easy scale up, great efficiency, short production and avoids the use of organic solvents.	Requires high energy	(Borthakur <i>et al.</i> , 2016)

### 2.3.2. Bio-based materials

Nanostructured delivery systems can be produced from natural and synthetic polymers, but they must be food-grade and GRAS (generally recognized as safe), to be used for encapsulation of food bioactive materials. Bio-based nanostructured delivery systems can be produced from a wide variety of natural materials, such as polysaccharides, proteins, and lipids (Ruiz Canizales *et al.*, 2019). The selection of the bio-based material mainly depends on the nanoencapsulation method, physicochemical properties of the food matrix as well as on the bioactive compound to be incorporated. However, there are other factors

that must be considered when choosing the encapsulating material, such as the stability and behaviour of the delivery system within the food matrix during processing and storage, as well as the release profile of the bioactive compound during the digestion process. Thus, the composition of the nanostructured delivery systems is the main responsible for the functional properties that it will exhibit either within food or in the GI tract (Rashidinejad and Jafari, 2020).

#### 2.3.2.1. Polysaccharides

Polysaccharides are polymeric carbohydrate molecules composed of monosaccharides units linked by glycosidic linkages. Polysaccharides can be obtained from natural sources, mostly through low-cost processing procedures. These polymers possess several important properties such as good stability, non-toxicity, biodegradability, and bioadhesivity that allow their use as delivery systems (Souza Simões *et al.*, 2017). According to their biological origin, polysaccharides-based delivery systems are organized into four categories: plant-based (e.g., pectin, starch, gums, and cellulose); animal-based (e.g., chitosan); algae-based (e.g., alginate and carrageenan); and microbial-based (e.g., dextran and xanthan gum). The most used bio-based polysaccharides in the manufacture of delivery systems include chitosan, alginate, carrageenan, and various gums (Rashidinejad and Jafari, 2020).

#### 2.3.2.2. Proteins

Proteins are polymers formed by a sequence of amino acids linked by peptide bonds. There are 20 different amino acids that can be classified as aliphatic, aromatic, charged (positive or negative), or polar. Proteins can adopt different structures (e.g., random coil, fibrous or globular shapes), which depend on their amino acid sequence, environmental conditions, and environmental history (Matalanis *et al.*, 2011). The type, number, and particular sequence of amino acids in a polypeptide chain determine the molecular weight, conformation, electrical charge, hydrophobicity, physical interactions, and functionalities of proteins. Several factors must be considered when selecting a suitable protein or combination of proteins to fabricate delivery systems. This usually requires knowledge of physicochemical characteristics of the proteins involved, such as denaturation temperature, isoelectric point, and chemical degradation reactions (Jones and McClements, 2010). Proteins exhibit unique functional properties, including emulsification, gelation, foaming, and water-binding capacity. Gelling is particularly important for the manufacture of distribution systems. This process generally comprises two main stages: the partial unfolding (denaturation) of the native globular structure and the intermolecular aggregation of the protein

structure (Souza Simões *et al.*, 2017). The most used proteins in the production of bio-based delivery systems include  $\beta$ -lactoglobulin, lactoferrin, sodium caseinate, and zein (Gonçalves *et al.*, 2018).

#### 2.3.2.3. Lipids

Lipids are often referred as fats (solid form) or oils (liquid form), depending on their physical state at room temperature (Souza Simões *et al.*, 2017). Fats and oils are classified as polar (e.g., phospholipids and monoglycerides) or nonpolar lipids (e.g., triacylglycerol and cholesterol). The microstructural and rheological characteristics and colloidal stability are factors controlled by the physicochemical properties of the lipids. For example, the melting point and moisture barrier properties of lipids can be affected by decreasing the length of its hydrocarbon chain attached to the glycerol structure, or by increasing the degree of unsaturation of the fatty acid chains. Lipid-based delivery systems are widely applied in the food industry owing to their many advantages, such as stability during process and storage, high encapsulation efficiency, and controlled and targeted release of the bioactive compound (Rashidinejad and Jafari, 2020). Some examples of lipids used in the production of the bio-based delivery systems include waxes, oils, sterols, monoglycerides, diglycerides, and triglycerides (Attama *et al.*, 2012). Beeswax is a natural wax often used for the formulation of these structures. It is commercially available and is approved as GRAS for direct application in foods, in addition of being characterized by high stability against oxidation processes (Bernal *et al.*, 2005; Silva Santos *et al.*, 2019). Phospholipids are a class of polar lipids that are essential for human health and the main constituents of cellular membranes (Souza Simões *et al.*, 2017). They are biocompatible and suitable for the protection, stabilization, and controlled release of food bioactive compounds. Thus, these components possess natural properties that allow to encapsulate both hydrophobic and hydrophilic bioactive compounds (Rashidinejad and Jafari, 2020). Phospholipids are widely distributed in animals and plants, and the main sources include vegetable oils (e.g., soybean, cotton seed, corn, sunflower, and rapeseed) and animal tissues (e.g., egg yolk and bovine brain). In terms of production, egg yolk and soybean are the most important sources for phospholipids. Phospholipids can be classified as natural or synthetic, according to their source. The term "lecithin" was first used to describe a sticky orange material isolated from the egg yolk (Li *et al.*, 2015). Lecithin is a mixture of choline, choline esters, fatty acids, glycerol, glycolipids, triglycerides, phosphoric acid, and phospholipids, such as phosphatidylcholine. Lecithin is considered to be GRAS by the U.S. Food and Drug Administration (Drugs and Lactation Database (LactMed), 2006).

### 2.3.3. Nanostructured delivery systems

Nanostructured delivery systems can be crystalline or amorphous solids at room temperature, can be spherical or non-spherical, have different surface characteristics and have different sizes, depending on the starting materials and the preparation conditions used in their manufacture (McClements and Xiao, 2017). Nanostructured delivery systems are produced mainly using naturally occurring substances such as lipids, proteins, and/or polysaccharides. These particles tend to be liquid, semi-solid (gelled) or solid (crystalline or amorphous) at room temperature, depending on their composition and processing conditions. Most of the organic nanostructured delivery systems used in food field are spherical, however, in some circumstances they may not have this shape (McClements and Xiao, 2017). These nanostructured delivery systems present a huge potential to provide new functionality to food and are widely applied to increase the absorption and bioavailability of compounds, such as antioxidants and vitamins (Sekhon, 2010; Pan and Zhong, 2016).

There are a few attributes that a delivery system must have to be suitable for application in the food industry (McClements *et al.*, 2007; McClements and Li, 2010a). Some of the most important functional and technical characteristics are described below:

- Food grade: The delivery system must be manufactured entirely from food ingredients, using production operations that have regulatory approval.
- Economic production: The delivery system should be economically produced using inexpensive ingredients.
- Protection from chemical degradation: The delivery system may have to protect an encapsulated bioactive compound against some form of chemical degradation (e.g., oxidation, hydrolysis, etc.).
- Loading capacity (LC): a delivery system should be capable of encapsulating a relatively large amount of bioactive compound per unit mass of carrier material ( $LC=ME/MC$ ).
- Delivery mechanism: The delivery system may have to be designed so that it releases the bioactive compound at the required site-of-action. The release may have to be a controlled release or in response to a specific environmental stimulus (e.g., pH, ionic strength, temperature, or enzyme activity).
- Food matrix compatibility: The delivery system should be compatible with the surrounding food matrix, that is, it should not adversely affect the appearance, texture, flavor, or stability of the final product.

- Bioavailability: A delivery system should enhance or at least not adversely affect the bioavailability (defined as the fraction of an ingested compound that is absorbed and available for physiological functions (i.e., reaches the systemic circulation in an active form) (Gonçalves *et al.*, 2018).

Different bio-based nanostructured delivery systems have been described in the literature and they present different sizes, structures, compositions, physicochemical properties, and may offer numerous functionalities [5]. A selected group of bio-based nanostructured systems that have been most used as delivery systems are described below (**Figure 3**).

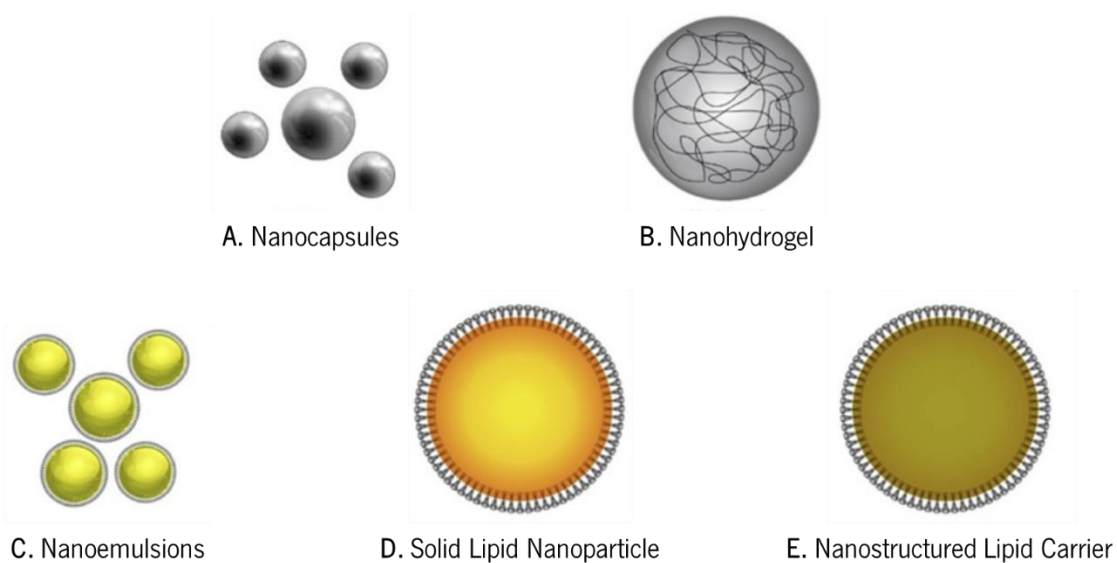


**Figure 3.** Bio-based nanostructured delivery systems that may be used for encapsulation of bioactive compounds for food applications. Adapted from (Souza Simões *et al.*, 2017).

#### 2.3.3.1. Nanocapsules

Nanocapsules (**Figure 3A**) are widely studied delivery systems for encapsulating bioactive compounds and consist of hollow vesicular structures that can entrap bioactive compounds by surrounding them with a biopolymer membrane, protecting from external environmental conditions. Nanocapsules can be easily produced from synthetic or natural compounds with different techniques whereas the most used is coacervation. These structures exhibit high stability during storage as well as in biological fluids, and significantly improve the stability of the bioactive compounds they incorporate. In addition, these systems allow the controlled release of bioactive compounds through complete disintegration of their structure or altering their porosity in response to external stimuli such as changes in ionic strength, pH or temperature (Souza Simões *et al.*, 2017). However, they must be biocompatible and biodegradable to be used in food systems (Jafari *et al.*, 2015). Granata *et al.*, 2018 studied the encapsulation of essential oils in polymer-

based nanocapsules to enhance their antimicrobial activity against food-borne pathogens. The results showed that the antimicrobial activity of essential oils encapsulated in nanocapsules (EO-NCs) was higher than the pure essential oils. Furthermore, EO-NCs showed a bactericidal activity even at the minimum inhibitory concentration, which makes them attractive as natural food preservatives.

#### 2.3.3.2. Nanohydrogels

Nanohydrogels (**Figure 3B**) are a three-dimensional hydrophilic or amphiphilic nanosized biopolymers that can associate to each other by forming covalent or non-covalent interactions (Martins *et al.*, 2015). In the presence of water, this structure has the capacity to swell about 30 times their initial size and hold a large amount of water while maintaining the structure (Souza Simões *et al.*, 2017). Furthermore, they are prevented from dissolving due to their chemically or physically cross-linked structure (Martins *et al.*, 2015). Bio-based nanohydrogels can be prepared from several materials using different strategies and the most common method includes gelation processes (Ramos *et al.*, 2017). Their reduced size enables a controlled release of bioactive compounds and improves the bioavailability of those compounds with poor absorption rates. Additionally, these structures have the ability to produce a response (e.g., swelling) to environmental stimuli (e.g. temperature, pH, ionic strength or enzymatic conditions), making them important systems for the delivery of bioactive compounds at specific sites and at a particular time in the GI tract (Liu and Urban, 2010; Martins *et al.*, 2015). One of the challenges of these nanostructured delivery systems is to provide components encapsulated at the desired point (e.g., stomach) without being destroyed under physiological conditions in the GI tract (Martins *et al.*, 2015). Thus, the use of hydrogels in the food industry is limited by their low mechanical resistance and rapid dissolution (Batista *et al.*, 2019). Guo *et al.*, 2017 developed and characterized  $\beta$ -lactoglobulin nanoparticles and studied their binding to caffeine. The authors observed that  $\beta$ -lactoglobulin nanohydrogels exhibited rapid peptic degradation but only 36.4% of entrapped caffeine was release under gastric conditions and total release was achieved at intestinal conditions. Bourbon *et al.*, 2016a encapsulated curcumin and caffeine in lactoferrin-glycomacropptide nanohydrogels and their ability to encapsulate and release both lipophilic and hydrophilic compounds was evaluated. The results showed that nanohydrogels are capable to encapsulate both lipophilic and hydrophilic compounds, with efficiencies of 95 % and 90 % for curcumin and caffeine, respectively. In addition, the encapsulation of bioactive compounds promoted an increase in antimicrobial activity when compared with active compounds in free solution.

### 2.3.3.3. Lipid-based nanostructured delivery systems

Lipid-based nanostructured delivery systems include nanoemulsions, solid lipid nanoparticles (SLNs), and nanostructured lipid carriers (NLCs), which are described below. In the production of lipid-based nanoparticles, emulsifiers, which are amphiphilic molecules, are used to facilitate the dispersion of lipid matrices in the water, reducing the surface tension between the aqueous phase and oil phase. The emulsifiers can be divided into 3 types: ionic, non-ionic, and Zwitterionic emulsifiers. The major representative of this last type of emulsifier are phospholipids, substances considered GRAS, which allow their use in foods. However, natural phospholipids are inefficient in the formation and stabilization of the lipid particles when used alone but might be effective when used in combination with co-emulsifiers. Co-emulsifiers, also called co-surfactants, are used to improve the flexibility of the interface of the emulsified systems. They act by promoting the increase in entropy at the oil-in-water interface and destabilizing the formation of crystalline structures, thereby conferring higher viscosity to the systems (McClements and Rao, 2011).

- Nanoemulsions

Emulsions are a mixture of two immiscible liquids in which one (dispersed phase) is spread in small droplets in a solution of the other one (continuous phase), forming a stable phase combination. Bioactive compounds can be incorporated into the dispersed droplets and protected in the continuous phase from external environmental conditions. These structures can be divided into oil-in-water (O/W), water-in-oil (W/O), liquid-in-liquid or solid-in-liquid emulsions. The emulsion characteristics and stability depend on factors such as the type of emulsifiers or surfactants used to stabilize the interface between phases, their composition, surfactant-to-oil ratio, the presence of co-solvents and co-solutes, and the homogenization conditions (Souza Simões *et al.*, 2017). Emulsions are produced mainly using high energy techniques, for instance, high-pressure valve homogenizers and sonicators, capable of generating intense disruptive forces that separate the oil and water phases, resulting in the formation of oil droplets. However, low energy methodologies, mainly dependent on the intrinsic physicochemical properties of surfactants and oily phases (i.e., phase inversion and solvent demixing methods), can be also employed (Cerqueira *et al.*, 2017; Souza Simões *et al.*, 2017).

Conventional emulsions are usually white opaque, nanoemulsions are optically transparent, and microemulsions are transparent. The main difference between microemulsions and nanoemulsions (**Figure 3C**) is related to physical stability. In fact, nanoemulsions are thermodynamically unstable, whereas microemulsions are thermodynamically stable (McClements, 2012). O/W nanoemulsions are a



mixture of two immiscible liquids, where a thin interfacial layer is created due to the adsorption of the emulsifier molecules surrounding the oil droplets. In the other hand, in W/O nanoemulsions, the oil is the continuous phase, where the emulsifier surrounds the water droplets (disperse phase) (Martins *et al.*, 2015). Nanoemulsions can be used to encapsulate, protect and deliver lipophilic compounds, such as essential oils (e.g.,  $\omega$ -3-rich oils), polyphenolics (e.g., curcumin), antioxidants (e.g., quercetin), antimicrobials (e.g., thymol), and vitamins (e.g., vitamin A) (Silva *et al.*, 2012; Martins *et al.*, 2015).

An advantage of the use of nanoemulsions is that it is expected that the bioavailability and bioefficacy of the liberated lipophilic bioactive compounds are superior when administered in the form of a nanoemulsion rather than a normal emulsion (Sagalowicz and Leser, 2010). Nanoemulsions allows improving the solubility and bioavailability of these compounds and preventing the degradation against light and oxidation (Martins *et al.*, 2015). The main challenges in their use are: i) the proper selection of the emulsifier, since there is a limited number of food-grade emulsifiers that can be used; ii) physical instability under environmental stresses; iii) limited control over oxidation of the bioactive compounds due to the very thin interfacial layer; and iv) the ability to provide better protection and stability for the encapsulated bioactive compounds during the passage through the GI tract (Martins *et al.*, 2015). Mayer *et al.*/2013 encapsulated vitamin E acetate into O/W nanoemulsions using either a low-energy method or a high-energy method. The influence of surfactant-to-oil on lipid digestion and vitamin bioaccessibility of nanoemulsions was determined using a GI tract model. The results showed an increase in the size and negative charge of the oil droplets after passage through the GI tract. The rate and extent of lipid digestion decreased with increasing surfactant concentration, but the bioaccessibility of vitamin E acetate was high in all samples. No appreciable influence of the preparation method (low-energy versus high-energy) on lipid digestion and vitamin bioaccessibility was observed (Mayer *et al.*, 2013). In a study conducted by Sari *et al.*, 2015, curcumin nanoemulsions have been developed in order to overcome curcumin's instability during processing and its low bioavailability, and the effect of nanoencapsulation was evaluated by a simulated digestion study. The results showed that the nanoemulsion has good stability against ionic strengths, pH, and pasteurization. *In vitro* GI studies showed that the curcumin's nanoemulsion was relatively resistant to pepsin digestion but pancreatin causes gradual release of curcumin from nanoemulsion. Ni *et al.*, 2017 developed quercetin-loaded nanoemulsions (QT-NE) using high-pressure homogenization. The prepared QT-NE had good physical and chemical stability and the *in vitro* digestion tests showed that the bioaccessibility of quercetin in simulated small intestinal conditions was improved by nanoencapsulation. The authors demonstrated that encapsulation of quercetin improves its stability and bioavailability.

- Solid lipid nanoparticles

SLNs (**Figure 3D**) are produced by a solid lipid or a blend of solid lipids in which the lipid droplets are fully crystallized. The most common lipids used in these nanostructured delivery systems include sunflower and palm oils (Souza Simões *et al.*, 2017). The major advantages of SLNs over nanoemulsions include large-scale production without the use of organic solvents and sterilization, high concentration of functional compounds in the system, long-term stability and the ability to be powdered (Khare and Vasisht, 2014). The main limitation is the low loading capacity during the storage process, due to the phenomena of crystallization. In this way, early releases can occur, which limits the use of these structures for certain applications as delivery systems (Tamjidi *et al.*, 2013). Patel and San Martin-Gonzalez, 2012 studied the encapsulation of ergocalciferol (vitamin D<sub>2</sub>) in SLNs in order to offer alternatives to milk and margarine as a source of vitamin D. In a study conducted by Sun *et al.*, 2013, curcumin was encapsulated in SLNs with the aim of improving its dispersibility and chemical stability, prolonging its antitumor activity and cell uptake, and increasing its bioavailability. Ban *et al.*, 2020 prepared SLNs using tristearin and PEGylated emulsifiers in order to control the bioavailability of curcumin. The authors evaluated the lipolysis of SLNs via GI digestion by altering the types and concentrations of emulsifiers. Their results suggested that the bioavailability of curcumin can be controlled by modulating the interfacial properties of SLNs, which will facilitate the development of curcumin formulations for use in functional foods and pharmaceuticals.

- Nanostructured lipid carriers

NLCs (**Figure 3E**) are a combination of solid and liquid lipids at room temperature (Gonçalves *et al.*, 2018). The formulation of these structures aims to produce particles in which the oil is incorporated into the core of a solid lipid to increase the charge ability and control the release. NLCs have been developed to overcome the limitations of SLNs, presenting higher encapsulation efficiency, control release, low toxicity, biodegradability, and bioavailability (Tamjidi *et al.*, 2013; Gonçalves *et al.*, 2018). Some of limitation of NLCs are the irritative and sensitising action of some surfactants, cytotoxic effects related to the nature of lipid matrix and concentration (Tamjidi *et al.*, 2013; Jaiswal *et al.*, 2016; Gonçalves *et al.*, 2018). Manea *et al.*, 2014 showed that green tea extract loaded into NLC could be used as a valuable natural source of antioxidant and antimicrobial agent. Babazadeh *et al.*, 2016 encapsulated rutin into NLCs in order to find a solution to eliminate the fortification difficulties and provide healthier functional foods. The results showed that rutin NLCs were stable during processing and storage period and they did not adversely affect the appearance of enriched food beverages when they were applied as the nutrient

carriers. This study indicated that the developed rutin NLCs could provide a method for designing new functional foods based on nanostructured delivery systems.

## 2.4. Characterization of nanostructured delivery systems

### 2.4.1. Physicochemical characterization techniques

#### 2.4.1.1. Dynamic light scattering

Dynamic light scattering (DLS) is a technique used for rapid determination of the size distribution profile of small particles in suspensions or polymers in solution. DLS allows calculating the mean size of the particles through the illumination of the particles with a laser and analyzing the intensity fluctuations in the scattered light. This method is often very used to evaluate size of nanostructured delivery systems as well as their size stability though storage (Silva *et al.*, 2012).

#### 2.4.1.2. Zeta potential

Zeta potential ( $\zeta$ -potential) is a term of electrokinetic potential in colloidal systems and measures the potential difference between the dispersion medium and the stationary layer of fluid attached to the dispersed particle. This technique measures the charge that a particle acquires in a specific medium and gives an indication of the potential stability of a system. Stability of the solution is evaluated through electrostatic repulsion interaction. It explains the reasons for the occurrence of dispersion, aggregation or flocculation and can be used to improve the conditions of the colloidal solution (Khare and Vasisht, 2014). A value of 30 mV (positive or negative) can be taken as the arbitrary value that separates low-charged surfaces from highly charged surfaces (Silva *et al.*, 2012).

#### 2.4.1.3. Fourier transform infrared spectroscopy

Fourier transformed infrared spectroscopy (FTIR) is based in an infrared radiation that passes through a sample where it is mostly absorbed by the sample and some of it is transmitted. The resulting spectrum represents the molecular absorption and transmission, creating a molecular fingerprint of the sample. Each sample fingerprint presents its characteristic absorption peaks that correspond to the frequencies of vibrations between the bonds of the atoms of the material. Because each different material is a unique combination of atoms, different compounds do not produce the exact same infrared spectrum. Therefore, infrared spectroscopy can result in a positive identification of different materials. In addition, the size of

the peaks in the spectrum is a direct indication of the amount of material present in the sample. The major advantages of FTIR are the fact that it can be used to determine the amount of components in a mixture and the quality or consistency of a sample, the small time required for analyses (because all frequencies are measured simultaneously), the fact that it is a very sensitive method, relatively simple to work with and internally calibrated. These advantages make measurements made by FTIR extremely accurate and reproducible (Silva *et al.*, 2012).

#### 2.4.1.4. Differential Scanning Calorimetry

Differential Scanning Calorimetry (DSC) is a technique in which the difference in the amount of heat required to increase the temperature of a sample is measured as a function of temperature. Generally, the temperature program for DSC analysis is designed so that the temperature of the sample holder increases linearly as a function of time (Silva *et al.*, 2012). This technique can be used to monitor thermal events in the samples, such as the glass transition temperature ( $T_g$ ) and the melting temperature ( $T_m$ ) (Espitia *et al.*, 2019).

#### 2.4.2. Imaging techniques

##### 2.4.2.1. Transmission electron microscopy

Transmission electron microscopy (TEM) is a technique whereby a beam of electrons is transmitted through an ultra-thin specimen and interacts as passes through the sample. An image is formed from the electrons transmitted through the specimen, magnified, and focused by an objective lens and appears on an imaging screen. Some materials require extensive sample preparation to produce a sample thin enough to be electron transparent, which makes TEM analysis a relatively time-consuming process with a low throughput of samples. The structure of the sample may be changed during the preparation process; the field of view is relatively small, and the sample may be damaged by the electron beam. In TEM, the crystalline sample interacts with the electron beam, mostly by diffraction rather than by absorption (Khare and Vasisht, 2014).

##### 2.4.2.2. Scanning electron microscopy

In scanning electron microscopy (SEM), an electron beam from a source strikes the surface of the sample for its visualization. The electrons suffer from the influence of an electromagnetic field (generated by electromagnetic “lenses”), which forces the electron beam to strike the surface of the sample. After this,

electrons are diffracted in different directions and generate a number of signals that can be imaged on the screen. The main problem with the application of SEM to nanoparticle characterization analysis is that sometimes it is not possible to clearly differentiate the nanoparticles from the substrate. Problems become even more exacerbated when the nanoparticles under study have the tendency to adhere strongly to each other, forming agglomerate. Nevertheless, SEM is also an expensive technique and requires high vacuum and a relatively high sample conductivity. The presence of surfactants during nanoemulsions preparation can sometimes inhibit their characterization via SEM due to the formation of a smooth camouflaging coating on the particle surfaces (Silva *et al.*, 2012).

#### 2.4.2.3. Confocal laser scanning microscopy

Confocal laser scanning microscopy (CLSM) is one of the most significant advances in optical microscopy. This technique is based on the use of a focused laser beam that is scanned in a raster pattern over the sample. The fluorescent light emitted from each point in the scan is then recorded with a detector to yield 2D image of the light emitted at the beam focus (Adams and Barbante, 2015a). The third dimension can be added by scanning in the axial direction (Adams and Barbante, 2015b). The CLSM has been widely used to observe the structure of multilayer emulsions, in which the oil phase is dyed with a fluorescent dye specific for oil (nile red) (Li and McClements, 2010).

## 2.5. Human gastrointestinal digestion

Human digestion is a complex biological process in which food products undergo a series of physicochemical and physiological changes that transform them into smaller and more basic components so they can be absorbed in the small intestine and reach the bloodstream (Souza Simões *et al.*, 2017). In this way, nanostructured delivery systems will undergo the same obstacles as they pass through the different regions of the GI before the release of the bioactive compound.

The consecutive changes in conditions such as pH of the medium, variations in the type and concentration of ions, the presence of different digestive enzymes and different temperatures can lead to the breakdown of nanostructured delivery systems (**Figure 4**). Thus, the fate of bio-based nanostructured delivery systems will depend not only on their initial physicochemical characteristics but also on the effect of changes experienced along the GI tract (Pinheiro *et al.*, 2017). Since the passage through the GI tract may cause a decrease in bioavailability, it is necessary to understand the fate of nanostructured delivery systems to predict and avoid this decrease (Martins *et al.*, 2015).

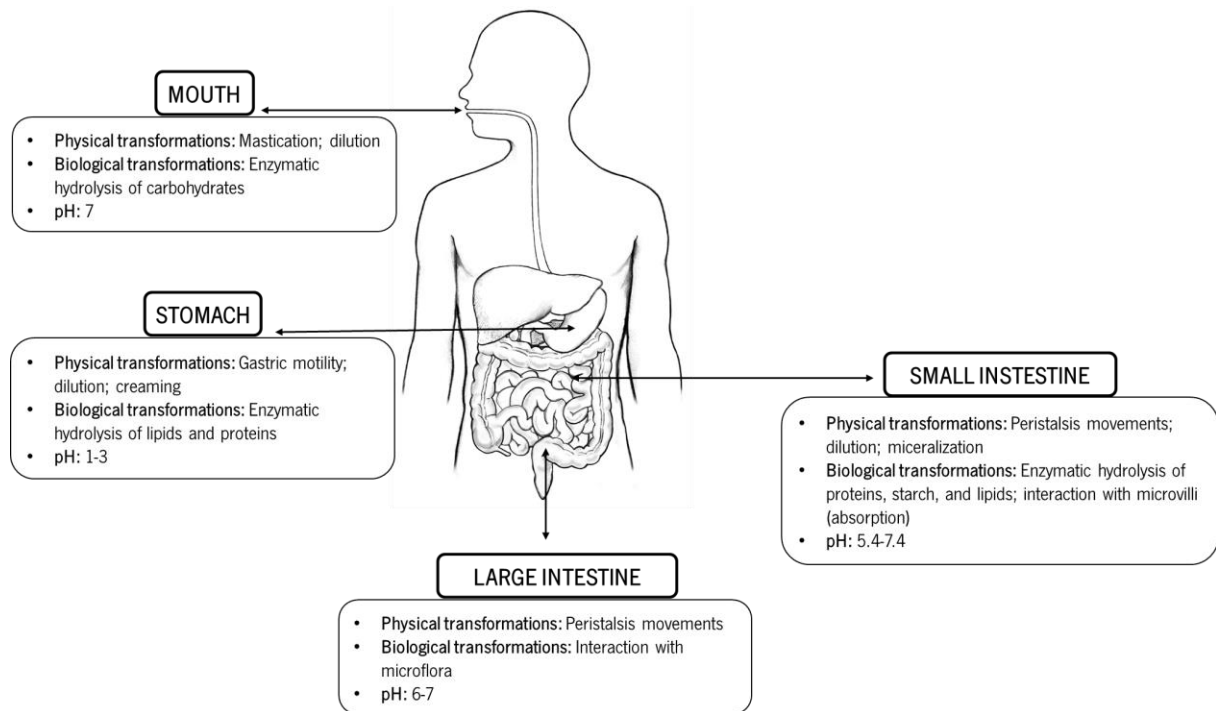


**Figure 4.** Physiological and physicochemical conditions present in the human digestive system (adapted from (Martins *et al.*, 2015; Gonçalves *et al.*, 2018)).

Immediately after ingestion, nanostructured delivery systems undergo a series of changes as they pass through the mouth, stomach, small intestine, and large intestine, which affect their ability to be digested and/or absorbed (McClements and Li, 2010b). In the oral phase, the delivery systems are mixed with saliva, diluted, influenced by digestion enzymes, pH, ionic strength, and temperature changes (Martins *et al.*, 2015). After reaching the stomach, the ingested nanostructured delivery systems are mixed with enzymes such as gastric lipases that initiate digestion of lipids and proteases that initiate digestion of proteins. Delivery systems are exposed to a highly acidic medium (i.e., pH between 1 and 3) and to peristaltic movements, which can further alter their composition and structure. (Martins *et al.*, 2015; Gonçalves *et al.*, 2018). Then, the ingested nanostructured delivery systems move into the small intestine, where most of the absorption occurs (McClements and Li, 2010b). In this phase, the delivery systems are mixed with bile salts, phospholipids, pancreatin, bicarbonate, and the pH increases, being almost neutral. Protease hydrolyses proteins to peptides and amino acids and pancreatin plays a critical role in the digestion of lipids, as it is responsible for the hydrolysis of triacylglycerol (TAG) to monoacylglycerol (MAG) and free fatty acids (FFA) (Martins *et al.*, 2015). Only a fraction of the components reaches the colon, since most of the ingested food is broken down and absorbed in the stomach and small intestine. Therefore, only the indigestible components are expected to reach the colon without being absorbed (Gonçalves *et al.*, 2018).

### 2.5.1. *In vitro* digestion models

*In vitro* digestion models are widely used to study the behaviour of the nanostructured delivery systems throughout the GI conditions (Pineiro *et al.*, 2017). These systems are often used to help understanding the digestibility of controlled release systems and to determine the bioavailability of functional compounds. *In vitro* experiments have the advantage of producing reproducible (without biological variations) and faster results in a more economical way, require less manpower, are easy to perform, do not involve ethical issues, and allow sampling at any point in the digestion process, when compared to *in vivo* experiments (Minekus *et al.*, 2014). *In vivo* studies generally provide more accurate results than *in vitro* systems, but they involve subjecting animals to uncomfortable conditions and/or sacrifices. In addition, often animal models do not mimic what happens in the human body, these feeding studies are generally expensive, time-consuming, subject to appreciable variations from subject to subject, and are limited by ethical constraints when potential harmful compounds are involved (McClements and Li, 2010b). *In vitro* models can be classified into static or dynamic digestion models, depending on their complexity.

#### 2.5.1.1. *In vitro* static digestion models

Several studies have used *in vitro* static digestion models to evaluate the behaviour of micro and nanostructured delivery systems, as well as the release and bioavailability of bioactive compounds. Static models are practical and inexpensive means to evaluate multiple experimental conditions, allowing a large number of samples to be tested (Souza Simões *et al.*, 2017). Most of the *in vitro* digestion models derived from the method described by Miller *et al.*, 1981. Many *in vitro* digestion methods are described in the literature, however, since there are significant differences between the parameters used in them, the comparison of results by the scientific community is difficult. Recently, the COST INFOGEST network described a general and practical standardized method of digestion, based on a set of conditions similar to physiological conditions, in order to standardize the existing protocols and to enable the production of comparable results (Minekus *et al.*, 2014). This protocol includes a set of delineated parameters including the oral, gastric and intestinal phase and also contains recommendations of the preparation of simulated digestion fluid stock solutions which are the simulated salivary fluid (SSF), simulated gastric fluid (SGF), and simulated intestinal fluid (SIF) (Minekus *et al.*, 2014).

The pH-stat method is probably the most analytical tool used in pharmaceutical and food research for *in vitro* digestion experiments and to monitor hydrolysis reactions (**Figure 5**) (McClements and Li, 2010a). In adequate pH conditions, lipid and protein hydrolyses may lead to the release or the consumption of

protons. In response, the automatic addition of an acidic or basic solution maintains the pH constant, so that the titration rate is proportional to the reaction rate. The quantity of titrant added can also be converted into a degree of hydrolysis ( $DH$ ) of the considered nutrient (Mat *et al.*, 2018). This method is very popular to measure the amount of FFA released from lipids, usually TAG, after lipase addition at pH values close to neutral. The sample containing the lipids is placed in a temperature-controlled reaction chamber with an appropriate concentration of small intestinal fluids (e.g., lipase, bile salts, and minerals). The lipase in the SSIF catalyzes lipid digestion leading to the generation of two FFA and one MAG per TAG molecule.

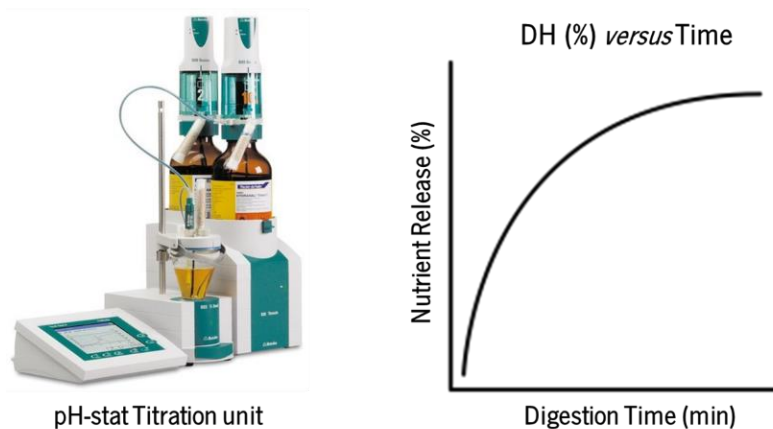


**Figure 5.** Schematic representation of pH-stat in vitro digestion model used to determine the digestion and release of nutrients. Adapted from (Li and McClements, 2010).

The concentration of NaOH that must be titrated into the digestion chamber to neutralize the FFA produced during lipid digestion, and thereby maintain the pH at the initial pre-set value (e.g., pH 7.0), is recorded *versus* time. This method is simple and rapid to carry out and enables comparison of different delivery systems under similar experimental conditions. This technique can be used to quickly screen the impact of different physicochemical factors expected to affect lipid digestion (McClements and Li, 2010a). Different static GI models have been used to evaluate the behavior of nanostructured delivery systems under digestion. Peram *et al.*, 2013 studied the influence of *in vitro* gastric digestion on  $\beta$ -lactoglobulin on native and heat-denatured state. The results showed that  $\beta$ -lactoglobulin in native state were resistant to the gastric conditions, suggesting that these protein could be used as delivery system for bioactive compounds. Zhang *et al.*, 2016 studied the influence of the initial lipid droplet size on the ability of O/W emulsions to increase carotenoid bioaccessibility from carrots using a simulated GI tract. The results demonstrated that the bioaccessibility of carotenoids increased significantly with the decrease in the size of the lipid droplets in the emulsions, which can be explained by the facilitated lipolysis due to the higher



surface area in smaller droplets of mixed micelles that could solubilize the carotenoids in intestinal fluids. Ahmad *et al.*, 2019 developed starch-based nanoparticles for nanoencapsulation of catechin. In this study, the authors concluded that nanoencapsulation offers protection to the catechin of the gastric environment, which helps to retain its bioactive properties during the digestion process.

#### 2.5.1.2. *In vitro* dynamic digestion models

Dynamic models are complex systems designed to mimic human digestion conditions as close as possible, allowing simulation of physicochemical changes such as pH transitions, enzymatic secretion changes and peristaltic movements that occur in GI tract. However, dynamic models are expensive to set up, more labor intense, time consuming, and require higher operating costs. Thus, these systems are more adequate to confirm the results obtained in static models and to obtain more detailed information about the changes that occur during the digestion (Alminger *et al.*, 2014; Souza Simões *et al.*, 2017).

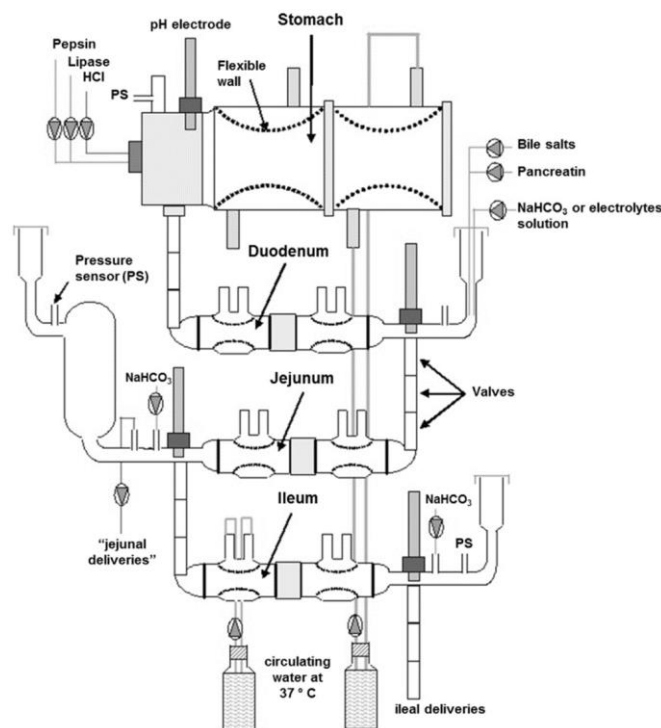


**Figure 6.** Schematic representation of modified TNO gastric-small Intestinal Model (TIM-1) (Villemejane *et al.*, 2016).

The TNO GI model TIM-1 was developed by TNO Nutrition and Food (Zeist, The Netherlands) and has been widely used in several studies (Alminger *et al.*, 2014). This model is controlled by a computer and it is composed of multiple compartments that simulates the main physiological digestive functions

(Villemejjane *et al.*, 2016). The system consists of four glass compartments simulating the stomach, duodenum, jejunum, and ileum.

This apparatus (**Figure 6**) allows to simulate not only peristaltic movements but also intestinal absorption: the jejunum and ileum compartments are connected to filtration units (semi-permeable hollow-fiber devices with a molecular weight cut-off of 5 kDa) which allow the quantification of bioaccessibility (defined as the fraction released during digestion) (Villemejjane *et al.*, 2016; Souza Simões *et al.*, 2017). Non-bioaccessible fractions (ileal delivery) are collected at the end of the ileum compartment and represent the unabsorbed material that will pass into the large intestine (Souza Simões *et al.*, 2017). Bourbon *et al.*, 2016b assessed the influence of chitosan coating on lactoferrin-glycomacropeptide (Lf-GMP) nanohydrogels. In this study, the authors used a dynamic *in vitro* system that simulated the digestive process to evaluate the digestibility of Lf-GMP nanohydrogels. The results demonstrated that the presence of chitosan improve the stability of nanohydrogels since proteins were hydrolyzed at a slower rate and were present in solution for a longer time.

## 2.6. Nanostructured delivery systems in food matrices

### 2.6.1. Food matrices

A food matrix has been described as a structural network of nutrients and non-nutrients interacting physically and chemically. The physicochemical properties of this complex has been shown to influence the release, mass transfer, accessibility, digestibility, and stability of many food components (Crowe, 2013). Food matrix directly affects the process of digestion and absorption of food nutrients and bioactive compounds in the GI tract (Aguilera, 2019). The physiological response and health benefits of different foods that contain the same nutrients and bioactive compounds are different. This is because the amount of nutrients actually digested and the amount actually absorbed are different for different foods (Geo Thomas *et al.*, 2018). Bioaccessibility (fraction released during digestion) and bioavailability of nutrients (fraction absorbed) are parameters that are directly related to the food matrix. The criterion used to assess the potential nutritional benefits derived from nutrients and bioactive compounds in foods and to support their health claims is bioavailability (Aguilera, 2019). Through the study of the interactions that a given bioactive compound has with various food matrices and their consequent physiological response in the body, it is possible to design a food matrix that improves the bioaccessibility and bioavailability of different bioactive compounds (Crowe, 2013; Geo Thomas *et al.*, 2018). The bioavailability of bioactive compounds

can be enhanced by retarding its metabolism, increasing its bioaccessibility, and/or promoting its absorption (Zheng and McClements, 2020).

#### 2.6.2. Nanostructured delivery systems incorporated into food matrices

There is currently an increasing trend towards natural foods that are rich in nutrients and may have biological functions. This demand encourages food manufacturers and researchers to introduce different bioactive ingredients in the formulation of functional foods. In fact, there are several studies that evaluate the incorporation of delivery systems encapsulating bioactive compounds in different food matrices. Campo *et al.*, 2019 incorporate zeaxanthin nanoparticles and zeaxanthin nanoemulsion in yogurt. The results showed that at the end of the storage time, the retention of zeaxanthin was higher in yogurt with incorporated nanoparticles (Y-NP) than yogurt with incorporated nanoemulsions (Y-NE). Bioaccessibility after *in vitro* digestion suggested that nanoencapsulation provided a controlled release of the carotenoid. The authors concluded that zeaxanthin nanoparticles can be incorporated into yogurt, allowing the dispersion of a hydrophobic compound in a hydrophilic matrix, providing stability. Mohammed *et al.*, 2020 developed ice-cream fortified with *Nigella sativa* oil (NSO) nanoemulsion. The results showed that NSO nanoemulsion improved the ice-cream physical properties and consumer acceptability. Zhong *et al.*, 2018 produced a fish oil/Y-oryzanol nanoemulsion and evaluated the effect of adding this nanoemulsion on the physicochemical and sensory characteristics of yogurts. Hamed *et al.*, 2019 prepared a functional yogurt fortified with fish O/W nanoemulsion. Park *et al.*, 2019 developed turmeric extract-loaded nanoemulsion and studied its stability in milk as a food model. Kumar *et al.*, 2016 prepared curcumin nanoemulsion with milk protein and evaluated its incorporation into ice. Almeida *et al.*, 2018 produced different formulations of curcumin and evaluated them as yogurt colorant.

#### 2.6.3. Evaluation of food matrices

The overall quality of a product consists of “external” and “internal” quality. External quality is usually assessed visually by the consumer and may include a combination of several aspects, such as size, shape, and colour (Siswantoro, 2019). External (“visual”) quality is thus an important criterion for consumers when purchasing a food product.

#### 2.6.3.1. Structure and morphology characterization

Size is an important physical parameter in food products and a critical factor when consumers choose it. The size of food products is important in harvesting, processing, sorting, packaging, transport, marketing and price (Siswanto, 2019).

#### 2.6.3.2. Colour analysis

Colour is generally considered one of the most important attribute in the appearance of any food (Macdougall, 2010). In fact, consumers often accept or reject a food product based on its colour. Through this visual feature, it is possible to detect the presence of damage, evaluate product changes during processing and also evaluate the maturity, for example, of the fruit (Siswanto, 2019). The opacity and colour can be quantitatively described using tristimulus color coordinates, such as the CIE (Commission International de L'Éclairage)  $L^*a^*b^*$  space, known as CIELAB (Macdougall, 2010). In this colour system,  $L^*$  represents the lightness, and  $a^*$  and  $b^*$  are color coordinates, where  $+a^*$  is the red direction,  $-a^*$  is the green direction;  $+b^*$  is the yellow direction,  $-b^*$  is the blue direction, low  $L^*$  is dark, and high  $L^*$  is light (McClements *et al.*, 2007).

#### 2.6.3.3. Rheological analysis

Rheology consists of studying the deformation and flow of a material, namely, its behaviour in the transitional area between solids and fluids (Tabilo-Munizaga and Barbosa-Cánovas, 2005). This science allows defining a relationship between the stress acting on a given material and the deformation and/or flow resulting. The rheological characterization allows quantifying the functional relationships between deformation, tension, and resulting rheological properties, namely viscosity, elasticity, or viscoelasticity (Fischer and Windhab, 2011; Day and Golding, 2016). In the food area, rheology allows the understanding of the physicochemical principles underlying the structuring of food materials, as well as their interaction. The degree of fluidity and consistency are important parameters to determine how food ingredients can be mixed and processed during their production, what type of texture can be obtained and how stable the food will remain (Day and Golding, 2016).

#### 2.6.3.4. Texture analysis

Texture is one of the main attributes of food and is used to define the quality of the product and its acceptability (Day and Golding, 2016). Texture measures are used throughout the food value chain in

order to monitor and control product quality, from harvest to evaluation of post-harvest handling and processing in the shelf life and consumer acceptance (Levine and Finley, 2018).

The sensory texture profile procedure was developed in the early 1960s by Szczesniak, 1963. Initially, the texture profile analysis (TPA) was performed on a texturometer, in which a probe simulates the action of a molar tooth. The movement of the probe simulates chewing, and two sequential bites are performed. Some modifications to the basic TPA procedure have been developed. Bourne, 2002 proposed a two-bite TPA. The texture parameters, such as hardness, adhesiveness, and cohesiveness can be obtained from the resulting force-time curve (**Figure 7; Table 2**) (Darras *et al.*, 2015; Kohyama, 2020).

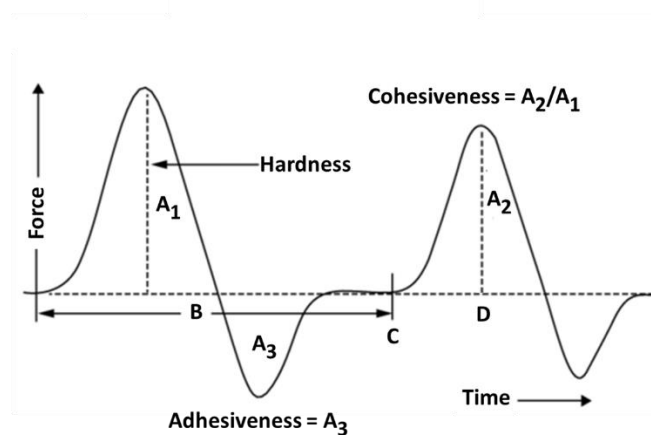


**Figure 7.** Example of TPA curve with typical parameters. Adapted from (Kohyama, 2020).

Compressive work is represented by the area under the curve for the first and the second compression ( $A_1$  and  $A_2$  in **Figure 7**). The height ( $A_1$ ) of the peak force of the first compression (this first compression is represented by  $B$  in **Figure 7** and corresponds to the first bite) was defined as hardness. The ratio of the positive force areas of the first and second compressions ( $A_2/A_1$  in **Figure 7**) was defined as cohesiveness. Adhesiveness is represented by the area of negative force during the first decompression ( $A_3$  in **Figure 7**). The distance at which the food regains its height during the time between the end of the first bite and the beginning of the second bite ( $CD$  in **Figure 7**) was defined as springiness. Two other parameters were derived by calculating the measured parameters: the gumminess was defined as the product of hardness  $\times$  cohesiveness; chewiness was defined as the product of gumminess  $\times$  springiness (Darras *et al.*, 2015; Kohyama, 2020).

**Table 2.** Definition of some texture parameters that can be obtained from the force-time curve of the TPA test.

Texture parameters	Definition	References
Hardness	Force required to break the sample into several pieces during the first bite by the molars	
Adhesiveness	Force required to remove material that adheres to the mouth, generally the palate, during the normal eating process	(Bourne, 2002; Darras <i>et al.</i> , 2015)
Gumminess	Energy required to disintegrate a semisolid food to a state of readiness for swallowing	
Chewiness	Energy required to masticate a solid food product	

## 2.7. Application of nanostructured delivery systems in food industry

Food industries such as Nestlé and Unilever are already applying nanotechnology in their products. Unilever has developed a healthier, lower-fat ice cream without compromising taste through the application of nanoemulsions. Nestlé has a patent of water-in-oil nanoemulsions that allow obtaining a faster and simpler thaw of food in the microwave (Silva *et al.*, 2012).

Another example of the application of the nanotechnology in the food industry is AQUANOVA AG, with their NovaSol® products. NovaSol® offers health solutions (coenzyme Q10, DL- $\alpha$ -tocopherol acetate, vitamins A, D, D3, E, and K and omega three fatty acids) and food additives ( $\beta$ -carotene, apocarotenal, chlorophyll, curcumin, lutein, and sweet pepper extract). AQUANOVA AG claims the significantly increased and clinically proven bioavailability of encapsulated functional compounds and food additives ('Aquanova AG (2020)').

The Portuguese company Improveat's mission is to develop technology-based products using edible and biodegradable materials to improve the quality and safety of food products. In this segment, it has been developing several products, namely, BioFruitCoat, BioNutriCoat, and BioCheeseCoat. These products have a coating technology that allows not only to increase the shelf life of the product but also its safety, preventing unwanted contamination ('Improveat').

## 2.8. Toxicological aspects

The great potential of nanotechnology in the food sector arises serious questions about their toxicity and safety. This concern is mainly based on the small size of nanostructured delivery systems since there is a risk of bioaccumulation in the organs and tissues of the body (Gonçalves *et al.*, 2018). In the case of

nanostructured delivery systems used as food additives, they come in direct contact with human organs which can lead to higher levels of exposure, depending on the concentration in the food and the amount of food consumed (He and Hwang, 2016). There are many factors that affect dissolution, including particle surface morphology, concentration, surface energy, aggregation, and adsorption (Singh *et al.*, 2017). Organic nanostructured delivery systems are thought to be less toxic because they are fully digested in the GI tract and are not bio-persistent (McClements and Xiao, 2017). In fact, during the passage through the GI tract, namely, in the gastric phase, the ingested nanostructured delivery systems are exposed to a highly acidic medium (pH 1–3), ionic composition changes, and the presence of digestive enzymes. Thus, at this stage, the original interfacial characteristics of ingested nanostructured delivery systems may be changed, as well as their size, which may no longer be at the nanometric scale. Then, the ingested nanostructured delivery systems move to the small intestine, where most of the absorption occurs. Again, within the small intestine changes in the particle size and interfacial characteristics may occur due to particle aggregation and competitive adsorption process (McClements and Xiao, 2012; Martins *et al.*, 2015).

In recent years, several studies have been conducted to understand the behaviour of nanostructured delivery systems in the GI tract. This knowledge will be crucial to assess the biological activity of nanostructured delivery systems *in vivo* and to know the potential health risks arising from their use (Cerqueira *et al.*, 2014). Toxicity assessment is essential to characterize the nanostructured delivery systems itself. For example, in terms of materials, structure, size, shape, surface area, load, solubility, hydrophobicity, stability, and state of aggregation (Gonçalves *et al.*, 2018). Loh *et al.*, 2012 reported that *in vitro* cytotoxicity of chitosan nanostructures against Caco-2 cells is less dependent on positive surface charges than on the particle size. There are many toxicological studies that have been made to evaluate the safety of nanostructured delivery systems (Chiu *et al.*, 2012; Lee *et al.*, 2012; Vecchione *et al.*, 2016). During the production, processing, and active packaging and consumption of nano-based food products, regulatory policies must be considered. However, most countries do not have specific regulations for the risk assessment of encapsulated nanoproducts, thus limiting the marketing of products between countries (Bazana *et al.*, 2019).

# CHAPTER 3

---

## EXPERIMENTAL APPROACH



### 3.1. Materials

Curcumin (from *Curcuma longa* (Turmeric) powder), pepsin (from Porcine gastric mucosa), bile (bile extract porcine), pancreatin (from porcine pancreas), Pefabloc® SC, and Nile red were purchased from Sigma-Aldrich (St. Louis, MO, USA). Beeswax (produced by *Apis mellifera*) was purchased from QUIMIND (Porto, Portugal). PHOSPHOLIPON® 90G was purchased from Lipoid (Ludwigshafen, Germany). Tween 80 was purchased from PanReac AppliChem ITW Reagents (Darmstadt, Germany). Gelatin (porcine Skin 90-110 BLOOM) was purchased from OXOID (UK). Chloroform was purchased from Fisher Scientific (N.J, USA).

### 3.2. Preparation of SLNs

SLNs were prepared according to Kheradmandnia *et al.*, 2010 with some modifications. Briefly, beeswax (3.0 %), Phospholipon 90G (1.5 %) and curcumin (0.1 %) were melted in a water bath at 85 °C. Tween 80 (1.5 %) was solubilized in distilled water at 85 °C in an Ultra-Turrax homogenizer (T18, Ika Werke, Germany) during 2 min at 3400 rpm. The aqueous solution was added to the lipid solution and mixed in an Ultra-Turrax homogenizer (T18, Ika-Werke, Germany) at 18 000 rpm for 8 min. Then, the resulting lipid solution was gradually dispersed at a volume ratio of 1:10 in cold water at 2 °C under stirring at 2000 rpm for 5 min. The SLN was stirred at 800 rpm for an additional 35 min on a mechanical stirrer. The SLNs were kept at 4 °C in the dark.

### 3.3. Nanostructures characterization

#### 3.3.1. Particle size

The average particle diameter (Z-average diameter) and polydispersity index (PDI) of SLNs were determined using DLS (Zetasizer Nano-ZS, Malvern Instruments Ltd., Malvern Hills, UK.). SLNs were diluted in distilled water at room temperature. PDI indicates the heterogeneity (monodisperse or polydisperse) of particles' size in a mixture. Each sample was analysed in a disposable sizing cuvette (DTS0012). The measurements were made in duplicate, with three readings for each of them. The results are given as the average  $\pm$  standard deviation of the six values obtained.

### 3.3.2. $\zeta$ -potential

The  $\zeta$ -potential of the SLNs was determined using DLS (Zetasizer Nano-ZS, Malvern Instruments Ltd., Malvern Hills, UK.). Each sample was analysed in a folded capillary cell. The measurements were made in duplicate, with three readings for each of them. The results are given as the average  $\pm$  standard deviation of the six values obtained.

### 3.3.3. Temperature stability

Thermal stability of the SLNs was assessed by DLS (Zetasizer Nano-ZS, Malvern Instruments Ltd., Malvern Hills, UK.) using the temperature range from 20 °C to 80 °C, with increments of 5 °C, with 60 s of equilibration before each measurement. Each sample was analysed in a glass cuvette (PCS1115). The measurements were made in quadruplicate with three readings. The results are given as the average  $\pm$  standard deviation of the twelve values obtained (Simões *et al.*, 2020).

## 3.4. Incorporation of bio-based nanostructures in food matrices

Gelatine control was prepared by dissolving 2.5 g of gelatine in 35 mL of distilled water at 45 °C under mechanical stirring to obtain a homogeneously dispersed sample. Then, 35 mL of distilled water at 4 °C was added to the solution. To prepare the gelatine with SLNs incorporated (gelatine-SLNs), the same gelatin/water ratio of gelatine control was maintained and since the final SLN solution contains 99.445 % water in its composition, 2.5 g of gelatin was dissolved in 35.2 mL of distilled water at 45 °C under mechanical stirring and then, 35 mL of previously prepared SLNs (section 3.2.) at 4 °C were added. The final solutions were placed in flasks, protected from light, and stored at 4 °C for the gelation process occur.

## 3.5. Understanding the effects of bio-based nanostructures in food matrices' shelf-life

Samples were stored at 4 °C for 21 days. To assess the storage stability of gelatine and gelatine-SLNs and the effect of SLNs incorporation, colour, texture, and rheology were measured once a week over 21 days.

### 3.5.1. Colour evolution

The surface colour parameters of gelatine and gelatine-SLNs were measured with a tristimulus colorimeter (Konica Minolta, CR-400, Japan) using the CIELAB system (CR-410, Japan). A white tile (Minolta calibration plate) with following standard value:  $Y=93.9$ ,  $x=0.3133$ ,  $y=0.3193$ , was used to calibrate the equipment. Results were calculated by the equipment into the Hunter Lab colour scale.  $L^*$  ranges from 0 (black) to 100 (white),  $a^*$  indicates degree of greenness for negative values and degree of redness for positive values,  $b^*$  ranges from negative to positive values indicating, respectively, degree of blueness to yellowness. Colour changes were assessed using total colour difference (TCD) (**Equation 1**):

$$\text{TCD}/\Delta E = \sqrt{(L^* - L_0^*)^2 + (a^* - a_0^*)^2 + (b^* - b_0^*)^2} \quad \text{Equation 1}$$

where  $L^*$ ,  $a^*$  and  $b^*$  are the colour parameters at the end of the period under analysis and  $L_0^*$ ,  $a_0^*$ , and  $b_0^*$  are the colour parameters at the beginning of that period. The results are given as the average  $\pm$  standard deviation of the fifteen values obtained.

### 3.5.2. Texture analysis

Texture measurements of the gelatine and gelatine-SLNs were performed through TPA test using a Texture Analyzer-HD Plus (Stable Micro Systems, Dias de Sousa, Portugal). The TPA test consists of two cycles of compression. In each cycle, the sample was compressed to 75 % of the sample length by a cylinder probe (25 mm diameter), at a crosshead speed of 5.0 mm.s<sup>-1</sup>. Pre-test speed and post-test speed was 1.0 mm.s<sup>-1</sup> and 5.0 mm.s<sup>-1</sup>, respectively. During each test time, force, and distance were measured. From each force time curve of the TPA test a few textural parameters were extracted, such as hardness, chewiness, gumminess, and adhesiveness. Measurements were made in triplicate. The results are given as the average  $\pm$  standard deviation of the three values obtained.

### 3.5.3. Rheology analysis

Viscoelastic properties of the gelatine and gelatine-SLNs were determined by small deformation dynamic oscillatory measurements in a rheometer model Hybrid Discovery HR1 (TA Instruments, United States), using a parallel plate geometry (40 mm diameter), with a Peltier temperature control. Firstly, a frequency sweep test was done at a range of frequencies (0.1 to 10 Hz) to find the frequency independent viscoelastic behaviour region. The frequency sweep test revealed that 1 Hz was within the linear

viscoelastic region (LVR) for the gelatine samples. For each test, 1 mL of the sample were loaded on the bottom plate of the rheometer. Before each measurement, the samples were allowed to equilibrate at temperature of 45 °C for 5 min, in order to achieve mechanical and temperature equilibrium between samples. For the oscillatory test, an amplitude sweep test was carried out at 4 °C, a frequency of 1 Hz and shear stress from 0.01 to 100 Pa. The measurements were made in triplicate. The results are given as the average  $\pm$  standard deviation of the three values obtained. Data obtained in each step were storage modulus ( $G'$ ) and loss modulus ( $G''$ ) that were used to calculate the complex viscosity ( $\eta^*$ ) (Equation 2):

$$\eta^* = \sqrt{G'^2 + G''^2} / \omega \quad \text{Equation 2}$$

where  $G'$  is the storage modulus,  $G''$  is the loss modulus, and  $\omega$  is the frequency.

### 3.6. *In vitro* digestion

#### 3.6.1. Digestion stock solutions

Stock electrolyte solutions were prepared as follow: SSF was constituted by KCl 15.1 mmol.L<sup>-1</sup>, KH<sub>2</sub>PO<sub>4</sub> 3.7 mmol.L<sup>-1</sup>, NaHCO<sub>3</sub> 13.6 mmol.L<sup>-1</sup>, MgCl<sub>2</sub>(H<sub>2</sub>O)<sub>6</sub> 0.15 mmol.L<sup>-1</sup>, (NH<sub>4</sub>)<sub>2</sub>CO<sub>3</sub> 0.06 mmol.L<sup>-1</sup> and HCl 1.1 mmol.L<sup>-1</sup> in Milli-Q water; SGF will composed by KCl 6.9 mmol.L<sup>-1</sup>, KH<sub>2</sub>PO<sub>4</sub> 0.9 mmol.L<sup>-1</sup>, NaHCO<sub>3</sub> 25 mmol.L<sup>-1</sup>, NaCl 47.2 mmol.L<sup>-1</sup>, MgCl<sub>2</sub>(H<sub>2</sub>O)<sub>6</sub> 0.12 mmol.L<sup>-1</sup>, (NH<sub>4</sub>)<sub>2</sub>CO<sub>3</sub> 0.5 mmol.L<sup>-1</sup>, and HCl 15.6 mmol.L<sup>-1</sup> in Milli-Q water; and SIF will made up of KCl 6.8 mmol.L<sup>-1</sup>, KH<sub>2</sub>PO<sub>4</sub> 0.8 mmol.L<sup>-1</sup>, NaHCO<sub>3</sub> 85 mmol.L<sup>-1</sup>, NaCl 38.4 mmol.L<sup>-1</sup>, MgCl<sub>2</sub>(H<sub>2</sub>O)<sub>6</sub> 0.33 mmol.L<sup>-1</sup>, CaCl<sub>2</sub>(H<sub>2</sub>O)<sub>2</sub> 0.6 mmol.L<sup>-1</sup> and HCl 8.4 mmol.L<sup>-1</sup> in Milli-Q water. All the electrolyte solutions (SSF, SGF and SIF) were prepared 1.25x concentrated (i.e., 4 parts of electrolyte stock solution + 1 part water will give the correct ionic composition in the simulated digestion fluids).

#### 3.6.2. *In vitro* static digestion

The oral phase simulation consisted in the addition of SSF solution, CaCl<sub>2</sub>(H<sub>2</sub>O)<sub>2</sub> 0.3 mol.L<sup>-1</sup> (to achieve a concentration of 1.5 mol.L<sup>-1</sup> in the fluid) and Milli-Q water (volume needed to achieve 1x concentration of SSF) to 5 mL of each sample. The mixture was incubated during 2 min at 37 °C under agitation at 120 rpm. In gastric phase, SGF, CaCl<sub>2</sub>(H<sub>2</sub>O)<sub>2</sub> 0.3 mol.L<sup>-1</sup> (to achieve 0.15 mmol.L<sup>-1</sup> in the fluid) and pepsin solution (with final activity of 3593 U.mL<sup>-1</sup> in the final mixture) were added. The pH was adjusted to 3.0

with HCl 1 M and Milli-Q water was added (volume needed to achieve 1x concentration of SGF). The samples were incubated for 2 h at 37 °C under orbital agitation at 200 rpm. The intestinal phase was simulated by the addition of SIF,  $\text{CaCl}_2(\text{H}_2\text{O})_2$  0.3 mol.L<sup>-1</sup> (to achieve 0.3 mmol.L<sup>-1</sup> in the mixture), bile salts (to reach the concentration of 10 mmol.L<sup>-1</sup> in the final mixture) and pancreatin solution (with final activity of 800 U.mL<sup>-1</sup> in the final mixture). The pH was adjusted to 7.0 with NaOH 1 mol.L<sup>-1</sup> or HCl 1 mol.L<sup>-1</sup> and then Milli-Q water was added (in order to achieve 1x concentration of the SIF). The samples were incubated for 2 h at 37 °C under orbital agitation at 200 rpm. The reaction of gastric phase (pepsin activity) was stopped by raising pH to 7.0 with NaHCO<sub>3</sub> (1 mg.mL<sup>-1</sup>) and after full digestion, the reaction was stopped by adding the enzyme inhibitor Pefabloc (1 mmol.L<sup>-1</sup>) (10 µL for each 1 mL of sample). All the samples were tested at least in triplicate.

### 3.6.3. Physicochemical characterization

#### 3.6.3.1. Particle size

The Z-average diameter of the SLNs and gelatine-SLNs was evaluated at each stage of the *in vitro* digestion (i.e., oral, gastric, and intestinal phases) by DLS (section 3.3.1.) with an equilibration at 37 °C for 60 s before each measurement. Samples of the oral and intestinal phases were diluted with Milli-Q water at pH 7, and samples of the gastric phase were diluted with Milli-Q water at pH 3. The measurements were performed in triplicate, with three readings of each of them. The results are given as the average ± standard deviation of the nine values obtained.

#### 3.6.3.2. ζ-potential

The ζ-potential of the SLNs and gelatine-SLNs was evaluated at each stage of the *in vitro* digestion (i.e., oral, gastric, and intestinal phases) by DLS (section 3.3.2.) with an equilibration at 37 °C for 60 s before each measurement. Samples of the oral and intestinal phases were diluted with Milli-Q water at pH 7, and samples of the gastric phase were diluted with Milli-Q water at pH 3. The measurements were performed in triplicate, with three readings of each of them. The results are given as the average ± standard deviation of the nine values obtained.

#### 3.6.4. Morphology

The structure of oil droplets in the SNLs was evaluated using a fluorescence microscope (Olympus BX51) with an x100 oil immersion objective lens. Samples were stained with Nile Red (9-diethylamino-5H-benzo[a]phenoxazine-5-one, 0.25 mg.mL<sup>-1</sup> in dimethyl sulfoxide, 1:10 (dye:sample), v/v), which enabled the oil droplets to become visible. Slides were prepared by taking a portion of the stained SNLs solution and placing in a concave glass microscope slide and covering with a glass cover slip.

#### 3.6.5. Evaluation of degree of hydrolysis of proteins by Lowry method

Protein release was the method used to measure the digestibility of the protein phase. Gelatine and gelatine-SLN samples at the end of the salivary phase were mixed with all salts of the gastric phase (section 3.6.2.). The pH of the reaction was maintained at 3.0 by the addition of 0.05 mol.L<sup>-1</sup> HCl solution using an automatic titration unit (pH-stat method) (Titrand 902, Metrohm, Switzerland) during 2 h in a heated jacketed reactor at 37 °C under agitation. The gastric digestion experiment was started by adding 1.0 mL of a pepsin solution to achieve 3593 U.mL<sup>-1</sup> activity in the mixture. Titration was immediately turned on. At the end of the experiment, 2.59 mL of the gelatine samples were collected for further analysis of the final *DH* using the Lowry assay method to calculate the mean degree of dissociation of the carboxylic groups ( $\alpha_{COOH}$ ) produced in the reaction (Lowry *et al.*, 1951). Finally, the volumes of acid titrant were converted into *DH* (Equation 3):

$$DH = 100 \times \frac{V \times N}{m \times h_{tot}} \times \frac{1}{1 - \alpha} \quad \text{Equation 3}$$

where *V* is the volume of titrant (mL), *N* its normality (mg.mL<sup>-1</sup>), *m* is the protein mass (g), and *h<sub>tot</sub>* is the number of peptide bonds per mass (g) of proteins (Mat *et al.*, 2018).

#### 3.6.6. Evaluation of the release of free fatty acids

FFA release was the method used to measure the digestibility of the lipid phase. Samples at the end of the gastric phase were mixed with all salts of intestinal phase (section 3.6.2.). The pH was maintained at 7 by the addition of 0.05 mol.L<sup>-1</sup> NaOH solution using an automatic titration unit (pH-stat method) (Titrand 902, Metrohm, Switzerland) during 2 h in a heated jacketed reactor at 37 °C under agitation. The intestinal digestion experiment was started by adding the pancreatin solution. At the end of the incubation at pH 7, NaOH was added to quickly reach pH 9 stopping the reaction and promoting the FFA

release. The FFA release was determined through the volume of NaOH used to achieve pH 9 to guarantee full ionization and titration of FFA (Wrolstad *et al.*, 2004; Helbig *et al.*, 2012). Blank assays were performed, consisting in the digestion conducted without pancreatin, to establish the NaOH volume necessary to achieve pH 9. The amount of FFA were determined through **Equation 4** (Wrolstad *et al.*, 2004):

$$\text{FFA} = \frac{(V_{\text{NaOHsample}} - V_{\text{NaOHblank}}) \times C \times 1000}{V_{\text{sample}}} \quad \text{Equation 4}$$

where  $V_{\text{NaOHsample}}$  and  $V_{\text{NaOHblank}}$  are the volume of NaOH titrated in the sample and blank assays, respectively,  $C$  is the molar concentration of NaOH titrant, in this case  $0.05 \text{ mol.L}^{-1}$ , and  $V_{\text{sample}}$  is the total volume of the sample.

### 3.6.7. Curcumin bioaccessibility, stability and effective bioavailability

Curcumin bioaccessibility was assumed as the fraction of curcumin present inside the micelle phase, while stability was assumed as the fraction of curcumin present in the whole digesta at the end of the digestion. The digesta (10 mL) was centrifuged (Allegra 64R, Beckman Coulter Inc., USA) at 18 500 g at room temperature for 30 min, collecting the supernatant which was assumed as the micelle phase. Samples of digesta or micelle phase (5 mL) were mixed with 5 mL of chloroform using a vortex and centrifuged at 700 g at room temperature for 10 min. The bottom layer was collected, and the top layer was subjected again to the extraction procedure. The second bottom layer was added to the first one and analyzed in an UV-VIS spectrophotometer (V-560, Jasco, USA) at 422 nm. Curcumin concentration was determined through a calibration curve of absorbance versus curcumin concentration in chloroform.

The bioaccessibility, stability and bioavailability were determined through the following equations (**Equation 5**, **Equation 6**, **Equation 7**):

$$\text{Bioaccessibility (\%)} (B) = \frac{C_{\text{Micelle}}}{C_{\text{Digesta}}} \times 100 \quad \text{Equation 5}$$

$$\text{Stability (\%)} (S) = \frac{C_{\text{Digesta}}}{C_{\text{Initial}}} \times 100 \quad \text{Equation 6}$$

$$\text{Bioavailability (\%)} = B \times S \quad \text{Equation 7}$$

where  $C_{Micelle}$  and  $C_{Digesta}$  are the curcumin concentrations measured at the end of the digestion in micellar phase and raw digesta, respectively.  $C_{Initial}$  is the curcumin concentration present in the SLNs at the beginning of digestion process.

### 3.7. Statistical analyses

Statistical analyses were performed to every data from each of the experimental results. Therefore, the mean values and standard deviations of the experimental data were calculated. Statistical analysis was carried out using Analysis of Variance (ANOVA) and Tukey mean comparison test ( $p < 0.05$ ), resorting Origin® Pro 8 software (Massachusetts, USA).



# CHAPTER 4

---

## RESULTS AND DISCUSSION

#### 4.1. Development of SLNs

SLNs are typically composed of lipid matrix, emulsifier, co-surfactant, water, and bioactive compounds. In this work, SLNs encapsulating curcumin were prepared by beeswax as the lipid core, PHOSPHOLIPON 90G® (i.e., lecithin) as emulsifier and Tween 80 as co-surfactant. **Figure 8** shows the visual appearance of the produced SLNs.



**Figure 8.** Visual appearance of the developed SLNs.

#### 4.2. Physicochemical characterization of SLNs

The mean diameter, particle size distribution, and polydispersity index (PDI) are important properties for lipid-based nanoparticles characterization. Determination of the mean diameter is fundamental for characterizing and confirming if the desired dimensions were obtained, and especially, if they are maintained during storage (McClements, 2013).  $\zeta$ -potential can be used to evaluate the charge on the surface of nanoparticles, and it is considered as one of the parameters that can be used to reflect their stability (Shah, R., Eldridge, D., Palombo, E., Harding, 2015). SLNs were characterized in terms of the Z-average diameter, PDI, and  $\zeta$ -potential over 21 days of storage to assess their physical stability.

##### 4.2.1. Particle size

The changes in the Z-average diameter of the SLNs as a function of the storage time are shown in **Figure 9**. SLNs maintained their initial size ( $p > 0.05$ ) over 21 days of storage. The Z-average diameter slightly increased from  $125.5 \pm 4.3$  nm at the beginning of storage to  $132.4 \pm 3.3$  nm at the end of 21 days. This minimal change in the average particle diameter of SLNs was expected, as lipid-based nanoparticles generally show an increase in size upon storage (Gupta *et al.*, 2016). The increase of droplet size with time is due to the movement of dispersed droplet through the continuous phase that increases the

opportunities for droplets' collisions (Li and Chiang, 2012). Other authors developed SLNs loaded with curcumin by solvent evaporation method and studied their long-term stability. The results showed good stability of the SLNs, in which the mean diameter ranged from 130 nm to 180 nm and no significant variations were observed during six months of storage (Santonocito *et al.*, 2020).

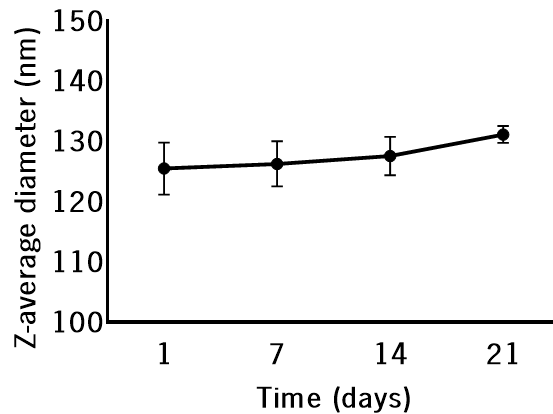


**Figure 9.** Evolution of Z-average diameter of the SLNs during 21 days of storage at 4 °C in the dark. The results are presented as the mean  $\pm$  SD.

The monodispersity of the SLNs can be evaluated by its PDI, which can range from 0 to 1 (with 0 being monodisperse and 1 being polydisperse). According to Tamjidi *et al.*, 2013, in order to obtain suspensions with long-term stability correlates with PDI, the PDI values should be in the range of 0.1–0.25. The changes in the PDI of the SLNs as a function of the storage time are shown in **Figure 10**.

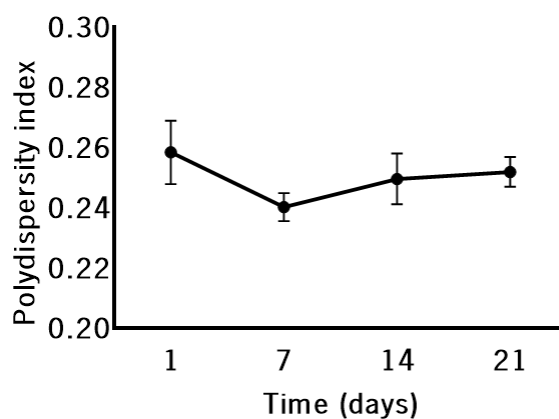


**Figure 10.** Evolution of PDI of the SLNs during 21 days of storage at 4 °C in the dark. The results are presented as the mean  $\pm$  SD.

The SLNs produced exhibit PDI values lower than 0.27, which indicates the existence of a narrow to moderate polydisperse population. The PDI at the beginning of storage was  $0.26 \pm 0.01$  remained the same ( $p > 0.05$ ) at the end of 21 days,  $0.26 \pm 0.02$ . In a previous study conducted by Kheradmandnia *et al.*, 2010 they developed ketoprofen-loaded SLNs (KP-loaded SLNs) made of beeswax and carnauba wax using Tween 80 and egg lecithin as emulsifiers. In their study they investigated the effect of surfactant composition on PDI of the KP-loaded SLNs and concluded that 50 % of Tween 80 in a surfactant mixture leads to a PDI of  $0.26 \pm 0.02$ . The results of this study are in agreement with their work since we use the same ratio of the surfactant mixture, i.e., 1:1 of Tween 80 and Phospholipon® 90G (lecithin) as surfactants.

#### 4.2.2. Particle charge

$\zeta$ -potential measurements allow predicting the stability of colloidal aqueous dispersions (Garud *et al.*, 2012).  $\zeta$ -potential of  $\pm 30$  mV indicates particle stability, where  $> \pm 30$  mV indicates a stable condition and  $< \pm 30$  mV indicates instability, aggregation, flocculation, etc. (Mahira *et al.*, 2020).  $\zeta$ -potential of the SLNs droplets can be positive, neutral or negative depending if a cationic, nonionic or anionic emulsifier, respectively, is selected (Zhang and McClements, 2018).

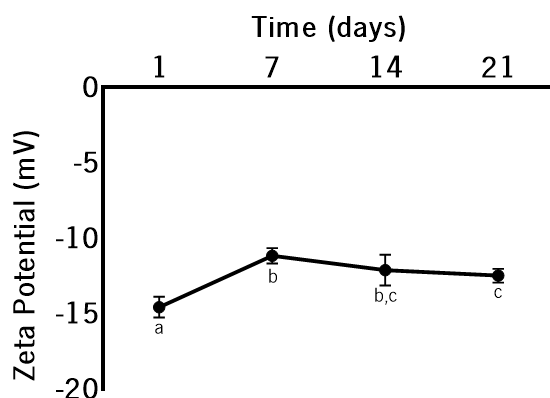


**Figure 11.** Changes of  $\zeta$ -potential of SLNs during 21 days of storage at 4 °C in the dark. The results are presented as the mean  $\pm$  SD. Different letters (a-c) indicate statistically significant between values ( $p < 0.05$ ).

$\zeta$ -potential of SLNs during 21 days of storage are represented in **Figure 11**. The surface charge of the SLNs over the 21 days of storage is negative, as expected since lecithin was used as surfactant. The surface charge of the SLNs was not maintained over 21 days of storage. In addition, the  $\zeta$ -potential values obtained are due to the combination of the steric effect caused by Tween 80 and the electrostatic

repulsion caused by lecithin (Soleimanian *et al.*, 2018). The  $\zeta$ -potential decreased ( $p < 0.05$ ) from  $-14.6 \pm 0.7$  mV at the beginning of storage to  $-12.5 \pm 0.5$  mV at the end of the storage (day 21). Since an absolute large negative or positive  $\zeta$ -potential is required for colloidal dispersion stability, the range of  $\zeta$ -potential values obtained for SLNs may not have been high enough to provide a strong electric field around the particles (Kheradmandnia *et al.*, 2010). This may explain the changes observed in the surface charge of the SLNs over the 21 days of storage. Kheradmandnia *et al.*, 2010 developed KP-loaded SLNs composed of beeswax and carnauba wax using Tween 80 and egg lecithin as emulsifiers. The results showed that combination of Tween 80 and egg lecithin had a significant effect on particle charge. The authors observed a slight variation of the  $\zeta$ -potential from -15 to -16 mV for SLNs prepared in the presence of 40 %, 50 %, and 60 % of Tween 80. These results are similar to those obtained in the present work, since a 1:1 ratio of Tween 80 and Phospholipon® 90G (lecithin) was used and a  $\zeta$ -potential value of  $-14.58 \pm 0.69$  mV was obtained after the preparation of the SLNs (day 1).

#### 4.2.3. Temperature stability

Heating is a common processing treatment in food industry. Therefore, it is crucial to evaluate the thermal stability of delivery systems at a temperature range of at least 20–80 °C (Simões *et al.*, 2020). The effect of temperature on particle size and PDI of the developed SLNs was evaluated at those conditions.

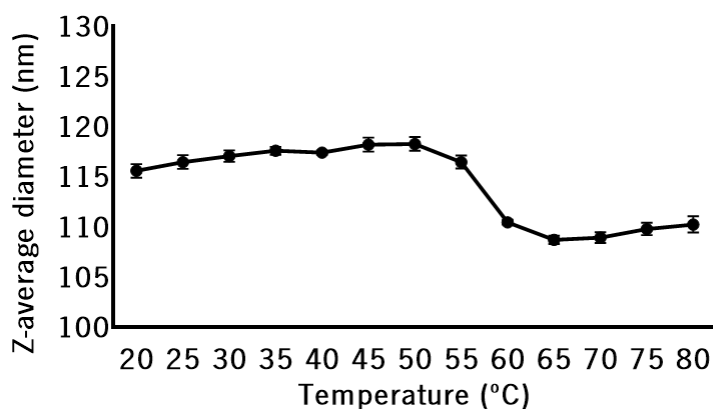


**Figure 12.** Effect of temperature on the Z-average diameter of the SLNs. The results are presented as the mean  $\pm$  SD.

**Figure 12** shows the effect of temperature on the Z-average diameter of the SLNs. The Z-average diameter decreased ( $p < 0.05$ ) from  $115.6 \pm 0.69$  nm at 20 °C to  $110.3 \pm 0.81$  nm at 80 °C. The Z-average

diameter was below 120 nm, independently of temperature. The particle size of SLNs did not change significantly ( $p>0.05$ ) for temperatures below 55 °C.

**Figure 13** shows the effect of temperature on the PDI of the SLNs. The PDI at the 20 °C was  $0.24 \pm 0.00$  and  $0.23 \pm 0.00$  at 80 °C. The PDI values of SLNs were always below 0.27, independently of temperature, indicating a good homogeneity within a narrow size distribution.

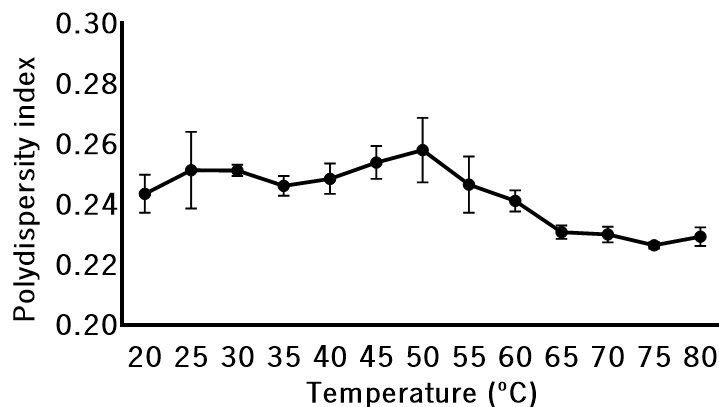


**Figure 13.** Effect of temperature on the PDI of the SLNs. The results are presented as the mean  $\pm$  SD.

It is possible to observe a decrease ( $p<0.05$ ) in both Z-average diameter and PDI of SLNs between 55 °C and 80 °C. This decrease is probably related to the melting and crystallization temperatures of beeswax. In fact, other authors studied the thermal behaviour of beeswax through DSC. The results showed that in the exothermic process the crystallization onset temperature ( $T_{oc}$ ) was at  $61.47 \pm 0.02$  °C and the dominant crystallization peak ( $T_c$ ) was at  $57.15 \pm 0.09$  °C. For the endothermic process, a clear melting onset temperature ( $T_{om}$ ) was observed at  $50.64 \pm 0.04$  °C, where the maximum melting peak ( $T_m$ ) appeared at  $63.09 \pm 0.06$  °C (Arredondo-Ochoa *et al.*, 2017).

### 4.3. Incorporation of SLNs into gelatine

In recent years, many studies have shown the use of curcumin as a functional ingredient and its incorporation into food products. To be successfully incorporated into a food product, SLNs need to be stable in the complex food and should be able to stabilize curcumin by preventing degradation both in the SLNs and in the food product (Aditya *et al.*, 2015). In this work, the SLNs containing curcumin were incorporated into a gelatine matrix, which was selected as a real food model. Thus, gelatine control (i.e., without SLNs) and gelatine-SLNs were prepared (**Figure 14**).

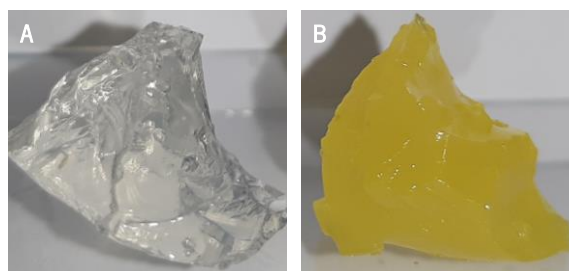


**Figure 14.** Visual appearance of gelatine (A) and gelatine-SLNs (B).

#### 4.3.1. Physicochemical characterization

The Z-average diameter, PDI, and  $\zeta$ -potential were analysed using DLS to evaluate the effect of the incorporation of the SLNs into gelatine. The Z-average diameter of SLNs and gelatine-SLNs is shown in **Figure 15**. There are no significant differences ( $p > 0.05$ ) between the Z-average diameter of SLNs and gelatine-SLNs ( $162.9 \pm 3.9$  nm and  $173.5 \pm 3.9$  nm, respectively). Thus, the incorporation of SLNs into gelatine does not affect its Z-average diameter. These results are in accordance with other works Park *et al.*, 2019 developed turmeric extract-loaded nanoemulsion (TE-NE) and studied its stability into milk as a colloidal food model. The Z-average diameter of the TE-NE and TE-NE incorporated in the milk were also not statistically different.

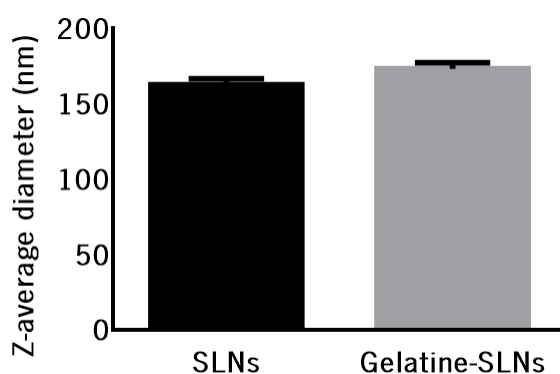


**Figure 15.** Z-average diameter of the SLNs and gelatine-SLNs. The results are presented as the mean  $\pm$  SD.

**Figure 16** shows the PDI of the SLNs and gelatine-SLNs. The PDI values were  $0.25 \pm 0.02$  and  $0.27 \pm 0.01$ , respectively, for the SLNs and gelatine-SLNs. The fact that gelatine-SLNs have a PDI below 0.3 just like SLNs means that the incorporation of SLNs into gelatine does not affect this parameter, which is in agreement with the results obtained in the Z-average diameter measurement.

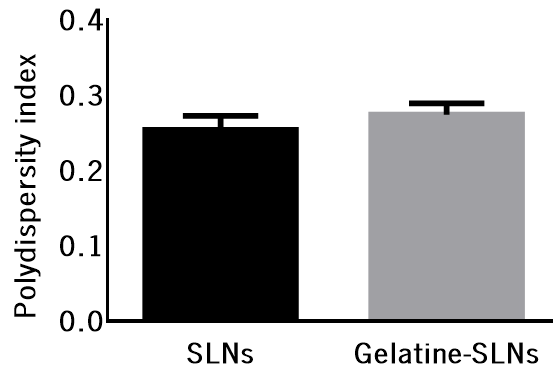


**Figure 16.** PDI of the SLNs and gelatine-SLNs. The results are presented as the mean  $\pm$  SD.

**Figure 17** shows the  $\zeta$ -potential of the gelatine, SLNs, and gelatine-SLNs. The  $\zeta$ -potential of the gelatine, SLNs, and gelatine-SLNs were  $1.6 \pm 0.1$  mV,  $-16.6 \pm 0.9$  mV, and  $0.5 \pm 0.2$  mV, respectively.  $\zeta$ -potential of SLNs and gelatine-SLNs is different and this is due to the fact that gelatine has a slightly positive  $\zeta$ -potential. Since the  $\zeta$ -potential measures the surface charge of the particles, the fact that the surface charge of the SLNs has been altered suggests that the gelatine compounds adhered to the surface of the SLNs.

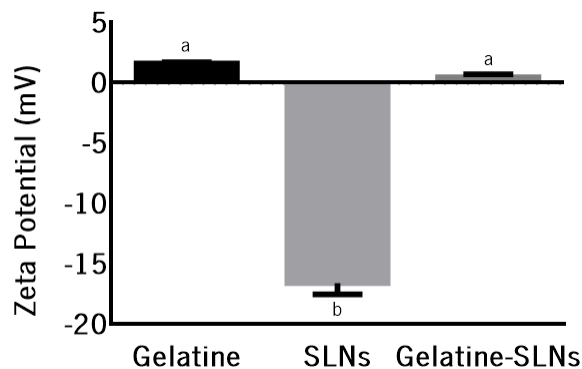


**Figure 17.**  $\zeta$ -potential of gelatine, SLNs, and gelatine-SLNs. The results are presented as the mean  $\pm$  SD. Different letters (a-b) indicate statistically significant between values ( $p < 0.05$ ).

#### 4.4. Evaluation the effects of SLNs incorporation in gelatine shelf life

##### 4.4.1. Colour evolution

Colour is an important factor since it directly influences product appearance and thus, consumer acceptability. Curcumin is one of the most commonly used natural food colorants. To better understand the colour change in gelatine-SLNs, colorimetric parameters were analysed at days 1, 7, 14, and 21 of



storage, and gelatine was used as a control. The evolution of TCD of gelatine and gelatine-SLNs during 21 days of storage at 4 °C in the dark are represented in **Figure 18**.

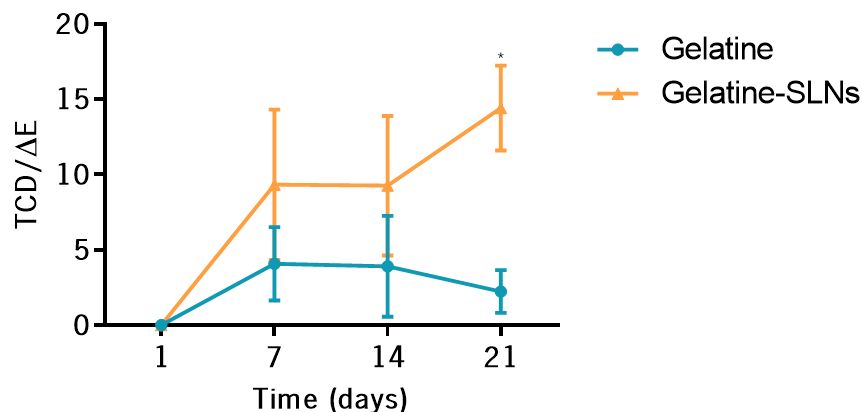


**Figure 18.** Evolution of TCD/ΔE of gelatine and gelatine-SLNs during 21 days of storage at 4 °C in the dark. \* significantly different from correspondent values in gelatine from same day ( $p < 0.05$ ).

Values of TCD of the gelatine were  $4.08 \pm 2.44$  and  $2.23 \pm 1.42$  for days 7 and 21, respectively. For gelatine-SLNs the values of TCD for days 7 and 21 were  $9.33 \pm 4.99$  and  $14.41 \pm 2.81$ , respectively. During the 21 days of storage, the TCD of the gelatine remained constant ( $p > 0.05$ ). However, for gelatine-SLNs, significant differences ( $p > 0.05$ ) were observed between day 1 and the remaining days (7, 14 and 21). From the day 7, there was no significant ( $p > 0.05$ ) change in TCD over time for the gelatine-SLNs. The variation of TCD is caused by changes in the colour parameters  $L^*$ ,  $a^*$ , and  $b^*$  (Annex I). The parameter  $b^*$  (yellowness) increased in gelatine-SLNs by the addition of SLNs that are yellow, due to the presence of curcumin. Gelatine and gelatine-SLNs only showed a significant difference ( $p < 0.05$ ) on day 21. The main factor responsible for this change is the parameter  $b^*$ , which becomes less negative, i.e., on day 21 the colour is more reddish than on the others. This variation is probably related to curcumin degradation reactions (Priyadarsini, 2014; Chuachoen *et al.*, 2019). Thus, considering the ability of curcumin to confer colour, incorporation of this bioactive compound in SLNs is an advantage, as it can be used as a natural dye in gelatine. In addition, SLNs also provide protection to curcumin, maintaining its beneficial properties in foods. Kumar *et al.*, 2016 prepared curcumin nanoemulsions with milk protein and evaluated its incorporation into ice cream. The colour was evaluated 24 h after the nanoemulsion incorporation and the results showed that was no significant difference between the control ice cream (without curcumin) and ice cream with curcumin nanoemulsions incorporated.

## 4.4.2. Texture evolution

TPA test consists of compressing a food sample twice, in a reciprocating motion that imitates the action of the jaw. TPA test was applied to study the textural characterization of gelatine and gelatine-SLNs and assess the effect of the storage in during shelf life (days 1, 7, 14, and 21). **Figure 19** shows the resulting force-time curves obtained from TPA test of gelatine and gelatine-SLNs over 21 days of storage.

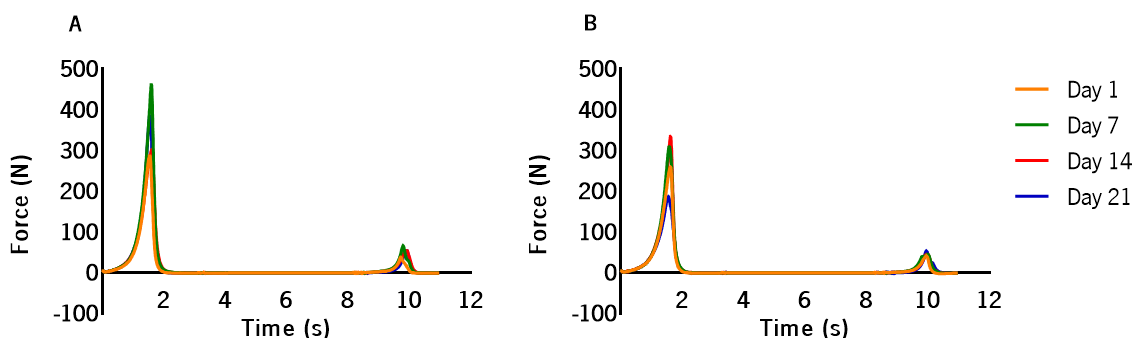


**Figure 19.** Force-time curve obtained from TPA test of gelatine (A) and gelatine-SLNs (B) over 21 days of storage at 4 °C in the dark. The results are presented as the mean.

Textural parameters obtained from the force-time curve have been described by Bourne, 2002. Hardness is the most assessed parameter for texture analyses, being defined as the necessary force to attain a given deformation. Adhesiveness is the work required to overcome the forces of attraction between the material and the probe surface. In practical terms, adhesiveness is the force necessary to separate the material that sticks to the teeth during feeding. Chewiness is the labour (also related with the time) required to chew a sample until it is reduced to a state suitable for consumption. Gumminess is defined as the energy required to break a semi-solid food into fragments until it is ready to swallow (Mousavi *et al.*, 2019).

Experimental values of the hardness, adhesiveness, gumminess, and chewiness are listed in **Table 3**. There are no significant differences ( $p > 0.05$ ) in the different textural parameters over the 21 days of storage for gelatine and gelatine-SLNs. Moreover, there are also no significant differences ( $p > 0.05$ ) when the same days were compared between the gelatine and gelatine-SLNs. It is possible to conclude that the texture attributes of gelatine and gelatine-SLNs are stable during the 21 days of storage. Furthermore, the addition of SLNs into gelatine does not affect the stability or texture parameters of the gelatine.

**Table 3.** Textural parameters obtained from the force-time curve from TPA test of gelatine and gelatine-SLNs over 21 days of storage at 4 °C in the dark. The results are presented as the mean  $\pm$  SD.

Days	Hardness (N)	Adhesiveness (N.s)	Gumminess	Chewiness
<b>Gelatine</b>				
1	302.5 $\pm$ 87.4	-5.0 $\pm$ 1.1	33.7 $\pm$ 8.4	26.3 $\pm$ 8.5
7	451.7 $\pm$ 28.3	-4.8 $\pm$ 0.8	68.7 $\pm$ 24.8	53.1 $\pm$ 20.9
14	325.3 $\pm$ 158.1	-4.9 $\pm$ 0.6	50.0 $\pm$ 19.6	38.9 $\pm$ 16.2
21	394.1 $\pm$ 88.4	-4.6 $\pm$ 0.3	49.3 $\pm$ 13.1	36.0 $\pm$ 11.1
<b>Gelatine-SLNs</b>				
1	256.0 $\pm$ 94.9	-4.2 $\pm$ 1.0	31.8 $\pm$ 7.3	22.7 $\pm$ 9.3
7	318.2 $\pm$ 99.9	-4.5 $\pm$ 1.4	47.7 $\pm$ 24.9	34.2 $\pm$ 21.5
14	369.7 $\pm$ 109.4	-4.3 $\pm$ 1.6	43.5 $\pm$ 21.5	32.2 $\pm$ 16.2
21	210.4 $\pm$ 68.7	-3.5 $\pm$ 2.1	39.4 $\pm$ 18.7	26.3 $\pm$ 9.6

Campo *et al.*, 2019 incorporated zeaxanthin nanoparticles (Zea-NP) and zeaxanthin nanoemulsions (Zea-NE) in yogurts. The results from textural analysis showed that the control yogurt presented higher firmness and consistency than yogurt with zeaxanthin nanoparticles and yogurt with zeaxanthin nanoemulsions. The authors explained that the addition of Zea-NP and Zea-NE in yogurt promoted a decrease in firmness and consistency due to the water content and zeaxanthin extract present in the nanoparticles and nanoemulsion formulation. The results of the present work are not in accordance with this study since there were no differences in the texture parameters of gelatine with SLNs and control gelatine. In fact, in the present work, for the preparation of the gelatine-SLNs sample, the same proportion of water present in the control gelatine was maintained, in order to eliminate the effects of other alteration in gelatine formulation besides the presence of SLNs.

#### 4.4.3. Rheology evolution

To evaluate the viscoelasticity behaviour of the gelatine and gelatine-SLNs, dynamic rheology was used at days 1, 7, 14, and 21 of storage. Frequency sweep experiments revealed that 1 Hz was within the LVR (Annex II). During rheological measurements  $G'$  was higher than  $G''$  for both gelatine and gelatine-SLNs over the 21 days, as expected since gelatine is a solid structure (Annex III). This means that gelatine showed predominantly a solid-like behaviour and the incorporation of SLNs did not alter this performance.

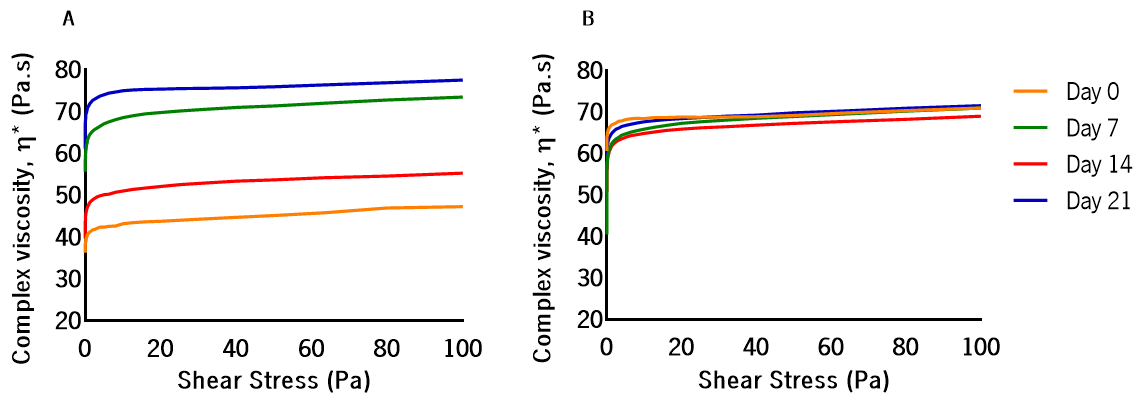


**Figure 20.** Complex viscosity ( $\eta^*$ ) versus time curve obtained from gelatine (A) and gelatine-SLNs (B) over 21 days of storage at 4 °C in the dark. The results are presented as the mean.

**Figure 20** shows the resulting  $\eta^*$  versus time curves obtained of gelatine and gelatine-SLNs over 21 days of storage. In general,  $\eta^*$  of the gelatine increases ( $p < 0.05$ ) over time, as expected since storage at 4 °C aids gelatine solidification. Gelatine-SLNs sample has higher  $\eta^*$  values on day 0 than gelatine. The results demonstrate that the incorporation of SLNs helps improving the solid behaviour of gelatine because gelatine control seems to take longer to reach the degree of solid behaviour exhibited by gelatine-SLNs sample from day 0. In this way, the addition of the SLNs into gelatine promoted a better  $\eta^*$  behaviour than gelatine without SLNs, due to its ability to maintain  $\eta^*$  constant during storage period, suggesting a promising application in food.

#### 4.5. *In vitro* digestion behaviour of gelatine with SLNs incorporated

SLNs may be designed to retain bioactive compounds during storage within a food product but control their release when they encounter specific environmental conditions, such as the ones found in the GI tract (Zhang and McClements, 2018). A number of studies have evaluated the behaviour of lipid-based nanoparticles within simulated gastrointestinal conditions, which have been reviewed in recent publications (Singh *et al.*, 2009; Golding *et al.*, 2011; Singh and Sarkar, 2011; McClements and Xiao, 2012; McClements, 2013).

The changes in size,  $\zeta$ -potential and morphology of the SLNs and gelatine-SLNs at different stages of the simulated *in vitro* digestion process, namely initial (before digestion), oral phase (mouth), gastric phase (stomach) and intestinal phase (intestine) were determined, as well as protein hydrolyse, release of FFA, and curcumin bioaccessibility, stability, and bioavailability.

## 4.5.1. Influence of digestion on particle size

**Figure 21** shows the Z-average diameter of SLNs and gelatine-SLNs at different stages of the simulated *in vitro* digestion. The Z-average diameter of SLNs and gelatine-SLNs were  $162.9 \pm 3.9$  nm, and  $173.5 \pm 3.9$  nm, respectively, before the *in vitro* digestion. There are no statistically significant differences ( $p > 0.05$ ) in the Z-average diameter of the SLNs over the four stages of digestion, which suggest that SLNs were relatively stable. It was expected that in the gastric phase there would be no significant increase in Z-average diameter since Tween 80 was used. It is known that this non-ionic surfactant provides steric stabilization and resistance to agglomeration in low pH (McClements, 2013).

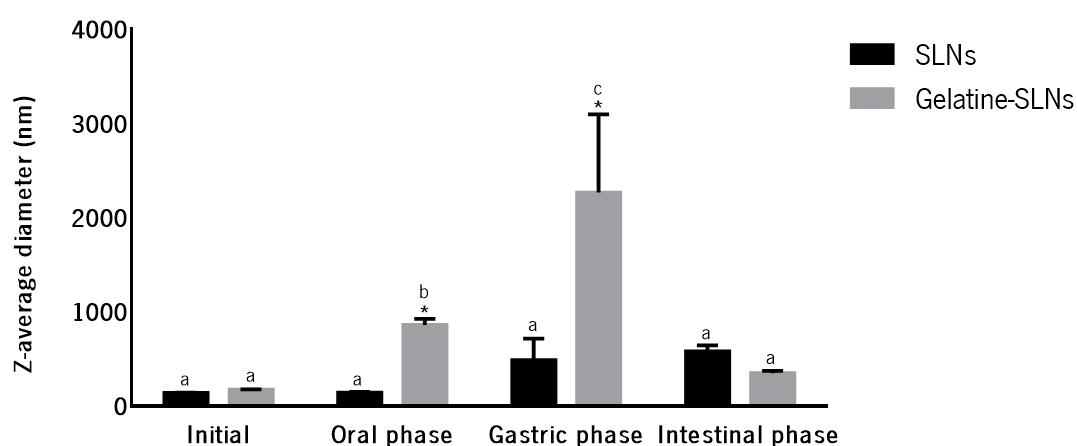


**Figure 21.** Z-average diameter of SLNs and gelatine-SLNs as they undergo the different stages of *in vitro* digestion. The results are presented as the mean  $\pm$  SD. \*significantly different from correspondent values in SLNs in the same phase ( $p < 0.05$ ). Different letters (a-c) indicate statistically significant between values from same sample during different phases ( $p < 0.05$ ).

The Z-average diameter of the gelatine-SLNs was relatively similar ( $p > 0.05$ ) between initial and intestinal phase. However, the Z-average diameter of the gelatine-SLNs increased ( $p < 0.05$ ) in the oral and gastric phases, which is confirmed by microscopy images that shows an aggregation of the droplet particles (**Figure 24**). This increase could be attributed to aggregation due to the action of the digestive enzymes as well as changes in pH and ionic strength (Pinheiro *et al.*, 2013). According to Yvon *et al.*, 1992, it is in the stomach that almost all the protein is hydrolysed by pepsin, being the low pH values and high ionic force parameters that have a high impact in denaturation of proteins during the gastric digestion. In fact, under the acidic conditions of the gastric phase, gelatine-SLNs were mixed with fluids, enzymes (i.e., pepsin) and the hydrolysis of proteins initiates. Since gelatine is mostly composed by protein, the action of protein-digesting enzymes in the gastric phase originates the gelatine matrix degradation and,

consequently, the SLNs that are incorporated in the gelatine may have been destabilized as well, leading to an increase in the Z-average diameter of the SLNs. The same reasons can explain the significant differences ( $p < 0.05$ ) in the Z-average diameter between gelatine-SLNs and SLNs in the oral and gastric phases. In addition, during the gastric phase, the products resulting from the hydrolysis of gelatine may have been adsorbed on the surface of SLNs leading to an increase in the Z-average diameter of gelatine-SLNs. The decrease in the Z-average diameter of the SLNs in the intestinal phase may suggest that the particles were digested and therefore their size became smaller. Our results of the intestinal phase are contrary to the study conducted by Aditya *et al.*, 2014, which developed and evaluated lipid nanocarriers, namely, SLNs, NLCs, and nanoemulsions to increase the bioaccessibility of quercetin. In Aditya's work, all three types of nanocarriers were stable under the simulated stomach conditions, however, after the simulated intestinal conditions, there was a significant increase in the size of all three types of nanocarriers. Pinheiro *et al.*, 2016 and Silva *et al.*, 2019 also obtained an increase in the droplet size of the nanoemulsions after intestinal phase, which they explain to be related to the action of the lipase enzyme that hydrolyses the lipids, producing FFA, MAG, and DAG leading to aggregation of the particles.

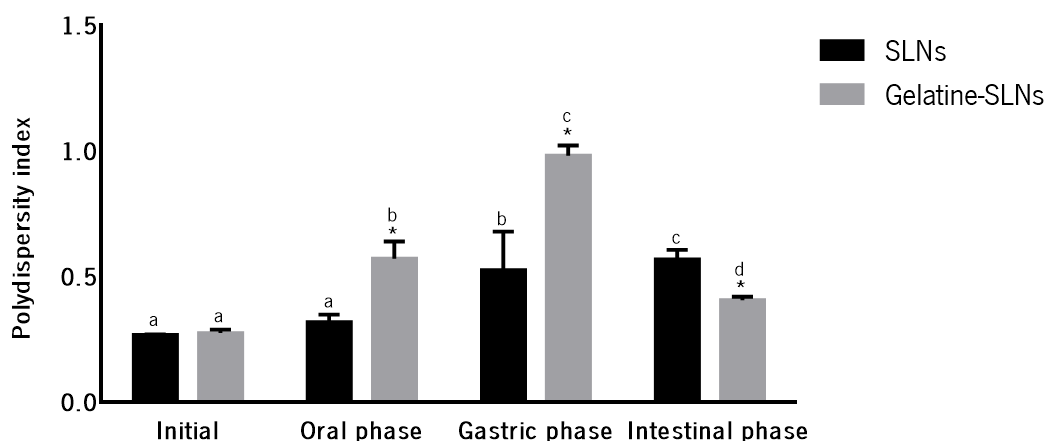


**Figure 22.** PDI of SLNs and gelatine-SLNs as they undergo the different stages of *in vitro* digestion. The results are presented as the mean  $\pm$  SD. \*significantly different from correspondent values in SLNs in the same phase ( $p < 0.05$ ). Different letters (a-d) indicate statistically significant between values from same sample during different phases ( $p < 0.05$ ).

**Figure 22** shows the PDI of SLNs and gelatine-SLNs at different stages of the simulated *in vitro* digestion. The PDI can range from 0 to 1 (with 0 being monodisperse and 1 being polydisperse). After the oral phase, the PDI values of the SLNs remained relatively similar, contrary to the behaviour in the gastric and intestinal phases, in which an increase ( $p < 0.05$ ) was observed. The PDI values of the gelatine-SLNs increased in the oral and gastric phases and decreased in the intestinal phase, following the same trend

as the size results (**Figure 21**). The observed increase in PDI values along digestion is related to the various pH conditions and ionic strength, as well as the action of the digestive enzymes, namely protein-digesting enzymes in the gastric phase and lipid-digesting enzymes present in the intestinal phase. In the oral, gastric, and intestinal phases, the PDI of the gelatine-SLNs is significantly different from SLNs ( $p < 0.05$ ), which means that the gelatine matrix had an influence on the dispersion of the SLNs since the sample gelatine-SLNs is not homogeneous. Moreover, the products resulting from the hydrolysis of gelatine may have been adsorbed on the surface of SLNs leading to an increase in the PDI of the gelatine-SLNs during gastric phase.

#### 4.5.2. Influence of digestion on particle charge

**Figure 23** shows the  $\zeta$ -potential of SLNs and gelatine-SLNs at different stages of the simulated *in vitro* digestion. Before the *in vitro* digestion, the  $\zeta$ -potential of SLNs and gelatine-SLNs were  $-22.5 \pm 0.6$  mV and  $0.5 \pm 0.2$  mV, respectively. After the *in vitro* digestion,  $\zeta$ -potential of the SLNs did not change significantly ( $p > 0.05$ ), suggesting that there was not a major change in interfacial surface charge. The surface charge of the gelatine-SLNs did not change significantly ( $p > 0.05$ ) from the initial values to the oral phase. The surface charge of the SLNs significantly decreased ( $p < 0.05$ ) after the oral phase, reaching more negative values. The  $\zeta$ -potential of the SLNs and gelatine-SLNs changed to positive values at the gastric phase since a change in pH and ionic strength may alter the electrical charge on ionic groups (McClements, 2013). These results are in agreement with the results of study conducted by Silva *et al.*, 2019. These authors developed curcumin nanoemulsions and curcumin multilayer nanoemulsions and evaluated the curcumin bioaccessibility using a dynamic GI tract. The results showed that  $\zeta$ -potential of the nanoemulsions at gastric conditions also changed from negative to positive values. The  $\zeta$ -potential of the SLNs and gelatine-SLNs changed to negative values at the intestinal phase. These results suggest that the anionic components, such as bile salts or FFA were adsorbed onto the surface of the SLNs conferring them the negative charge (Salvia-Trujillo *et al.*, 2019; Silva *et al.*, 2019; Tan *et al.*, 2020). In the all phases of digestion, the  $\zeta$ -potential values of the gelatine-SLNs are significantly different from the ones of SLNs ( $p < 0.05$ ).

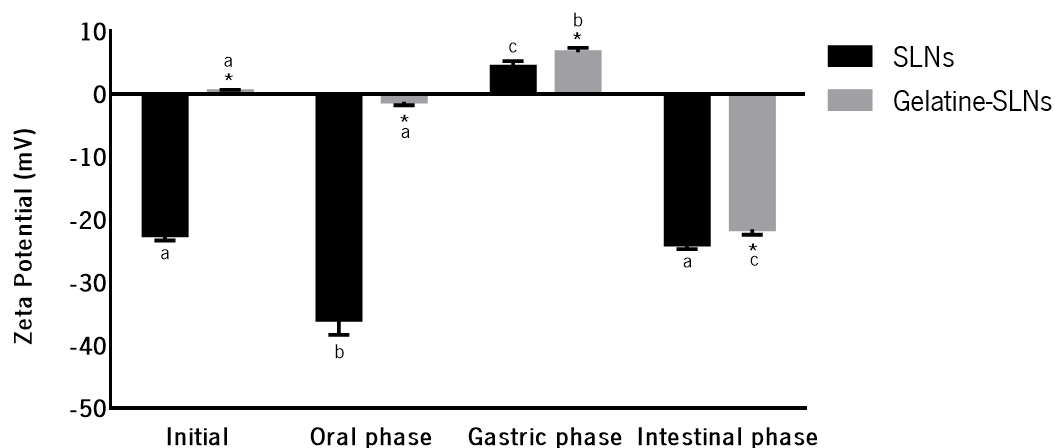


**Figure 23.**  $\zeta$ -potential of SLNs and gelatine-SLNs as they undergo the different stages of *in vitro* digestion. The results are presented as the mean  $\pm$  SD. \*significantly different from correspondent values in SLNs in the same phase ( $p < 0.05$ ). Different letters (a-c) indicate statistically significant between values from same sample during different phases ( $p < 0.05$ ).

#### 4.5.3. Influence of digestion on morphology

The morphology of the SLNs and gelatine-SLNs at each stage of the simulated *in vitro* digestion was evaluated by fluorescence microscopy (**Figure 24**). Since the Nile Red dye only stains the oil, in the microscopy images we observe exclusively the SLNs and not the constituents of the gelatine. The microscopy images showed that SLNs maintains its size throughout the different stages of digestion, which corroborates the results of the Z-average diameter (**Figure 21**). Before digestion, the images showed that SLNs incorporated in gelatine contain lower droplets compared with the ones present in the different phases of digestion, which is in accordance with the Z-average diameter results (**Figure 21**). Except for the gastric phase of the gelatine-SLNs, in the remaining phases of digestion the SLNs exhibit a spherical morphology. However, during the oral and gastric phases, aggregates have been formed, which is in accordance with the increase of Z-average diameter of the SLNs incorporated into gelatine observed in these phases. In the gastric phase, it is possible to observe some flocculation in the SLNs incorporated in the gelatine which may be related to the fact that the products resulting from the hydrolysis of the gelatine may have been adsorbed on the surface of the SLNs. However, the oil droplets are again dispersed in the intestinal phase, hence the observed decrease in the Z-average diameter results from the gastric phase to the intestinal phase. The images of the intestinal phase demonstrate that the size of the SLNs in this phase is lower than the size found in the previous phases but slightly larger than the size observed in the initial phase, which once again corroborates the results of the Z-average diameter.



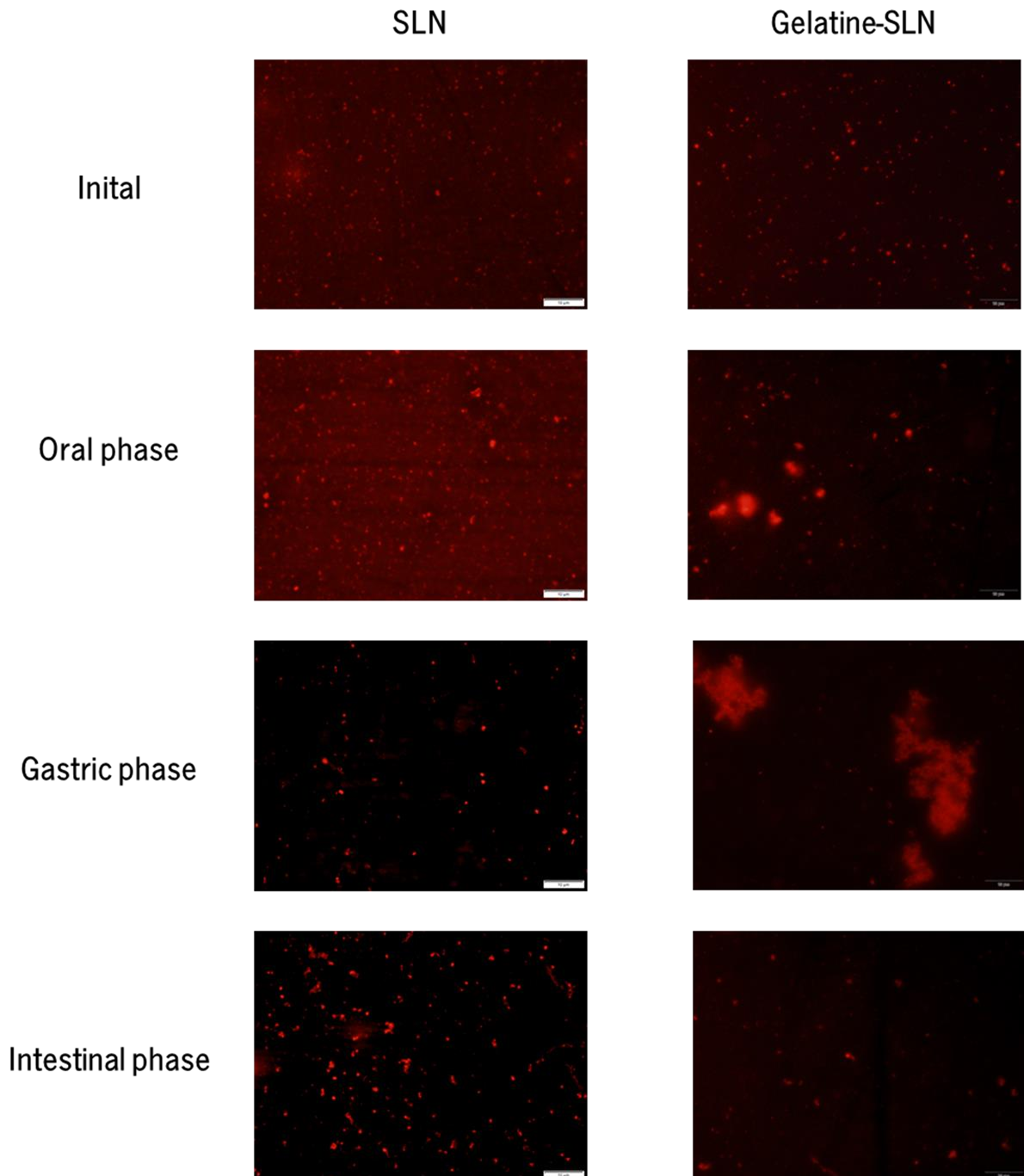


**Figure 24.** Microscopy images of the SLNs and gelatine-SLNs as they undergo the different stages of the simulated *in vitro* digestion.

#### 4.5.4. Evaluation of protein hydrolysis

Several studies have been shown that pH-stat technique can be used during the intestinal phase of *in vitro* digestion to monitor both the lipolysis and proteolysis of foods (Asselin *et al.*, 1989; McClements and Li, 2010a; Mat *et al.*, 2016). Considering the high number of studies in which this technique is applied to evaluate the digestion at intestinal phase, it is surprising that the use of the pH-stat technique

during the gastric phase is little explored. In this work, the evaluation of protein hydrolysis was studied using the pH-stat method to monitor the protein hydrolysis during the gastric phase of the simulated *in vitro* digestion of the control gelatine and gelatine-SLNs.

The *DH* estimated using the Lowry method at the end of the gastric digestion for the gelatine sample was  $47.3 \pm 1.9$  %. Reversing the Eq. (3) with a *DH* of 47.3 % and a titrant volume at the end of the gastric digestion of gelatine of 0.85 mL added, leads to a mean degree of dissociation of peptide's C-terminus carboxylic groups ( $\alpha\text{COOH}$ ) of 0.998. Thus, using the equation and the  $\alpha\text{COOH}$  calculated, it was possible to estimate the *DH* (%) of each volume added over the 2 h of the gastric stage (**Figure 25**).

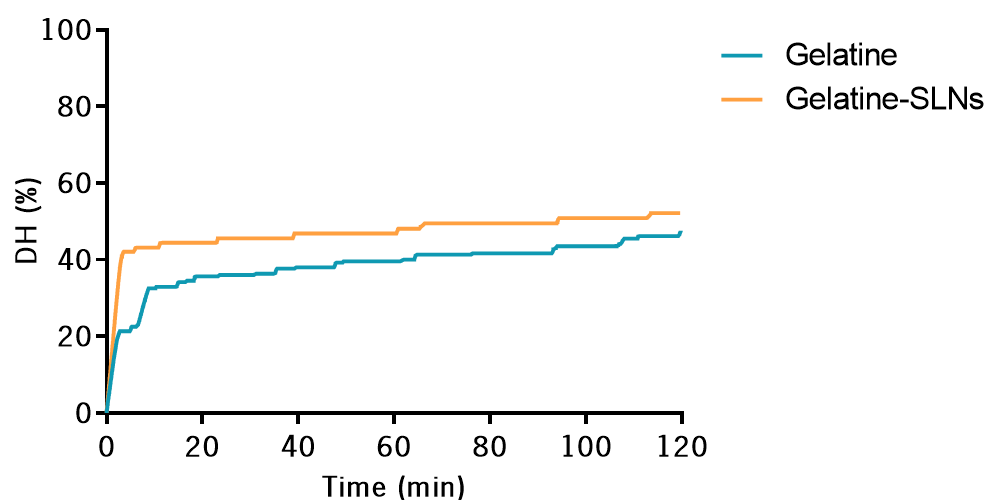


**Figure 25.** *DH* (%) during the protein hydrolysis in the simulated gastric digestion of the gelatine and gelatine-SLNs.

*DH* (%) of protein in the gelatine and gelatine-SLNs were 47.8 % and 52.2 %, respectively, at the end of the gastric digestion. These results are in line with what was expected since although gelatine contains other components, it is mostly composed by proteins, which are hydrolysed at this stage by pepsin. The trend observed is typical of an enzymatic reaction, with a high initial rate of reaction followed by a progressive slowdown.

#### 4.5.5. Evaluation of release of free fatty acids

The extent of lipolysis was evaluated by determining the amount of FFA release from SLNs and gelatine-SLNs using the pH-stat method. The volume of NaOH that was added into the gelatine and gelatine-SLNs to maintain a constant pH of 7 was then measured as a function of digestion time, and then the amount of FFA released from the mixture was calculated. **Figure 26** shows the results of the production of total

FFA during the simulated intestinal *in vitro* digestion of gelatine and gelatine-SLNs. The total production of FFA after the simulated intestinal digestion of the gelatine, gelatine-SLNs, and SLNs were  $23.4 \pm 4.2 \mu\text{mol.mL}^{-1}$ ,  $28.0 \pm 2.2 \mu\text{mol.mL}^{-1}$ , and  $14.7 \pm 2.5 \mu\text{mol.mL}^{-1}$  respectively. Gelatine-SLNs have slightly more production of FFA than gelatine. However, this difference is not statistically significant ( $p > 0.05$ ).

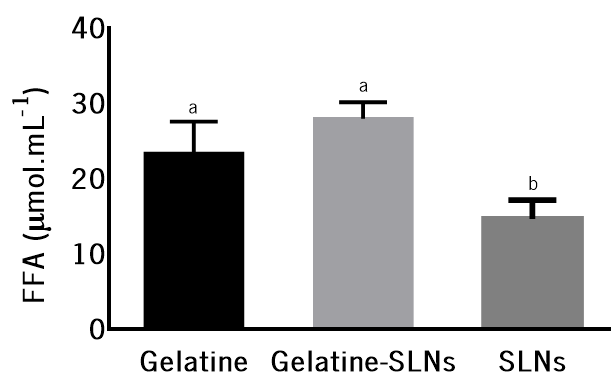


**Figure 26.** Total production of FFA after the simulated intestinal digestion of the gelatine, gelatine-SLNs, and SLNs. Different letters (a-b) indicate statistically significant between values ( $p < 0.05$ ).

Gelatine samples showed a higher concentration of FFA than the SLNs, however, these results should be carefully analysed, since it is possible that hydrolysis of gelatine protein occurs due to the action of the protease present in pancreatin. In fact, during the hydrolysis of proteins, amino acids are formed that lower the pH, as well as the FFA, and can influence the results. On the other hand, gelatine is not composed exclusively of proteins and may have other oil components that were hydrolysed into FFA in the intestinal phase. Moreover, SLNs have lipids in their constitution that can be hydrolysed at this stage, contributing to the increase in the concentration of FFA produced, however this amount is not enough to make a difference statistic. These results suggest that incorporation of the SLNs into gelatine may be useful for controlling the rate of lipid digestion and FFA adsorption within the GI tract, but it does not totally prevent the adsorption of pancreatin to the lipid droplet and their consequent digestion. These results are similar to the ones of Pinheiro *et al.*, 2013. These authors evaluated the behaviour of curcumin nanoemulsions during *in vitro* digestion. The results showed that the nanoemulsions stabilized with Tween 20 produced around  $20 \mu\text{mol.mL}^{-1}$  of FFA after the intestinal phase.

#### 4.5.6. Curcumin bioaccessibility, stability and bioavailability

Curcumin has numerous biological and pharmacological activities that may be beneficial to human health. However, pure curcumin has low water solubility, poor chemical stability, and low bioavailability, mainly due to low bioaccessibility and chemical transformation owing to metabolic enzymes present in the GI tract. As discussed before, one of the most effective approaches to protect curcumin against chemical degradation, increasing its water dispersibility, and improving its bioavailability is to use encapsulation technologies. The bioavailability of curcumin can be enhanced by retarding its metabolism, increasing its bioaccessibility, and/or promoting its absorption. Encapsulation of curcumin within a lipid phase can increase their bioaccessibility and chemical stability. Furthermore, the use of a digestible lipid phase leads to the production of lipid digestion products that are incorporated into mixed micelles. These mixed micelles can then solubilize curcumin, thereby increasing its bioaccessibility. (Zheng and McClements, 2020). Most studies have shown that the health effects of a bioactive compound within a food matrix are generally higher than that of the free form (Dima *et al.*, 2020). Measuring bioaccessibility after *in vitro* digestion is of the utmost importance once it provides information about the potential health benefits of curcumin loaded into SLNs. Therefore, the curcumin concentrations in the whole digesta and in the mixed micelle phase collected after intestinal digestion of the gelatine-SLNs were measured. The concentration in the whole digesta (before centrifugation) is a measure of the amount of curcumin that has not been chemically degraded. The concentration in the mixed micelle phase (collected after centrifugation) is a measure of the amount of curcumin that is chemically stable, solubilized within the mixed micelles, and ready for intestinal absorption. These values were used to calculate the bioaccessibility and stability of curcumin, i.e., the fraction of curcumin in the raw digesta that was solubilized within the mixed micelles and the fraction of curcumin present in the whole digesta at the end of the digestion, respectively. Then, by calculating these two parameters, it was possible to estimate bioavailability.

The bioaccessibility, stability, and bioavailability of curcumin after *in vitro* digestion of SLNs and gelatine with SLNs incorporated were measured as the curcumin concentration presented in mixed micelles (Figure 27).

The bioaccessibility of curcumin after the *in vitro* digestion of the SLNs and gelatine-SLNs were  $53.3 \pm 3.7 \%$  and  $46.7 \pm 12.7 \%$ , respectively. Curcumin bioaccessibility after *in vitro* digestion is not statistically different ( $p > 0.05$ ) when in SLNs or gelatine-SLNs, which are in agreement with the results of FFA. Curcumin bioaccessibility tends to increase with digestion time, and this behaviour can be attributed to the formation of digestion products that have the ability to form mixed micelles capable of solubilizing

highly lipophilic components such as curcumin (Pinheiro *et al.*, 2013). Campo *et al.*, 2019 incorporate zeaxanthin nanoparticles and zeaxanthin nanoemulsion in yogurt. The results showed that after of *in vitro* digestion the bioavailability was  $3.66 \pm 0.07$  % for Y-NP (yogurt-zeaxanthin nanoparticles) and  $4.46 \pm 0.25$ % for Y-NE (yogurt nanoemulsions). According to their results, at the end of the digestion, zeaxanthin concentration into micelles and bioaccessibility was significantly higher in Y-NE than in Y-NP. Donhowe *et al.*, 2014 evaluated the influence of microencapsulation on the *in vitro* release of  $\beta$ -carotene. The authors reported that microencapsulated  $\beta$ -carotene showed significantly lower bioaccessibility than free  $\beta$ -carotene and attributed this result to the soluble fibers present in gelatine, that was used as wall material in microencapsulation, which formed bonds with bile salts, reducing the carotenoid release and micelle formation. This may explain the slightly lower curcumin bioaccessibility obtained for the gelatine-SLN sample, i.e., the gelatine could have formed bonds with bile salts, consequently reducing curcumin release.

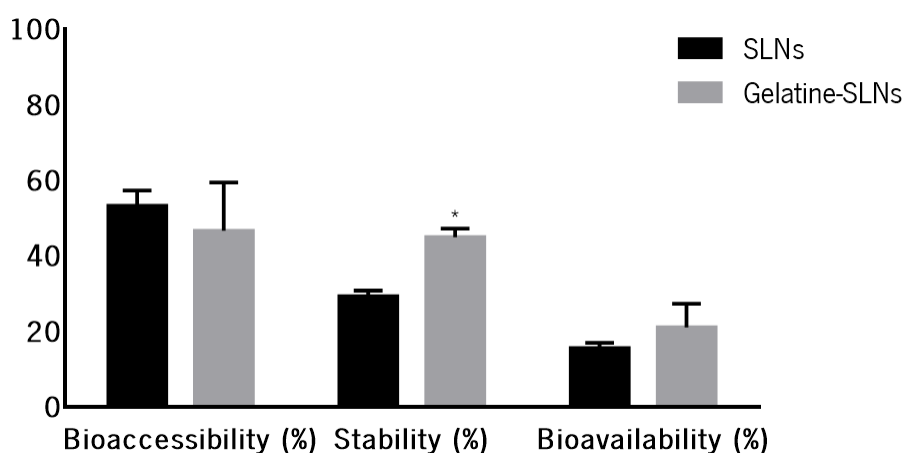


**Figure 27.** Bioaccessibility (%), stability (%), and bioavailability (%) of curcumin after *in vitro* digestion of SLNs and gelatine-SLNs. The results are presented as the mean  $\pm$  SD. \*significantly different from correspondent values in SLNs ( $p < 0.05$ ).

Stability of curcumin at the end of the *in vitro* digestion was  $29.3 \pm 1.4$  % in SLNs and increased ( $p < 0.05$ ) to  $45.0 \pm 2.2$  % in gelatine-SLNs. These results suggest that gelatine-SLNs provides a protective effect to curcumin. One possible explanation could be related to the fact that curcumin is encapsulated in SLNs, which in its turn is incorporated into a gelatine matrix, further protecting the curcumin and, consequently, making it less accessible to the action of the components of intestinal digestion, namely those that catalyse lipid degradation.

Curcumin bioavailability at the end of the simulated *in vitro* digestion was  $15.6 \pm 1.3 \%$  and  $21.1 \pm 6.2 \%$  for SLNs and gelatine-SLNs, respectively. These results are in line with the ones achieved by Pinheiro *et al.*, 2013, which obtained around 15 % of curcumin bioavailability after intestinal phase, for curcumin encapsulated in Tween 20-stabilized nanoemulsions. The slight increase ( $p > 0.05$ ) in the bioavailability of curcumin in gelatine-SLNs compared to SLNs is in accordance with the results of Z-average diameter after the intestinal phase (**Figure 21**), in which the SLNs showed  $580.2 \pm 61.0$  nm and the gelatine-SLNs  $352.2 \pm 21.4$  nm. Once the mean diameter of the gelatine-SLNs is lower than SLNs, it would be expected to have higher bioavailability of curcumin. In fact, previous studies have found that the rate of lipid digestion increased when the droplet size decreased, which was attributed to the increase in the surface area of the lipid phase exposed to the aqueous phase (Ahmed *et al.*, 2012b). Consequently, greater digestion of lipids leads to the greater formation of digestion products that will form mixed micelles and result in higher bioavailability. In addition, these results are also in accordance with the concentration of FFA which in the gelatine-SLNs was practically double than the FFA of the SLNs sample, although there is the issue of amino acid formation during the hydrolysis of gelatine proteins.

The value of the curcumin bioavailability is estimative and it must be analysed with care, once there are other factors that influence the bioavailability that are not considered, such as absorption and metabolism (Zou *et al.*, 2016).

# CHAPTER 5

---

## CONCLUSIONS AND FUTURE REMARKS

## 5.1. Conclusions

Curcumin has numerous biological activities that may be beneficial to human health; however, due to its low water solubility, poor chemical stability, and low bioavailability its incorporation in food products is both a need and a challenge. Encapsulation is one of the most common approaches to protect curcumin against chemical degradation, increasing its water dispersibility, and improving its bioavailability. The purpose of this study was to develop and characterize SLNs encapsulating curcumin and evaluate its potential to be incorporated into a food product (i.e., gelatine matrix).

The results of the incorporation of the SLNs into gelatine showed that neither the initial size nor initial PDI of the SLNs was changed. Considering the colour capacity of curcumin, and since there were no colour variations of gelatine-SLNs for 14 days, it is concluded that SLNs can be incorporated into gelatine as a natural dye. The results of the texture analysis showed that it is possible to incorporate the SLNs into the gelatine without compromising the textural parameters of the gelatine. Through the analysis of rheology, it was possible to conclude that the addition of SLNs gives a more solid behaviour to gelatine from the beginning of storage and maintains this behaviour until the end of storage. The *DH* results showed that the incorporation of SLNs into gelatine did not influence the hydrolysis of the protein. Moreover, *DH* was slightly higher in the gelatine-SLNs sample. Although there appears to be an increase in the production of FFA in gelatine-SLNs, the difference observed is not statistically significant. The incorporation of SLNs in gelatine did not significantly affect the bioaccessibility of curcumin, however, the bioavailability was slightly higher in the sample of gelatine-SLNs. The results showed that curcumin stability was superior in the gelatine-SLNs sample, concluding that the gelatine confers a further stability to this bioactive compound.

Finally, given the ability of SLNs loaded with curcumin to confer colour and solid behaviour to gelatine, and the fact that this matrix provides stability to SLNs makes this approach a very promising application as it enables the development of a functional gelatine enhancing the characteristics of curcumin.

## 5.2. Future recommendations

In future work, a more detailed physicochemical characterization of the SLNs should be carried out. The incorporation of the SLNs into gelatine must be optimized and evaluated under different storage conditions for longer storage periods. Moreover, it would be of great interest to evaluate the incorporation into food matrices with different natures, characters, and complexities. Finally, it would be fundamental to assess the food nutritional composition of gelatine after the incorporation of the SLNs.



It would be also very interesting to study the toxicity of SLNs alone and incorporated into food matrices through *in vitro* cytotoxicity assays. Finally, it should be noted that the assessment of bioavailability by *in vitro* methods is less accurate than by *in vivo* methods, due to the differences between the simulation conditions of biological processes and the actual biological processes in the human body. Thus, reliable *in vitro* models vs *in vivo* animal models (different species) will be needed to complete the investigation.

# CHAPTER 6



## REFERENCES

- Adams F, Barbante C. 2015a. History and Present Status of Micro- and Nano-Imaging Analysis. In *Comprehensive Analytical Chemistry* 67–124.
- Adams F, Barbante C. 2015b. Spectroscopic Imaging. In *Comprehensive Analytical Chemistry* 339–384.
- Aditya NP, Macedo AS, Doktorovova S, Souto EB, Kim S, Chang P-S, Ko S. 2014. Development and evaluation of lipid nanocarriers for quercetin delivery: A comparative study of solid lipid nanoparticles (SLN), nanostructured lipid carriers (NLC), and lipid nanoemulsions (LNE). *LWT - Food Science and Technology* **59**: 115–121.
- Aditya NP, Aditya S, Yang H-J, Kim HW, Park SO, Lee J, Ko S. 2015. Curcumin and catechin co-loaded water-in-oil-in-water emulsion and its beverage application. *Journal of Functional Foods* **15**: 35–43.
- Aguilera JM. 2019. The food matrix: implications in processing, nutrition and health. *Critical Reviews in Food Science and Nutrition* **59**: 3612–3629.
- Ahmad M, Mudgil P, Gani A, Hamed F, Masoodi FA, Maqsood S. 2019. Nano-encapsulation of catechin in starch nanoparticles: Characterization, release behavior and bioactivity retention during simulated in-vitro digestion. *Food Chemistry* **270**: 95–104.
- Ahmed K, Li Y, McClements DJ, Xiao H. 2012a. Nanoemulsion- and emulsion-based delivery systems for curcumin: Encapsulation and release properties. *Food Chemistry* **132**: 799–807.
- Ahmed K, Li Y, McClements DJ, Xiao H. 2012b. Nanoemulsion- and emulsion-based delivery systems for curcumin: Encapsulation and release properties. *Food Chemistry* **132**: 799–807.
- Almeida HHS, Barros L, Barreira JCM, Calhêla RC, Heleno SA, Sayer C, Miranda CG, Leimann FV, Barreiro MF, Ferreira ICFR. 2018. Bioactive evaluation and application of different formulations of the natural colorant curcumin (E100) in a hydrophilic matrix (yogurt). *Food Chemistry* **261**: 224–232.
- Alminger M, Aura A-M, Bohn T, Dufour C, El SN, Gomes A, Karakaya S, Martínez-Cuesta MC, McDougall GJ, Requena T, et al. 2014. In Vitro Models for Studying Secondary Plant Metabolite Digestion and Bioaccessibility. *Comprehensive Reviews in Food Science and Food Safety* **13**: 413–436.
- Aquanova AG (2020).
- Arredondo-Ochoa T, García-Almendárez B, Escamilla-García M, Martín-Belloso O, Rossi-Márquez G, Medina-Torres L, Regalado-González C. 2017. Physicochemical and Antimicrobial Characterization of Beeswax–Starch Food-Grade Nanoemulsions Incorporating Natural Antimicrobials. *International Journal of Molecular Sciences* **18**: 2712.
- Assadpour E, Mahdi Jafari S. 2019. A systematic review on nanoencapsulation of food bioactive ingredients and nutraceuticals by various nanocarriers. *Critical Reviews in Food Science and*

*Nutrition* **59**: 3129–3151.

Asselin J, Hébert J, Amiot J. 1989. Effects of In Vitro Proteolysis on the Allergenicity of Major Whey Proteins. *Journal of Food Science* **54**: 1037–1039.

Attama AA, Momoh MA, Builders PF. 2012. Lipid Nanoparticulate Drug Delivery Systems: A Revolution in Dosage Form Design and Development. In *Recent Advances in Novel Drug Carrier Systems* InTech; 107–140.

Babazadeh A, Ghanbarzadeh B, Hamishehkar H. 2016. Novel nanostructured lipid carriers as a promising food grade delivery system for rutin. *Journal of Functional Foods* **26**: 167–175.

Ban C, Jo M, Park YH, Kim JH, Han JY, Lee KW, Kweon D-H, Choi YJ. 2020. Enhancing the oral bioavailability of curcumin using solid lipid nanoparticles. *Food Chemistry* **302**: 125328.

Batista RA, Espitia PJP, Quintans J de SS, Freitas MM, Cerqueira MÃ, Teixeira JA, Cardoso JC. 2019. Hydrogel as an alternative structure for food packaging systems. *Carbohydrate Polymers* **205**: 106–116.

Bazana MT, Codevilla CF, de Menezes CR. 2019. Nanoencapsulation of bioactive compounds: challenges and perspectives. *Current Opinion in Food Science* **26**: 47–56.

Bernal JL, Jiménez JJ, del Nozal MJ, Toribio L, Martín MT. 2005. Physico-chemical parameters for the characterization of pure beeswax and detection of adulterations. *European Journal of Lipid Science and Technology* **107**: 158–166.

Borthakur P, Boruah PK, Sharma B, Das MR. 2016. Nanoemulsion: preparation and its application in food industry. In *Emulsions* Elsevier; 153–191.

Bourbon AI, Cerqueira MA, Vicente AA. 2016a. Encapsulation and controlled release of bioactive compounds in lactoferrin-glycomacropeptide nanohydrogels: Curcumin and caffeine as model compounds. *Journal of Food Engineering* **180**: 110–119.

Bourbon AI, Pinheiro AC, Cerqueira MA, Vicente AA. 2016b. Influence of chitosan coating on protein-based nanohydrogels properties and in vitro gastric digestibility. *Food Hydrocolloids* **60**: 109–118.

Bourne MC. 2002. Sensory Methods of Texture and Viscosity Measurement. In *Food Texture and Viscosity* Elsevier; 257–291.

Campo C, Queiroz Assis R, Marques da Silva M, Haas Costa TM, Paese K, Stanisçuaski Guterres S, de Oliveira Rios A, Hickmann Flôres S. 2019. Incorporation of zeaxanthin nanoparticles in yogurt: Influence on physicochemical properties, carotenoid stability and sensory analysis. *Food Chemistry* **301**: 125230.

Cerqueira MA, Pinheiro AC, Silva HD, Ramos PE, Azevedo MA, Flores-López ML, Rivera MC, Bourbon AI,

- Ramos ÓL, Vicente AA. 2014. Design of Bio-nanosystems for Oral Delivery of Functional Compounds. *Food Engineering Reviews* **6**: 1–19.
- Cerqueira MÃ, Pinheiro AC, Ramos OL, Silva H, Bourbon AI, Vicente AA. 2017. Advances in Food Nanotechnology. In *Emerging Nanotechnologies in Food Science* Elsevier; 11–38.
- Chiu G, Tan, Liu, Chang, Lim. 2012. Perorally active nanomicellar formulation of quercetin in the treatment of lung cancer. *International Journal of Nanomedicine* **7**: 651.
- Chuacharoen T, Prasongsuk S, Sabliov CM. 2019. Effect of Surfactant Concentrations on Physicochemical Properties and Functionality of Curcumin Nanoemulsions Under Conditions Relevant to Commercial Utilization. *Molecules* **24**: 2744.
- Crowe KM. 2013. Designing Functional Foods with Bioactive Polyphenols: Highlighting Lessons Learned from Original Plant Matrices. *J Hum Nutr Food Sci* **1**: 1018.
- Darras BT, Ryan MM, De Vivo DC. 2015. Preface to the Second Edition. In *Neuromuscular Disorders of Infancy, Childhood, and Adolescence* Elsevier; xxv–xxvi.
- Day L, Golding M. 2016. Food Structure, Rheology, and Texture. In *Encyclopedia of Food Chemistry* Elsevier; 125–129.
- Dima C, Assadpour E, Dima S, Jafari SM. 2020. Bioavailability of nutraceuticals: Role of the food matrix, processing conditions, the gastrointestinal tract, and nanodelivery systems. *Comprehensive Reviews in Food Science and Food Safety* **19**: 954–994.
- Donhowe EG, Flores FP, Kerr WL, Wicker L, Kong F. 2014. Characterization and in vitro bioavailability of  $\beta$ -carotene: Effects of microencapsulation method and food matrix. *LWT - Food Science and Technology* **57**: 42–48.
- Drugs and Lactation Database (LactMed) [Internet]. 2006. *Lecithin*. National Library of Medicine (US): Bethesda (MD).
- Duncan T V. 2011. Applications of nanotechnology in food packaging and food safety: Barrier materials, antimicrobials and sensors. *Journal of Colloid and Interface Science* **363**: 1–24.
- Espitia PJP, Fuenmayor CA, Otoni CG. 2019. Nanoemulsions: Synthesis, Characterization, and Application in Bio-Based Active Food Packaging. *Comprehensive Reviews in Food Science and Food Safety* **18**: 264–285.
- Ezhilarasi PN, Karthik P, Chhanwal N, Anandharamakrishnan C. 2013. Nanoencapsulation Techniques for Food Bioactive Components: A Review. *Food and Bioprocess Technology* **6**: 628–647.
- Fischer P, Windhab EJ. 2011. Rheology of food materials. *Current Opinion in Colloid & Interface Science* **16**: 36–40.

- Garud A, Singh D, Garud N. 2012. Solid Lipid Nanoparticles (SLN): Method, Characterization and Applications. *International Current Pharmaceutical Journal* **1**: 384–393.
- Gasa-Falcon A, Odriozola-Serrano I, Oms-Oliu G, Martín-Belloso O. 2020. Nanostructured Lipid-Based Delivery Systems as a Strategy to Increase Functionality of Bioactive Compounds. *Foods* **9**: 325.
- Geo Thomas, Adarsh M Kalla, Rajunaik B, Ashok Kumar. 2018. Food matrix: A new tool to enhance nutritional quality of food. In *Journal of Pharmacognosy and Phytochemistry* 1011–1014.
- Golding M, Wooster TJ, Day L, Xu M, Lundin L, Keogh J, Clifton P. 2011. Impact of gastric structuring on the lipolysis of emulsified lipids. *Soft Matter* **7**: 3513.
- Gonçalves RFS, Martins JT, Duarte CMM, Vicente AA, Pinheiro AC. 2018. Advances in nutraceutical delivery systems: From formulation design for bioavailability enhancement to efficacy and safety evaluation. *Trends in Food Science & Technology* **78**: 270–291.
- Granata G, Stracquadanio S, Leonardi M, Napoli E, Consoli GML, Cafiso V, Stefani S, Geraci C. 2018. Essential oils encapsulated in polymer-based nanocapsules as potential candidates for application in food preservation. *Food Chemistry* **269**: 286–292.
- Guo Y, Harris P, Kaur A, Pastrana L, Jauregi P. 2017. Characterisation of  $\beta$ -lactoglobulin nanoparticles and their binding to caffeine. *Food Hydrocolloids* **71**: 85–93.
- Gupta B, Poudel BK, Pathak S, Tak JW, Lee HH, Jeong J-H, Choi H-G, Yong CS, Kim JO. 2016. Effects of Formulation Variables on the Particle Size and Drug Encapsulation of Imatinib-Loaded Solid Lipid Nanoparticles. *AAPS PharmSciTech* **17**: 652–662.
- Hamed S, Soliman T, Hassan L, Abo-Elwafa G. 2019. Preparation of Functional Yogurt Fortified with Fish Oil-In-Water Nanoemulsion. *Egyptian Journal of Chemistry* **62**: 6–7.
- He X, Hwang H. 2016. Nanotechnology in food science: Functionality, applicability, and safety assessment. *Journal of Food and Drug Analysis* **24**: 671–681.
- Helbig A, Silletti E, Timmerman E, Hamer RJ, Gruppen H. 2012. In vitro study of intestinal lipolysis using pH-stat and gas chromatography. *Food Hydrocolloids* **28**: 10–19.
- Improveat.
- Jafari SM, Fathi M, Mandala I. 2015. Emerging product formation. In *Food Waste Recovery* Elsevier; 293–317.
- Jaiswal P, Gidwani B, Vyas A. 2016. Nanostructured lipid carriers and their current application in targeted drug delivery. *Artificial Cells, Nanomedicine, and Biotechnology* **44**: 27–40.
- Jones OG, McClements DJ. 2010. Functional Biopolymer Particles: Design, Fabrication, and Applications. *Comprehensive Reviews in Food Science and Food Safety* **9**: 374–397.

- Khare AR, Vasisht N. 2014. Nanoencapsulation in the Food Industry. In *Microencapsulation in the Food Industry* Elsevier; 151–155.
- Kheradmandnia S, Vasheghani-Farahani E, Nosrati M, Atiyabi F. 2010. Preparation and characterization of ketoprofen-loaded solid lipid nanoparticles made from beeswax and carnauba wax. *Nanomedicine: Nanotechnology, Biology and Medicine* **6**: 753–759.
- Kohyama K. 2020. Food Texture – Sensory Evaluation and Instrumental Measurement. In *Textural Characteristics of World Foods* Wiley; 1–13.
- Kumar DD, Mann B, Pothuraju R, Sharma R, Bajaj R, Minaxi M. 2016. Formulation and characterization of nanoencapsulated curcumin using sodium caseinate and its incorporation in ice cream. *Food & Function* **7**: 417–424.
- Lee C-W, Yen F-L, Huang H-W, Wu T-H, Ko H-H, Tzeng W-S, Lin C-C. 2012. Resveratrol Nanoparticle System Improves Dissolution Properties and Enhances the Hepatoprotective Effect of Resveratrol through Antioxidant and Anti-Inflammatory Pathways. *Journal of Agricultural and Food Chemistry* **60**: 4662–4671.
- Levine H, Finley JW. 2018. *Principles of Food Chemistry*. Springer International Publishing: Cham.
- Li J, Wang X, Zhang T, Wang C, Huang Z, Luo X, Deng Y. 2015. A review on phospholipids and their main applications in drug delivery systems. *Asian Journal of Pharmaceutical Sciences* **10**: 81–98.
- Li P-H, Chiang B-H. 2012. Process optimization and stability of d-limonene-in-water nanoemulsions prepared by ultrasonic emulsification using response surface methodology. *Ultrasonics Sonochemistry* **19**: 192–197.
- Li Y, McClements DJ. 2010. New Mathematical Model for Interpreting pH-Stat Digestion Profiles: Impact of Lipid Droplet Characteristics on in Vitro Digestibility. *Journal of Agricultural and Food Chemistry* **58**: 8085–8092.
- Liu F, Urban MW. 2010. Recent advances and challenges in designing stimuli-responsive polymers. *Progress in Polymer Science* **35**: 3–23.
- Loh JW, Saunders M, Lim L-Y. 2012. Cytotoxicity of monodispersed chitosan nanoparticles against the Caco-2 cells. *Toxicology and Applied Pharmacology* **262**: 273–282.
- Lowry OH, Rosebrough NJ, Farr AL, Randall RJ. 1951. Protein measurement with the Folin phenol reagent. *The Journal of biological chemistry* **193**: 265–75.
- Macdougall D. 2010. Colour measurement of food: principles and practice. In *Colour Measurement* Elsevier; 312–342.
- Mahira S, Rayapolu RG, Khan W. 2020. Nanoscale characterization of nanocarriers. In *Smart*

*Nanocontainers* Elsevier; 49–65.

- Manea A-M, Vasile BS, Meghea A. 2014. Antioxidant and antimicrobial activities of green tea extract loaded into nanostructured lipid carriers. *Comptes Rendus Chimie* **17**: 331–341.
- Martins JT, Ramos ÓL, Pinheiro AC, Bourbon AI, Silva HD, Rivera MC, Cerqueira MA, Pastrana L, Malcata FX, González-Fernández Á, et al. 2015. Edible Bio-Based Nanostructures: Delivery, Absorption and Potential Toxicity. *Food Engineering Reviews* **7**: 491–513.
- Mat DJL, Le Feunteun S, Michon C, Souchon I. 2016. In vitro digestion of foods using pH-stat and the INFOGEST protocol: Impact of matrix structure on digestion kinetics of macronutrients, proteins and lipids. *Food Research International* **88**: 226–233.
- Mat DJL, Cattenoz T, Souchon I, Michon C, Le Feunteun S. 2018. Monitoring protein hydrolysis by pepsin using pH-stat: In vitro gastric digestions in static and dynamic pH conditions. *Food Chemistry* **239**: 268–275.
- Matalanis A, Jones OG, McClements DJ. 2011. Structured biopolymer-based delivery systems for encapsulation, protection, and release of lipophilic compounds. *Food Hydrocolloids* **25**: 1865–1880.
- Mayer S, Weiss J, McClements DJ. 2013. Behavior of vitamin E acetate delivery systems under simulated gastrointestinal conditions: Lipid digestion and bioaccessibility of low-energy nanoemulsions. *Journal of Colloid and Interface Science* **404**: 215–222.
- McClements DJ. 2012. Nanoemulsions versus microemulsions: terminology, differences, and similarities. *Soft Matter* **8**: 1719–1729.
- McClements DJ. 2013. Edible lipid nanoparticles: Digestion, absorption, and potential toxicity. *Progress in Lipid Research* **52**: 409–423.
- McClements DJ, Li Y. 2010a. Structured emulsion-based delivery systems: Controlling the digestion and release of lipophilic food components. *Advances in Colloid and Interface Science* **159**: 213–228.
- McClements DJ, Li Y. 2010b. Review of in vitro digestion models for rapid screening of emulsion-based systems. *Food & Function* **1**: 32.
- McClements DJ, Rao J. 2011. Food-Grade Nanoemulsions: Formulation, Fabrication, Properties, Performance, Biological Fate, and Potential Toxicity. *Critical Reviews in Food Science and Nutrition* **51**: 285–330.
- McClements DJ, Xiao H. 2012. Potential biological fate of ingested nanoemulsions: influence of particle characteristics. *Food Funct.* **3**: 202–220.
- McClements DJ, Xiao H. 2017. Is nano safe in foods? Establishing the factors impacting the



- gastrointestinal fate and toxicity of organic and inorganic food-grade nanoparticles. *npj Science of Food* **1**: 6.
- McClements DJ, Decker EA, Weiss J. 2007. Emulsion-Based Delivery Systems for Lipophilic Bioactive Components. *Journal of Food Science* **72**: R109–R124.
- Miller DD, Schricker BR, Rasmussen RR, Van Campen D. 1981. An in vitro method for estimation of iron availability from meals. *The American Journal of Clinical Nutrition* **34**: 2248–2256.
- Minekus M, Alminger M, Alvito P, Ballance S, Bohn T, Bourlieu C, Carrière F, Boutrou R, Corredig M, Dupont D, et al. 2014. A standardised static in vitro digestion method suitable for food – an international consensus. *Food Funct.* **5**: 1113–1124.
- Mohammed NK, Muhiadin BJ, Meor Hussin AS. 2020. Characterization of nanoemulsion of Nigella sativa oil and its application in ice cream. *Food Science & Nutrition* **8**: 2608–2618.
- Mousavi M, Heshmati A, Daraei Garmakhany A, Vahidinia A, Taheri M. 2019. Texture and sensory characterization of functional yogurt supplemented with flaxseed during cold storage. *Food Science & Nutrition* **7**: 907–917.
- Mozafari MR, Flanagan J, Matia-Merino L, Awati A, Omri A, Suntres ZE, Singh H. 2006. Recent trends in the lipid-based nanoencapsulation of antioxidants and their role in foods. *Journal of the Science of Food and Agriculture* **86**: 2038–2045.
- Neethirajan S, Jayas DS. 2011. Nanotechnology for the Food and Bioprocessing Industries. *Food and Bioprocess Technology* **4**: 39–47.
- Ni S, Hu C, Sun R, Zhao G, Xia Q. 2017. Nanoemulsions-Based Delivery Systems for Encapsulation of Quercetin: Preparation, Characterization, and Cytotoxicity Studies. *Journal of Food Process Engineering* **40**: e12374.
- Pan K, Zhong Q. 2016. Organic Nanoparticles in Foods: Fabrication, Characterization, and Utilization. *Annual Review of Food Science and Technology* **7**: 245–266.
- Panigrahi SS, Syed I, Sivabalan S, Sarkar P. 2019. Nanoencapsulation strategies for lipid-soluble vitamins. *Chemical Papers* **73**: 1–16.
- Paredes AJ, Asencio CM, Manuel LJ, Allemendi DA, Palma SD. 2016. Nanoencapsulation in the food industry: manufacture, applications and characterization. *Journal of Food Bioengineering and Nanoprocessing* **1**: 56–79.
- Park SJ, Hong SJ, Garcia C V., Lee SB, Shin GH, Kim JT. 2019. Stability evaluation of turmeric extract nanoemulsion powder after application in milk as a food model. *Journal of Food Engineering* **259**: 12–20.

- Patel MR, San Martin-Gonzalez MF. 2012. Characterization of Ergocalciferol Loaded Solid Lipid Nanoparticles. *Journal of Food Science* **77**: N8–N13.
- Pathakoti K, Manubolu M, Hwang H. 2017. Nanostructures: Current uses and future applications in food science. *Journal of Food and Drug Analysis* **25**: 245–253.
- Peram MR, Loveday SM, Ye A, Singh H. 2013. In vitro gastric digestion of heat-induced aggregates of  $\beta$ -lactoglobulin. *Journal of Dairy Science* **96**: 63–74.
- Peters R, Dam G ten, Bouwmeester H, Helsper H, Allmaier G, Kammer F vd, Ramsch R, Solans C, Tomaniová M, Hajslova J, et al. 2011. Identification and characterization of organic nanoparticles in food. *TrAC Trends in Analytical Chemistry* **30**: 100–112.
- Pinheiro AC, Lad M, Silva HD, Coimbra MA, Boland M, Vicente AA. 2013. Unravelling the behaviour of curcumin nanoemulsions during in vitro digestion: effect of the surface charge. *Soft Matter* **9**: 3147.
- Pinheiro AC, Coimbra MA, Vicente AA. 2016. In vitro behaviour of curcumin nanoemulsions stabilized by biopolymer emulsifiers – Effect of interfacial composition. *Food Hydrocolloids* **52**: 460–467.
- Pinheiro AC, Gonçalves RF, Madalena DA, Vicente AA. 2017. Towards the understanding of the behavior of bio-based nanostructures during in vitro digestion. *Current Opinion in Food Science* **15**: 79–86.
- Plaza-Oliver M, Baranda JFS de, Rodríguez Robledo V, Castro-Vázquez L, Gonzalez-Fuentes J, Marcos P, Lozano MV, Santander-Ortega MJ, Arroyo-Jimenez MM. 2015. Design of the interface of edible nanoemulsions to modulate the bioaccessibility of neuroprotective antioxidants. *International Journal of Pharmaceutics* **490**: 209–218.
- Priyadarsini K. 2014. The Chemistry of Curcumin: From Extraction to Therapeutic Agent. *Molecules* **19**: 20091–20112.
- Quirós-Sauceda AE, Ayala-Zavala JF, Olivas GI, González-Aguilar GA. 2014. Edible coatings as encapsulating matrices for bioactive compounds: a review. *Journal of Food Science and Technology* **51**: 1674–1685.
- Rafiee Z, Nejatian M, Daeihamed M, Jafari SM. 2019. Application of different nanocarriers for encapsulation of curcumin. *Critical Reviews in Food Science and Nutrition* **59**: 3468–3497.
- Ramos OL, Pereira RN, Martins A, Rodrigues R, Fuciños C, Teixeira JA, Pastrana L, Malcata FX, Vicente AA. 2017. Design of whey protein nanostructures for incorporation and release of nutraceutical compounds in food. *Critical Reviews in Food Science and Nutrition* **57**: 1377–1393.
- Rashidinejad A, Jafari SM. 2020. Nanoencapsulation of bioactive food ingredients. In *Handbook of Food Nanotechnology* Elsevier; 279–344.
- Risch SJ. 1995. Encapsulation: Overview of Uses and Techniques. 2–7.

- Ruiz Canizales J, Velderrain Rodríguez GR, Domínguez Avila JA, Preciado Saldaña AM, Alvarez Parrilla E, Villegas Ochoa MA, González Aguilar GA. 2019. Encapsulation to Protect Different Bioactives to Be Used as Nutraceuticals and Food Ingredients. 2163–2182.
- Sagalowicz L, Leser ME. 2010. Delivery systems for liquid food products. *Current Opinion in Colloid & Interface Science* **15**: 61–72.
- Salvia-Trujillo L, Verkempinck S, Rijal SK, Van Loey A, Grauwet T, Hendrickx M. 2019. Lipid nanoparticles with fats or oils containing  $\beta$ -carotene: Storage stability and in vitro digestibility kinetics. *Food Chemistry* **278**: 396–405.
- Santonocito D, Sarpietro MG, Carbone C, Panico A, Campisi A, Siciliano EA, Sposito G, Castelli F, Puglia C. 2020. Curcumin Containing PEGylated Solid Lipid Nanoparticles for Systemic Administration: A Preliminary Study. *Molecules* **25**: 2991.
- Sari TP, Mann B, Kumar R, Singh RRB, Sharma R, Bhardwaj M, Athira S. 2015. Preparation and characterization of nanoemulsion encapsulating curcumin. *Food Hydrocolloids* **43**: 540–546.
- Sekhon BS. 2010. Food nanotechnology - an overview. *Nanotechnology, science and applications* **3**: 1–15.
- Shah, R., Eldridge, D., Palombo, E., Harding I. 2015. Production Techniques. In *ASTM Manual on Zirconium and Hafnium* ASTM International: 100 Barr Harbor Drive, PO Box C700, West Conshohocken, PA 19428-2959; 56-56–8.
- Shah MA, Mir SA, Bashir M. 2017. Nanoencapsulation of Food Ingredients. In *Integrating Biologically-Inspired Nanotechnology into Medical Practice* 132–152.
- Silva HD, Cerqueira MÃ, Vicente AA. 2012. Nanoemulsions for Food Applications: Development and Characterization. *Food and Bioprocess Technology* **5**: 854–867.
- Silva HD, Beldíková E, Poejo J, Abrunhosa L, Serra AT, Duarte CMM, Brányik T, Cerqueira MA, Pinheiro AC, Vicente AA. 2019. Evaluating the effect of chitosan layer on bioaccessibility and cellular uptake of curcumin nanoemulsions. *Journal of Food Engineering* **243**: 89–100.
- Silva Santos V, Badan Ribeiro AP, Andrade Santana MH. 2019. Solid lipid nanoparticles as carriers for lipophilic compounds for applications in foods. *Food Research International* **122**: 610–626.
- Simões LS, Abrunhosa L, Vicente AA, Ramos OL. 2020. Suitability of  $\beta$ -lactoglobulin micro- and nanostructures for loading and release of bioactive compounds. *Food Hydrocolloids* **101**: 105492.
- Singh H, Sarkar A. 2011. Behaviour of protein-stabilised emulsions under various physiological conditions. *Advances in Colloid and Interface Science* **165**: 47–57.
- Singh H, Ye A, Horne D. 2009. Structuring food emulsions in the gastrointestinal tract to modify lipid

- digestion. *Progress in Lipid Research* **48**: 92–100.
- Singh T, Shukla S, Kumar P, Wahla V, Bajpai VK, Rather IA. 2017. Application of Nanotechnology in Food Science: Perception and Overview. *Frontiers in Microbiology* **8**: 1–7.
- Siswanto J. 2019. Application of Color and Size Measurement in Food Products Inspection. *Indonesian Journal of Information Systems* **1**: 90.
- Soleimanian Y, Goli SAH, Varshosaz J, Sahafi SM. 2018. Formulation and characterization of novel nanostructured lipid carriers made from beeswax, propolis wax and pomegranate seed oil. *Food Chemistry* **244**: 83–92.
- Souza Simões L de, Madalena DA, Pinheiro AC, Teixeira JA, Vicente AA, Ramos ÓL. 2017. Micro- and nano bio-based delivery systems for food applications: In vitro behavior. *Advances in Colloid and Interface Science* **243**: 23–45.
- Sun J, Bi C, Chan HM, Sun S, Zhang Q, Zheng Y. 2013. Curcumin-loaded solid lipid nanoparticles have prolonged in vitro antitumour activity, cellular uptake and improved in vivo bioavailability. *Colloids and Surfaces B: Biointerfaces* **111**: 367–375.
- Szczesniak AS. 1963. Objective Measurements of Food Texture. *Journal of Food Science* **28**: 410–420.
- Tabilo-Munizaga G, Barbosa-Cánovas G V. 2005. Rheology for the food industry. *Journal of Food Engineering* **67**: 147–156.
- Tajkarimi MM, Ibrahim SA, Cliver DO. 2010. Antimicrobial herb and spice compounds in food. *Food Control* **21**: 1199–1218.
- Tamjidi F, Shahedi M, Varshosaz J, Nasirpour A. 2013. Nanostructured lipid carriers (NLC): A potential delivery system for bioactive food molecules. *Innovative Food Science & Emerging Technologies* **19**: 29–43.
- Tan Y, Zhang Z, Zhou H, Xiao H, McClements DJ. 2020. Factors impacting lipid digestion and  $\beta$ -carotene bioaccessibility assessed by standardized gastrointestinal model (INFOGEST): oil droplet concentration. *Food & Function* **11**: 7126–7137.
- Vecchione R, Quagliariello V, Calabria D, Calcagno V, De Luca E, Iaffaioli R V., Netti PA. 2016. Curcumin bioavailability from oil in water nano-emulsions: In vitro and in vivo study on the dimensional, compositional and interactional dependence. *Journal of Controlled Release* **233**: 88–100.
- Villemejjane C, Denis S, Marsset-Baglieri A, Alric M, Aymard P, Michon C. 2016. In vitro digestion of short-dough biscuits enriched in proteins and/or fibres using a multi-compartmental and dynamic system (2): Protein and starch hydrolyses. *Food Chemistry* **190**: 164–172.
- Wang X, Jiang Y, Wang Y-W, Huang M-T, Ho C-T, Huang Q. 2008. Enhancing anti-inflammation activity of

- curcumin through O/W nanoemulsions. *Food Chemistry* **108**: 419–424.
- Wrolstad RE, Acree TE, Decker EA, Penner MH, Reid DS, Schwartz SJ, Shoemaker CF, Smith D, Sporns P. 2004. *Handbook of Food Analytical Chemistry*. John Wiley & Sons, Inc.: Hoboken, NJ, USA.
- Yvon M, Beucher S, Scanff P, Thirouin S, Pelissier JP. 1992. In vitro simulation of gastric digestion of milk proteins: comparison between in vitro and in vivo data. *Journal of Agricultural and Food Chemistry* **40**: 239–244.
- Zhang R, Zhang Z, Zou L, Xiao H, Zhang G, Decker EA, McClements DJ. 2016. Enhancement of carotenoid bioaccessibility from carrots using excipient emulsions: influence of particle size of digestible lipid droplets. *Food & Function* **7**: 93–103.
- Zhang Z, McClements DJ. 2018. Overview of Nanoemulsion Properties: Stability, Rheology, and Appearance. In *Nanoemulsions* Elsevier; 21–49.
- Zheng B, McClements DJ. 2020. Formulation of More Efficacious Curcumin Delivery Systems Using Colloid Science: Enhanced Solubility, Stability, and Bioavailability. *Molecules* **25**: 2791.
- Zhong J, Yang R, Cao X, Liu X, Qin X. 2018. Improved Physicochemical Properties of Yogurt Fortified with Fish Oil/ $\gamma$ -Oryzanol by Nanoemulsion Technology. *Molecules* **23**: 56.
- Zou L, Zheng B, Zhang R, Zhang Z, Liu W, Liu C, Zhang G, Xiao H, McClements DJ. 2016. Influence of Lipid Phase Composition of Excipient Emulsions on Curcumin Solubility, Stability, and Bioaccessibility. *Food Biophysics* **11**: 213–225.

---

## ANNEXES

Annex I – Evolution of the colour parameters of the gelatine and gelatine-SLNs

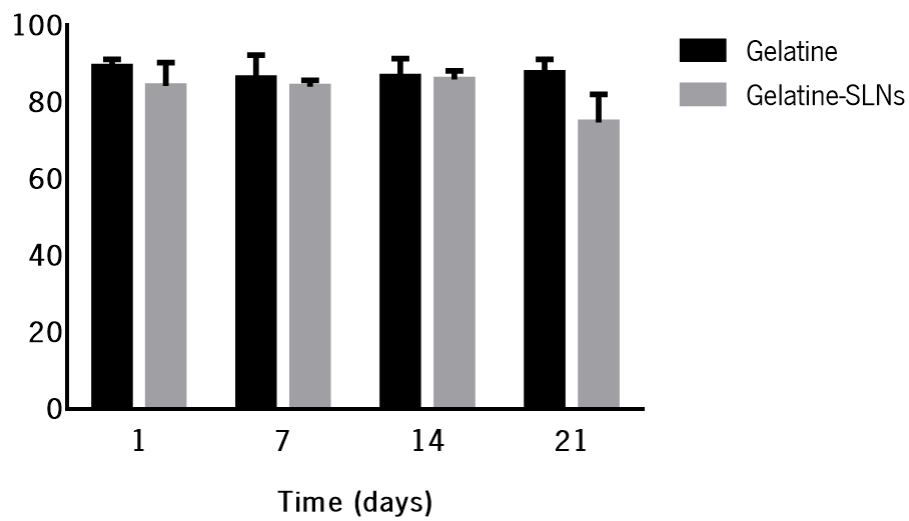


**Figure A. 1.** Evolution of colour parameter  $L^*$  of the gelatine and gelatine-SLNs, during 21 days of storage at 4 °C in the dark.

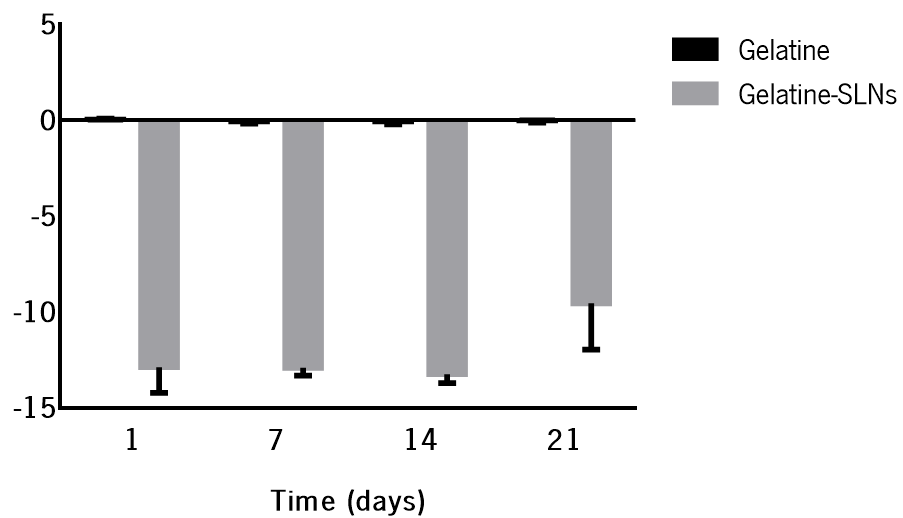


**Figure A. 2.** Evolution of colour parameter  $a^*$  of the gelatine and gelatine-SLNs, during 21 days of storage at 4 °C in the dark.

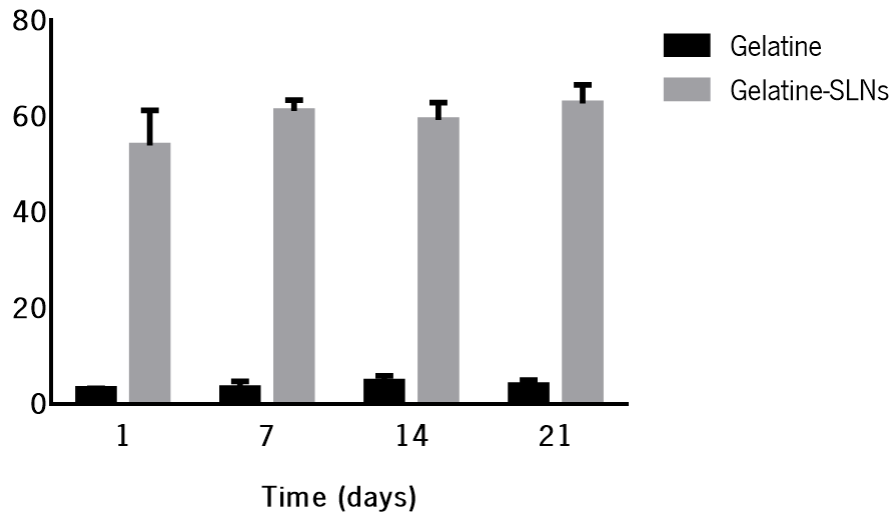


**Figure A. 3.** Evolution of colour parameter  $b^*$  of the gelatine and gelatine-SLNs, during 21 days of storage at 4 °C in the dark.

#### Annex II – Frequency sweep test

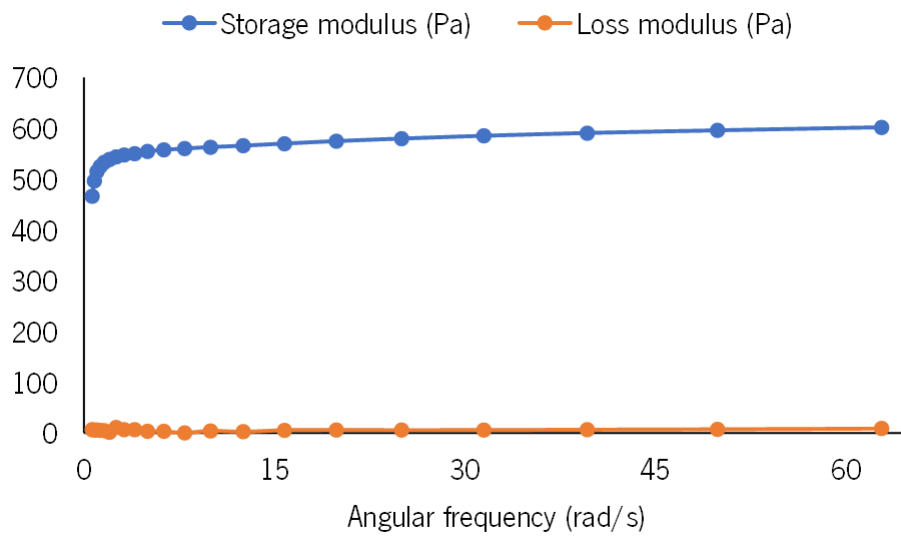


**Figure A. 4.** Frequency sweep test of the gelatine control.



Annex III – Storage and loss modulus of the rheological analysis

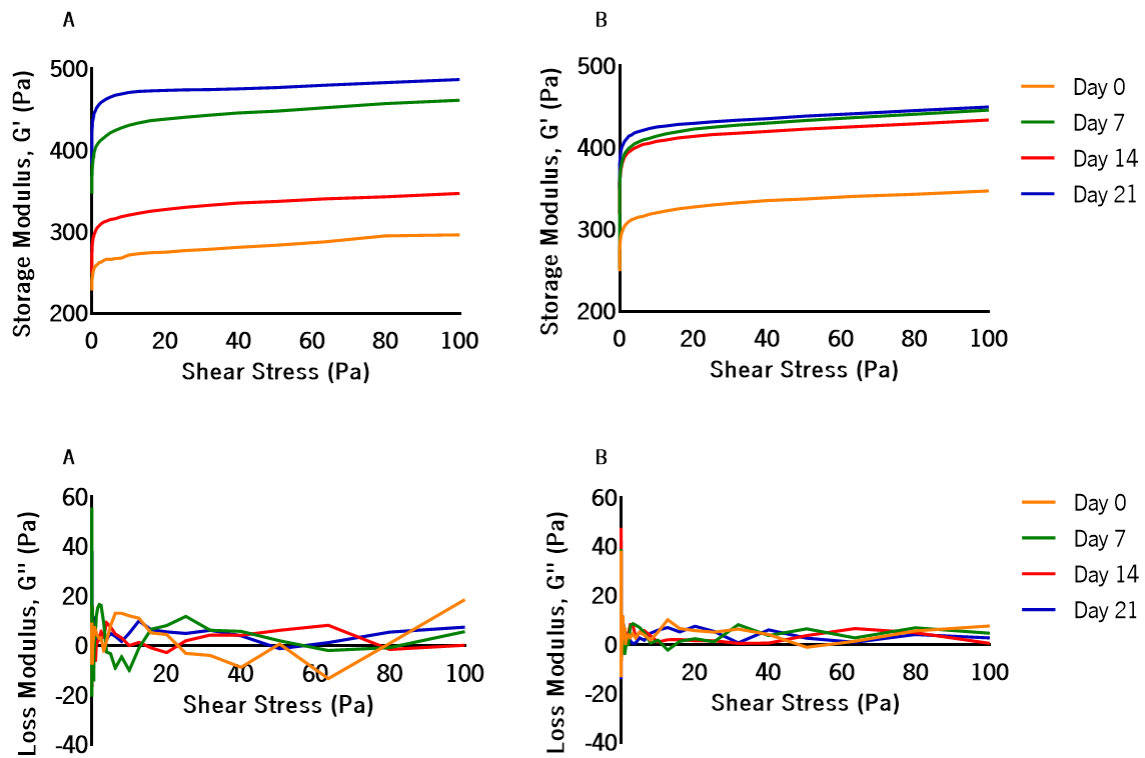


**Figure A. 5.** Storage modulus (G') and loss modulus (G'') obtained from gelatine (A) and gelatine-SLNs (B) over 21 days of storage at 4°C in the dark. The results are presented as the mean.

Annex IV – Folin-BSA calibration curve

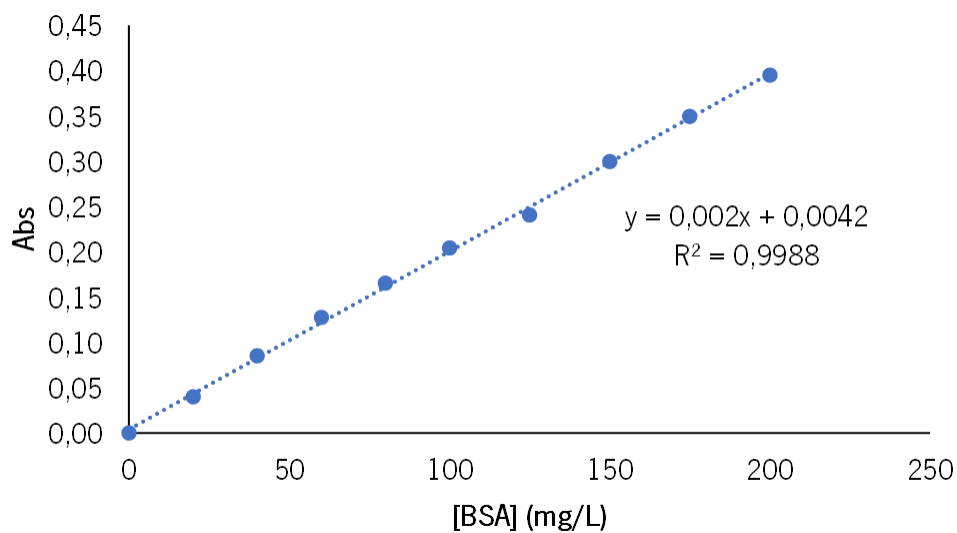


**Figure A. 6.** Folin-BSA calibration curve.

Annex V – Curcumin-chloroform calibration curve

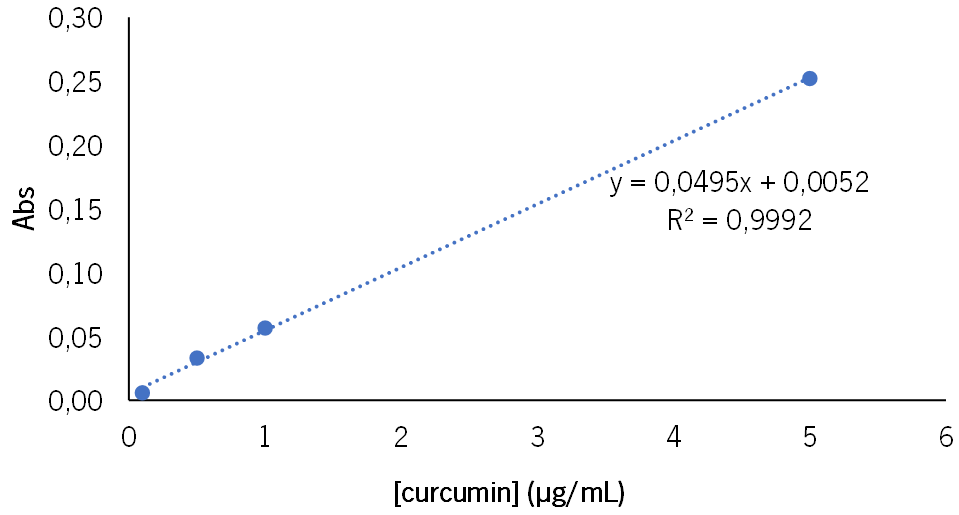


Figure A. 7. Curcumin-chloroform calibration curve.